



AALBORG UNIVERSITET
STUDENTERRAPPORT

Energy Storages and Flexible Loads to Support Large Wind Power Penetration



Group No: WPS4-1050

Authors:

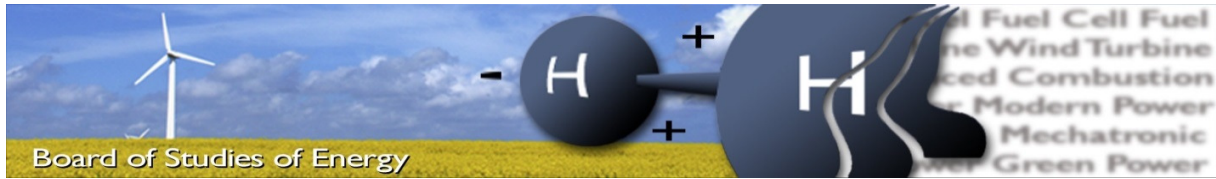
Umur Uslu

Boyang Zhang

Semester: 10th Semester

Department of Energy Technology

Aalborg University



Title: Energy Storages and Flexible Loads to Support Large Wind Power Penetration

Semester: 10th Semester

Semester theme: Master Thesis

Project period: 2/2/2016-1/6/2016

ECTS: 30

Supervisors: Jayakrishnan Radhakrishna Pillai and Sanjay Chaudhary

Project Group: WPS4-1050

Umur Uslu

Boyang Zhang

Copies: [3]

Pages, total: [114]

SYNOPSIS:

The Danish Energy Strategy Plan aims to transform Denmark into a fossil-free country by 2050. Large-scale wind power penetration is expected to increase in the power system. The high penetration level of wind farms creates challenges to the power system control and operation. The conventional grid would have to transform into a Smart grid in order to cope with the challenges. Smart Energy System presents flexible loads like electric vehicles, heat pumps, electrolysers in a Smart grid environment as demand response resources and indirect storage units that provides a supporting role to integrate more wind power in the grid.

In this thesis, the focus is on the employment of electrolyzer, aggregation of heat pumps, electrical vehicles as flexible loads and associated energy storage units for power balancing in wind power dominated power systems. Dynamic analysis on an IEEE standard grid model are conducted under various grid operating conditions and scenarios in DIgSILENT Power Factory. In dynamic analysis, flexible loads is modelled for Load Frequency Control and coordination.

By signing this document, each member of the group confirms that all group members have participated in the project work, and thereby all members are collectively liable for the contents of the report. Furthermore, all group members confirm that the report does not include plagiarism.

Content

1	Introduction	6
1.1	Background.....	6
1.1.1	Wind power in Denmark.....	7
1.1.2	Impact of large scale wind power penetration in the Danish grid	8
1.1.3	Demand side management.....	8
1.1.4	Energy Storages	9
1.2	Problem description	10
1.3	Objectives.....	10
1.4	Limitations.....	11
1.5	Methodology	11
1.6	Outline of the thesis	12
2	Demand Response Resources for frequency reserves in wind dominated power systems	13
2.1	Danish electricity system	13
2.2	Transmission network	14
2.3	Distribution network	14
2.4	District heating in Denmark	15
2.4.1	Combined heat and power plants in Denmark.....	15
2.5	Danish gas network	15
2.6	Wind power plants in Danmark	16
2.7	Danish electricity market	16
2.7.1	Energy markets	16
2.8	Smart energy system and future markets.....	18
2.9	Power to Gas	19
2.9.1	Theory and topologies of water electrolysis	20
2.9.2	Injection of Hydrogen in the Danish gas network	20
2.10	Heat pump.....	21
2.10.1	Coefficient of performance.....	21

2.10.2	Heat pumps in the Danish households	22
2.11	Electrical vehicles	22
2.11.1	EV battery technologies.....	22
2.11.2	EVs in Danish garages	23
2.12	Technical requirements for frequency control	24
2.12.1	Swing equation	24
2.12.2	Grid frequency response during disturbances	24
2.12.3	Primary frequency response.....	25
2.12.4	Governor droop settings.....	26
2.12.5	Secondary frequency response – Single area system.....	26
2.13	Summary	27
3	Load Frequency Control.....	28
3.1	Case study description	29
3.2	Integration of flexible loads in LFC.....	31
3.3	Centralized combined heat and power plant	34
3.3.1	Aggregated steam turbine model.....	34
3.4	Decentralized combined heat and power plant	37
3.4.1	Aggregated gas turbine model	37
3.5	Wind power generation	38
3.6	Passive load	39
3.7	Load model.....	40
3.8	Simulation results.....	40
3.8.1	Primary response	40
3.8.2	Step reference power	42
3.8.3	Secondary response.....	43
3.8.4	Base Case	45
4	Dynamic modelling of Flexible Loads in DiGSILENT PowerFactory	49
4.1	Implementation of Alkaline Electrolyzer.....	50
4.1.1	Modelling of Alkaline Electrolyzer	51

4.1.2	Test of the Alkaline Electrolyzer	54
4.2	Implementation of Heat Pump	55
4.2.1	Heat demand	56
4.2.2	Modelling of Heat Pump	57
4.2.3	Test of the Heat Pump	60
4.3	Electric vehicle (EV)	61
4.3.1	Modelling of the EV	64
5	Integration of Flexible Loads in a Wind Dominated Power System	69
5.1	Frequency support from AE	69
5.1.1	Winter scenario.....	69
5.1.2	Summer scenario	73
5.2	Frequency support from HP	75
5.2.1	Winter scenario.....	75
5.2.2	Summer scenario	78
5.3	Frequency support from EV	79
5.3.1	Winter scenario.....	80
5.3.2	Summer scenario	82
5.4	Frequency support from all three Flexible Loads	84
5.4.1	Winter scenario.....	84
5.4.2	Summer scenario	87
5.5	Statistical analysis.....	90
6	Conclusion.....	93
6.1	Future work	95
7	Bibliography	109

Preface

This master thesis has been written by WPS4-1050 on the 10th semester at the Department of Energy Technology at Aalborg University in the period from the 2nd of February 2016 until 1st of June 2016.

We would like to thank our supervisors Jayakrishnan Radhakrishna Pillai and Sanjay Chaudhary for their guidance and support throughout this project.

In this project, DigSILENT PowerFactory 15.1 has been used to simulate the electrical grid and the elements in the grid. Additionally, MATLAB/SIMULINK has been used to analyze and test the different models in the project.

Reader's Guide The information in this project has been collected in literature, web pages, articles and reports. The references can be found in the bibliography. The referring method for the references is the IEEE citation style, with numbers.

1 Introduction

This thesis presents the analysis of demand side participation of flexible loads and its associated storages in a power system with large-scale wind power penetration. A new solution for Load Frequency Control (LFC) are developed and presented dealing with compensation of frequency fluctuation caused by large wind power plants with coordination from different type of flexible loads in order to ensure system balance of the power system.

1.1 Background

The energy demand grows rapidly with the growth of the society and technology. It is not only desired to satisfy the growing energy demand, but also be able to generate electricity from more environment friendly energy sources. Fossil fuels were the main sources of energy for decades. These sources have caused climate change and environmental issues [1]. This had led countries opting for renewable energy sources (RES) such as wind power in order to reduce the use of fossil fuels. Nowadays, RES has a significant growth worldwide due to the mentioned issues. Wind power is one of the fastest growing RES and recognized as a mainstream technology. The main reasons for the large scale integration of wind power into the power system are [1]:

- Sustainable economic and industrial development
- Low CO2 emissions

According to [2], 432 GW wind power has been installed globally until the end of 2015. China has the biggest wind power share worldwide with the capacity of 145 GW. However, renewable energy sources (RES) are well known for being uncontrollable energy source of power because of fluctuation in power generation. Large scale of wind power penetration brings new challenges to the power system regarding the stability and reliability. These challenges will be explained further in the subsection 1.1.2. According to [3], one solution to these challenges would be the use demand side management in the power system.

1.1.1 Wind power in Denmark

Denmark is leading in development of wind power technology. The electricity generation from wind power began late in 1970s and increased with a huge growth late in the 1990s [4]. The Danish government has set an energy strategy where the aim is reduction of greenhouse gas emissions. The plan is become fossil fuel free by 2050 where 100% of the Danish electricity consumption has to be supplied by RES [5]. Many large conventional power plants are planned to be decommissioned and replaced by new large wind farms.

Figure 1.1 shows the wind power generation and the electricity consumption of Denmark for few weeks both present and in 2050.

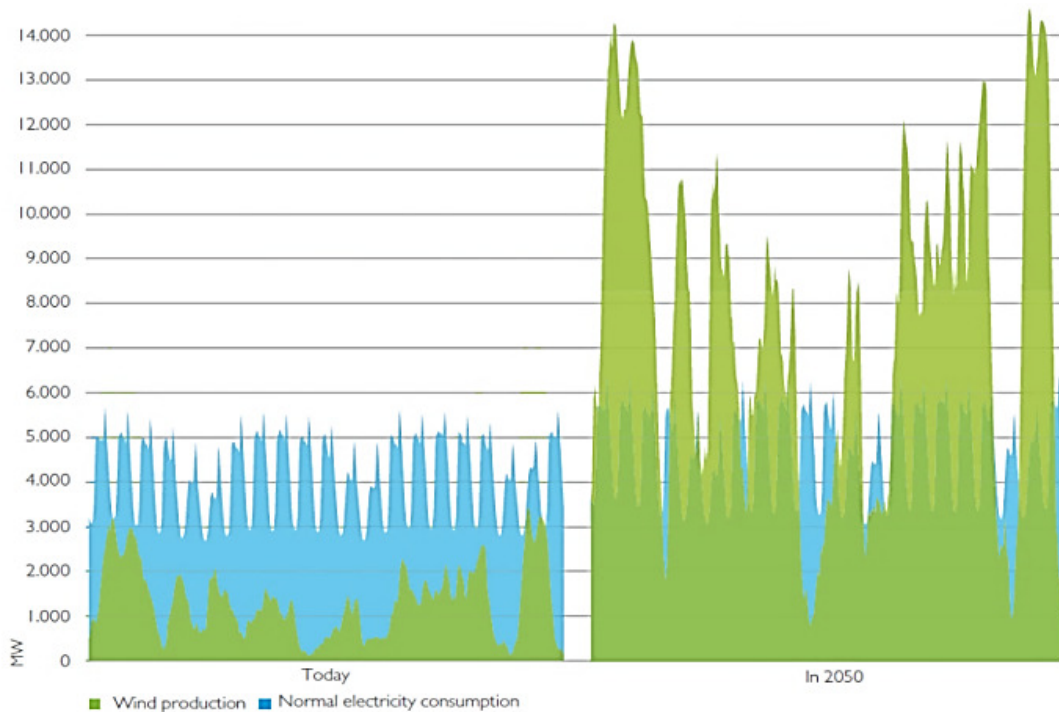


Figure 1.1 - Wind power production and consumption for present and 2050 in Denmark [6]

It can be seen that the electricity production from wind power in 2050 will considerably increase and exceed the electricity consumption for several hours. Therefore, it is required to minimize the imbalance between the demand and generation in order to maintain the grid stability. According to [3], smart energy systems are predicted to be one of the possible options to minimize the negative impacts of excess of wind power production.

1.1.2 Impact of large scale wind power penetration in the Danish grid

Large-scale wind power penetration has made the power system operators concerned regarding the stability and reliability of the power system operation. The intermittent nature of wind can lead to fluctuations in power generation, which can lead to challenges in the balancing and control systems. Power balance is the main challenge that needs to be taken into account for a large-scale wind power integration [7]. The transmission system operator (TSO) must ensure the power balance between generation and demand. Their duty is to keep the cost at minimum and at the same time ensure power system stability. The stability issues could be voltage fluctuation, frequency deviation and small-signal stability. According to [8], the imbalance between generation and demand will also create frequency problems in the grid. The frequency in the grid will increase if the generation is higher than the demand in the power system and vice versa. Therefore, it is very important to find a solution for this imbalance by control methods.

The WPPs will replace many large conventional power plants. Traditionally, the conventional power plants have the duty for ensuring active power balance and capable of meeting the guidelines in the grid code. In a traditional power system, the load changes almost follow the same pattern. These variations in load are compensated with extra power generation capacity kept as reserves. These reserves are provided by the conventional power plants, which are the called ancillary services to regulate for the grid frequency and voltage.

Therefore, the TSO will have to find new methods to integrating large-scale wind power plants into the power system while keeping the cost at minimum.

1.1.3 Demand side management

In order to use of electricity more efficient, the strategy for a Smart Grid Network of Denmark was set up in 2011 by Danish Minister for Climate and Energy [9]. The purpose of this concept is to create a flexible electricity consumption and production from the customers. The TSO is responsible for ensuring the stability of the entire power system and request the flexibility according to the demand. In this strategy, the customers are expected to make agreements with the players in the power system market.

The idea is shifting the customer load demand in order to get a desired load profile, which is beneficial for the TSO balancing services. These can be both economic and technical benefits. In this project, these loads are set to be electrolyser farms, heat pumps and electrical vehicles. An intelligent control of these loads will hereby turn them into flexible loads.

The most common applications of demand side management are:

- Peak shaving: *Reduce the consumption by going off-grid at peak times*
- Valley filling: *Increment of consumption during off-peak times*
- Load shifting: *Reschedule peak to off-peak times*

According to [10], it is possible to change the load shapes by using demand side management.

1.1.4 Energy Storages

As mentioned, the unpredictable nature of wind could lead to wind power fluctuation, which could affect the stability of the power system and cause some serious problems, such as frequency fluctuation and voltage instability.

Energy storage is one of the best resources, which can play a major role in the future Smart Energy Systems [11]. It has received lots of attention recently due to the high wind power penetration in Denmark by 2050. The issues on the transmission network have to be dealt by the TSO who would like to invest in new solutions to avoid problems in the power system [12]. Here, storage systems are associated with the flexible loads, because they can provide a buffer to support the power system.

Controlling the flexible loads, a long term value to the power system can be achieved by offsetting the excess of power from large scale wind power penetration. According to [13], Hydrogen (H_2) has a high potential for long term storage with a huge capacity up to 20 TWh and with a discharge time of months. Therefore, Power-To-Gas (P2G) solutions have the possibility of providing seasonal energy. However, the efficiency of P2G is very low and therefore it is not very attractive because of the technical limitations [13]. Apart from P2G, the Vehicle-to-Grid (V2G) technology will also be implemented in the future Smart Grid as EVs are going to be a more common transportation by 2050 and aggregated heat pumps are also feasible in the future Smart Grid [12].

In a smart energy system, the heat pumps could be used with flexibility in order to consume the excess of electrical energy from wind, which could be used for heating purposes together with the P2G technology to support the grid and the gas network. Heat pumps do have water storage tanks, which is an indirect storage system that can be used to store energy. The V2G technology can also provide additional support to the grid by consuming the excess of power from the wind or provide additional power into the grid.

The storage system of flexible loads can provide ancillary service like regulation in the system in order to reduce the power imbalance. The owners of these flexible loads will be able to benefit during low electricity prices by providing ancillary service to the TSO.

In this thesis, the main work is focused on the employment of P2G, Heat pump and EV technologies as demand-response resources with their associated energy storage capability to provide frequency regulation.

1.2 Problem description

Today's trends of power production are moving towards renewable energy sources, mostly wind power. However, the integration of these renewable energy sources is not straight forward, because it brings challenges to the power system stability and quality. A special case is with large scale wind power penetration where the frequency stability is becoming an important topic for the system operators.

Traditionally, the needed reserve power was provided by conventional power plants to stabilize the grid frequency. The replacement of conventional power plants with wind power plants reduces the reserve availability in the power system. Therefore, alternative solutions for providing reserves is necessary.

Flexible loads such as electrolysers, heat pumps and EVs could be a candidate solution to provide flexible consumption or additional power to the grid during high wind situations due to their storage ability.

Therefore, a proper investigation of flexible loads providing grid support has to be made.

1.3 Objectives

This thesis investigates the integration of flexible loads and energy storages in Load Frequency Control (LFC) for their active contribute in active power balance control as system services.

The objectives defined for this analysis are:

- *Analyze the integration of the LFC in a power system with flexible loads*
- *Study the flexible loads capability to provide system services, participating in the LFC control strategy*

The objectives are split into different tasks:

- *To model the flexible load components: Electrolyzer, Heat Pump and Electrical Vehicles.*
- *To integrate LFC with flexible loads with regards to frequency regulation.*
- *To perform dynamic analysis of the system subjected to changes in power generation and demand.*

1.4 Limitations

- Aggregated models are used for the wind farms, base loads and flexible loads.
- Fault scenarios are not considered.
- N-1 and N-2 contingencies are not considered.
- The hot water tank for HPs and the gas network for AE are not modelled.
- A total disconnection of wind is not considered.
- Voltage analysis is not considered.

1.5 Methodology

First, the project work will begin with a literature review for the background knowledge about grid stability problems. Later, the technologies behind the flexible loads will be studied. Based on the information, a suitable technology will be chosen for the requirements of this project. The models of these technologies will be implemented in MATLAB/SIMULINK for testing purpose. The next step is to implement the models in Digsilent Power Factory with an existing IEEE 9-bus network, which is chosen for this study case. A Load Frequency Control strategy will be implemented for the flexible loads. Dynamic analysis of the system will be conducted with different scenarios for wind penetration and load demand in Digsilent in order to assess the behavior of the system.

These steps are separated as tasks below:

- Literature review of the flexible loads: Electrolyzer, Heat Pumps and Electrical Vehicles
- Selection of technology
- Creating the models for the flexible loads in MATLAB
- Modeling of the system in Digsilent Power Factory with the IEEE 9-bus network
- Integrate LFC with the flexible loads
- Simulate winter and summer scenarios with respect with changes in electrical generation and demand
- Dynamic analysis of the impact of the flexible loads on the IEEE 9-bus network

1.6 Outline of the thesis

The introduction is followed by the main chapters of the thesis organized as following:

Chapter 2 – The second chapter presents the Danish power system where the reader gets information about the current power system division in the country. Hereby the current CHP plants in Denmark is presented together with the increasing penetration of wind power plants. The newest technologies behind electrolyzer, heat pumps and electrical vehicles is found in this chapter. The market is analyzed and the technical requirements for frequency control is introduced.

Chapter 3 – The third chapter presents the modelling of the LFC controller. The chapter explains how the system is interconnected. Furthermore, the test results of the system behavior is also analyzed. Finally, the base case simulation results are presented. The wind power curves and consumption curves for the different scenarios is also shown.

Chapter 4 – The fourth chapter presents the modelling of the flexible loads. The DigSILENT models for AE, HP and EV are introduced in details. This chapter includes a description of the models and a standalone test.

Chapter 5 – The fifth chapter analyzes the results and compares it to the base case values. The flexible loads are first added to the power system one by one. Then, all three flexible load is added into the power system and the results are discussed.

Chapter 6 – The sixth chapter presents the conclusion of this study case. Hereafter, the possible future work is listed.

Chapter 7 – The seventh chapter presents the list of the references used in this study case.

2 Demand Response Resources for frequency reserves in wind dominated power systems

In this chapter, the state of art behind the demand response resources for frequency reserves will be presented. First, an introduction to the Danish electricity and hereafter the gas and electricity systems are presented. Moreover, the flexible loads and storages relevant for the Danish grid services and markets will be presented. Furthermore, the relevant grid codes to this study case will also be presented in this chapter.

2.1 Danish electricity system

The electricity system of Denmark is divided into two networks, which are West Denmark (Jutland and Funen) and East Denmark (Zealand). Figure 2.1 shows the interconnections of the Danish electricity system.

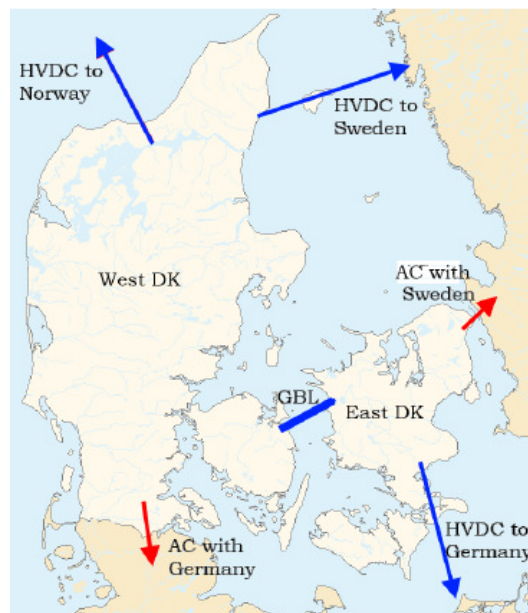


Figure 2.1 - Danish electricity system interconnections [14]

The electricity system is divided into two levels, transmission and distribution levels, which are 400kV to 132 kV and for the transmission network and 60kV to 0.4kV for the distribution network [14]. The power supply of Zealand is mainly supplied from both centralized CHPs, decentralized CHPs and wind power plants (*WPP*) both onshore and offshore spread around the island. The East Danish power system is synchronized to the Nordic power system. The Nordic power system is mostly supplied by large hydro and nuclear power plants.

These power plants are well known for having a predictable power output, which gives a stable frequency for the Nordic power system [14].

The West Danish power system is also supplied by CHPs and WPPs. It is also worth to mention that more WPPs are connected to the West Danish power system both onshore and offshore [15] [16], which makes West Danish power system weaker against large scale wind power production. The West Danish power system is connected to Sweden and Norway through a HVDC connection and to Germany through a HVAC connection. Therefore, Jutland and Funen are synchronized with the German power system. The HVAC interconnection with Germany links the West Danish power system with the European power system.

2.2 Transmission network

Energinet.dk is official operator of the Danish transmission network, which is owned by the Danish Ministry of Energy, Utilities and Climate. Their responsibility covers security and supply to the consumers [14]. In Denmark, the increasing integration of wind power are going to present challenges. Newly integrated WPPs will replace the conventional generators, which means that less frequency reserves will be available. Therefore, frequency fluctuation in the power system network will be a major concern because of the process. This might be solved by flexible loads provided in the distribution network.

2.3 Distribution network

The Distribution Operator (DSO) is responsible for the operation of the distribution network and to deliver power supply to the end users. Since the last decade, the Danish distribution network has gone through lots of changes. Many distribution generators (*DG*) are introduced at the Medium Voltage level presenting several challenges in the distribution grid. The frequency of the power system is 50 Hz if the consumption and generation is equal. However, the introduction of DGs has contributed to the power imbalance in the grid, which has led to frequency fluctuation. As a solution, flexible loads come into mind because they will be integrated in the distribution networks. The aggregated control of flexible loads in the distribution network will help to reduce the power imbalance, which will result in reducing the frequency fluctuation. The location of the flexible loads are as following: The electrolyzer will be installed at the Medium Voltage level, the HPs and EVs are installed at the Low Voltage level.

2.4 District heating in Denmark

District heating is the main way of heating in Denmark. The heat is produced in centralized power plants and transported to the end-users through water pipes. In 2013, the CHPs plants constituted 72.4% of the total supply [17]. According to [18], large heat pumps (larger than a few MW) can be also be found at district heating plants and small heat pumps are installed at house levels. The small heat pumps are mostly used in rural areas where district heating cannot be provided.

2.4.1 Combined heat and power plants in Denmark

The combined heat and power plant (CHP) technology in Denmark, which produces electricity and heat as a by-product from fuel sources. This technology can be used together with the P2G technology because the electrolyzer converts electricity into gas. Table 1 shows the amount of installed centralized (CHP) and decentralized (DCHP) in Denmark in 2013:

Table 1 - CHPs in Denmark [17]

Type of CHPs	Number of units	Electricity capacity MW	Heat capacity MJ/s
Centralized	32	6244	6301
Decentralized	637	1890	2333

2.5 Danish gas network

Denmark is exporting gas to countries like Sweden and Germany. The owner of the Danish Gas network is the Danish transmission operator by Energinet.dk. There are two gas storage facilities, one at Lille Torup and the other at Stenlille. The storage capability of these facilities are as following [19]:

- Lille Torup (Jutland) : 440 million Nm³, (5300 GWh)
- Stenlille (Zealand) : 558 million Nm³, (6820 GWh)

The stored gas in the future from the electrolyzer can be used whenever needed and wherever it is needed by consumers like CHP plants or fuel cell owners. The gas can be both used to heat the households or convert it back to electricity in order to deliver power the Danish power system.

2.6 Wind power plants in Denmark

The installed wind power capacity reached 4.89 GW in the Danish power system (2013) and this number is expected to go much higher by 2020 [20]. Compared with the onshore technology, offshore wind turbines are increasing significantly in Denmark and rest of Europe. The reason is that the offshore wind speed is higher than the onshore wind speed. Denmark has many offshore wind farms and a lot more are expected to be installed in the future. Two of the upcoming ones are listed below:

Some of the upcoming offshore wind farm projects in Denmark are listed below:

- **Horns rev 3** – The total capacity of the wind farm is 400 MW.
- **Krigers Flak** - The farm has a total capacity of 600 MW.

As mentioned in the introduction, Denmark has an aim of having 50 % of the power supply from wind turbines by 2020 and 100% power production from RES. Therefore, a lot more wind farms will be installed in Denmark in the future.

2.7 Danish electricity market

It is important to have a clear overview of the Danish electricity market, as the demand side response is expected to benefit all the players in the market. The control of the flexible loads depends pretty much on the price of the electricity. The intelligent control will begin when the electricity price is low due to excess of wind power in the grid. Therefore, a new market will be in need in order to buy and sell this flexible reserve/demand side response in the market.

The players in the Danish electricity market are free to offer and buy the electricity, which leads to an increasing competition. The offers and purchases are made in the Nord Pool market, which is a shared market for electricity between the Nordic countries. The Danish TSO, Energinet.dk, can purchase the regulated power in the Nordic Regulation Market.

2.7.1 Energy markets

The power in the grid is normally offered and bought in the day ahead market, which is called **Elspot**. Due to unexpected changes, a second market is needed, which is called **Elbas** that ensures a balance between generation and consumption every hour. The imbalances which occur within the hour of consumption needs to be dealt in a different way. These imbalances are regulated through two other markets: Regulating Power Market and Reserves Capacity Market.

Regulating Power- and Reserves Capacity market

The power imbalances are caused by many factors such as forecast imprecision or the intermittency of RES or due to outages in the grid. The TSO makes agreements with balance responsible parties (BRP) to provide up- and downwards regulation. The TSO pays these large players in the market to either reduce or increase their generation of power into the grid depending on the imbalance status of the power system. Figure 2.2 shows the activation time of these reserves in the power system, which is agreed time ranges by the European TSOs through the European Network of Transmission System Operators for Electricity(ENTSO – E) [21].

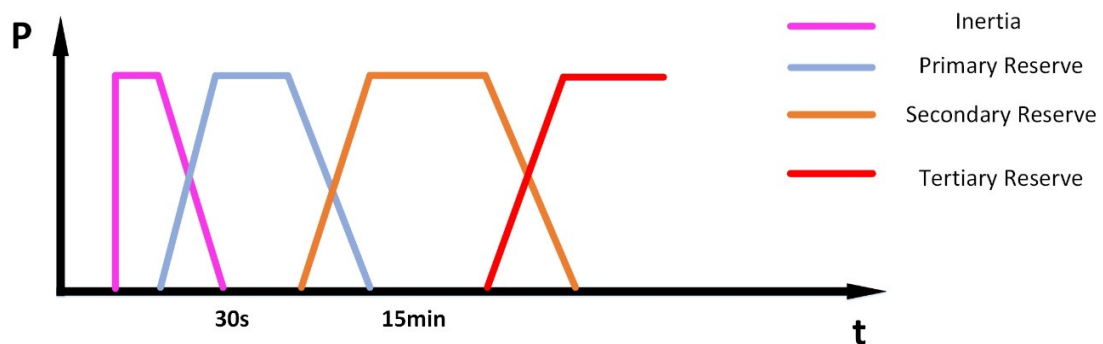


Figure 2.2 - Regulating power reserves

According to Energinet.dk, primary reserves in West Denmark operates within a frequency range of 49.8-50.2 Hz. Primary reserve should be able to fully operate within 30 seconds [21]. Secondary reserve, the so-called Load Frequency Control is to support the primary reserve if the frequency goes beyond 49.8-50.2 Hz. Secondary reserve should be activated latest after 30 seconds must fully operate within 15 minutes [21]. West Denmark and Germany has automated computer network, which handles all the offers by itself. In Nordic countries and East Denmark, the secondary control is made manually by phone call [22].

In order to participate as a reserve, a minimum amount of offer is needed. In Denmark, the minimum offer is 10 MW where the maximum offer is 50 MW. Energinet.dk purchases these offers from the Regulation Power Market. Energinet.dk needs to ensure enough reserves during faults or other issues, and therefore they sign contracts with BRPs in order to have available reserves to balance the system. The TSO and BRPs meet and agree on reserves in the reserve market [23]. The technical details behind primary and secondary reserves will explained further in section 2.12.

2.8 Smart energy system and future markets

Demand side response is directly connected with regulation of power and therefore it is interesting when discussing Regulation Power/Reserves capacity Market and Elbas Market, which are balancing markets of Denmark. A proposed solution to the mentioned challenges in the power system is a smart energy system where the idea is to integrate a smart grid to cope with the challenges. Smart grid contains many elements where the view as a big package could speed up with integration of renewable energy sources and get rid of fossil-fuels based systems [24].

The electricity prices often depend on the wind forecast and therefore an error in the forecast will lead to losses to the wind power producer. A windy day will result in low electricity price or even negative prices if there is too much excess of wind power in the grid. A low wind situation might lead to rise of the electricity prices. The flexible loads, which are covered in this project, can be used to consume this excess of wind power and store it in their storage system and use it whenever it is needed. The Electrolyzer and HP will be able to assist the power system with down regulation, where the EV will be able to assist with both up and down regulation [25]. Therefore, all three flexible loads have a big role in the balancing market due to its regulation ability.

The smart grid will be able to offer the needed services to balance the power system. The need for reinforcements of the grid will be reduced by making flexible consumption available. It will take use of the energy when it is cheap.

Wind power production is usually cheaper than a traditional power production. Wind turbines owners receive a support by the government. This support comes from the taxes payed by the end-customer, which is called PSO tariff. Energinet.dk uses these tax monies to invest in new technologies on behalf of the government. Therefore, the potential for wind power production in Denmark is expected to rise in the future. In the future, it is expected that electrolyzer projects will increase in Denmark, the end- consumers will have an EV charging in the garage, and HPs providing heat to the households. The end-customers will be glad to provide flexibility on windy days because of the cheap electricity price.

The DSOs are expected to have less role in the future due to the agreements with the government in order to operate the distribution networks. The trade between the end-users and system operators will be dealt in a new layer, which consists of the aggregators and traders. The aggregators will offer services to end-users and make sure of competitiveness in the market. Intelligent control of the flexible loads is necessary in order to have a successful smart grid. During over frequency periods in the grid, the electrolyzer and heat pump could start consuming the excess of wind power in order to bring the frequency within the allowed limits. The EV could do the same job, but the EV could also deliver power to the grid whenever there is under frequency.

The traders will sell and buy energy in the market. The price of energy will primarily depend on wind conditions. Therefore, the system operators will be in need for a flexible market inside the Nord Pool market, as it can be seen in Figure 2.3.



Figure 2.3 - Future market [26]

According to [26], a new market will appear in the future, where the commercial players will offer the flexibility. The owner of the flexible loads will have to make agreements with the commercial players in order to apply intelligent control for the HPs or EVs. For instance, the heat pump without control should consume more energy than the controlled heat pump. The idea is to have a flexible control of these loads and at the same time benefit all the players in the new market for flexibility. The next section explains the technology behind flexible loads and their current state.

2.9 Power to Gas

As mentioned in the introduction, Power-To-Gas (P2G) technology has ability for long-term storage. The electrolyzer converts electricity into hydrogen and stores it in the gas network. In the following subsections, different technologies for electrolyzers are presented.

2.9.1 Theory and topologies of water electrolysis

The P2G technology can be used to both store and transport energy. This technology is very suitable for accompany with variable source of renewable energy such as wind and solar, that because the P2G system can effectively convert instantaneous generated electricity into gas which can be stored in long periods. The production process of power-to-gas consists of electrolysis and optionally methanation can be included. In a water electrolysis, water can be decomposed into hydrogen and oxygen by applying an electric current. The electrolyzer is supplied by a DC power supply, where the current flows between the anode and cathode. The hydrogen is generated at the cathode and the oxygen is generated at the anode in the electrolysis process. There are three main technologies named Alkaline Electrolysis, Proton Exchange Membrane Electrolysis and Solid Oxide electrolysis, which have different advantages and drawbacks. A detailed explanation of these technologies can be found in Appendix A. The comparison for each type electrolyzer efficiencies are shown in Table 2:

Table 2 - Comparison of P2G technologies [27] [28]

	Alkaline electrolysis	Proton exchange membrane electrolysis	Solid oxide electrolysis
Efficiency	47% - 82%	48% - 65%	- 85%

2.9.2 Injection of Hydrogen in the Danish gas network

The problem with production of hydrogen is the final use of it due to the restrictions regarding materials in the pipelines. In order to provide the same energy as natural gas, the volume of hydrogen should be three times more, which limits the concentration of hydrogen in the gas pipelines [29]. According to [30], the concentration of hydrogen in the gas pipelines must not be greater than 10%. This sets a limitation for how much pure hydrogen the Alkaline Electrolyzer can produce in the project. Another feasible solution to this could be to convert the pure hydrogen into methane by a chemical process and store it in the gas network [30]. Many electrolyzer plants are being built and installed in Europe for this purpose. In Denmark, P2G-BioCat project is currently being developed in Denmark with a purpose to provide energy storage to the Danish energy system. The project is owned by many companies and one of them is the Danish transmission operator, Energinet.dk. The size of the electrolyzer plant is 1 MW. In Germany, the P2G plant installed in Falkenhagen, with a size of 2 MW alkaline electrolyzer [31].

2.10 Heat pump

Heat pump is a device that can use a small amount of energy, normally by applying electricity to extract an amount of heat from a lower temperature level source named heat source. It transfers thermal energy to a higher temperature source called heat sink electricity [32]. Heat pump is a high-efficiency appliance, which can be used for water heating or expanding conventional heating systems in building. It can be classified into different types according to the heat source.

2.10.1 Coefficient of performance

The performance of a heat pump is determined by coefficient of performance (COP). It is a ratio of the total amount of energy generated to the total amount of energy expended. In the reality, the value of COP is determined by the type of heat pump and operating conditions of the environment. Normally, the COP of a commercial heat pump product is around 4, which means the thermal energy released by the heat pump is four times of electrical input [32]. Hence, heat pump is not only more effective compared with other traditional heating appliances but also provides a sustainable and environmentally friendly heating solution.

Nowadays, many companies such as Danfoss, Dakin, Atlantic, have developed their own technology and launch their products into the market. A simple comparison of the different type of heat pumps, is shown in Table 3.

Table 3 - Comparison of HP technologies [33]

	Danfoss	Dakin	Atlantic
Model	DHP-A Opti 6	ERLQ008CV3	ALFÉA EXTENSA+ 5
COP	3.94	4.45	4.52
Input power	1.71kw	1.66kw	0.996kw
Heating capacity	6.18kw	7.40kw	4.5kw

2.10.2 Heat pumps in the Danish households

Heat pumps are very attractive in a smart energy system. First, the efficiency is very high. Second, less fossil fuel will be used if the HPs are implemented in the Danish households. HPs are very flexible due to the storage tank. As mentioned, there are many types of HPs and they can be used for many tasks. The most common type of HP is air-air source in Denmark.

A feasible solution to operate heat pumps would be to stop consumption of power when the electricity has high price and start consuming when the electricity has lowered its price. Although, during the winter period the HP will be running most of the time due to the low temperature outside, which will make the HP less effective. In this case, ground source heat pumps can be used as the ground is warmer than the air. Therefore, ground HPs might be better suited for flexible uses during the winter period. However, it is costlier to install the ground HP than the air source HP. Intelligent control of these HPs can earn savings for the end-user as well as reduce the peak consumption in the power system. According to Energinet.dk, a large scale integration of HPs will support the future energy system and will be a good economic investment [34]. However, many papers state that implementing large scale HPs in the distribution networks will result in high start-up currents. It might even lead to flicker issues in the grid due to its ON-OFF operation [35] [36].

2.11 Electrical vehicles

As mentioned previously, the EV technology has ability for both consuming power and deliver power to the grid. EVs have a converter inside the car which is connected to the battery. This converter can be intelligently controlled in order to change direction of the power flow between the grid and the EV. In the following subsections, different technologies for EVs are presented.

2.11.1 EV battery technologies

Regarding EV batteries, multiple factors have to be considered such as high power (up to a hundred kW), high-energy capacity (up to tens of kWh), weight and space limitation, and affordable price. The main battery technologies used in EVs are nickel metal hydride (NiMH) and lithium ion (Li-ion) [37]. However, due to the advantage of higher energy density, the Li-ion has tremendous development potential and it is expected that Li-ion battery can gain more market share in the future. An explanation of these technologies can be found in Appendix B.

2.11.2 EVs in Danish garages

Nowadays, road transport sector has become one of the most essential parts in global trade. The road transportation has vital contribution to global greenhouse gas emissions and climate change. According to [38], 17-18% of global CO₂ emissions of fossil fuels are coming from automobiles. It is expected that the worldwide number of cars will be tripled by 2050 especially in developing and transitional countries. In order to reduce the impact of environment, a new technology called Electric Vehicles has emerged in recent year and brings a new revolution for changing the development automobile industry in the world.

The driving/charging patterns of EVs have a big role when investigating demand side response. Many driving patterns have been investigated until now and some of them are found in [25] [39] [40].

Integration of EVs into the grid is typically referred as Vehicle-to-Grid (V2G). Like the other flexible loads, V2G concept can be used to support the grid in order to reach a stable frequency in the power system when there is over frequency periods during excess of wind power generation or deliver power to the grid during low frequency periods when there is a lack of power generation in the grid. The end-users which are the EV owners, are expected to make agreements with the aggregators in order to intelligently control the EVs. The aggregators will hereby sell their control flexibility on a larger scale to the TSO in order to provide up- and down regulation. The aggregators and BRPs are expected to make an agreement on the amount of power that can be regulated. This means that the State of Charge (SOC) for an EV should be below 100% in order to provide flexibility. If the EV is 100% charged, it cannot be used to provide flexible consumption. Therefore, a limit for the SOC is needed. According to [41], the SOC should be at least 85 % before the control of the EVs can begin. The lower limit is set accordingly to not have negative impacts on the driving distance of the EV owner. The end-user should still be able to plug the EV out from the charger and drive to his/her destination without any problem. The upper limit is set considering that the life time of the battery decreases by fully charging and discharging close to 100 % SOC.

2.12 Technical requirements for frequency control

In this section, the technical requirements for frequency control will be introduced. This section explains the theory behind frequency fluctuation in the grid followed by theory behind primary and secondary control.

2.12.1 Swing equation

An important parameter in a power system is frequency. It is necessary to keep the frequency within the allowable range in order to maintain a stable power system.

$$\frac{2H}{f_0} \frac{df}{dt} = P_m - P_e = \Delta P_s \quad (2.1)$$

Eq. (2.1) shows the swing equation of the equivalent system generator, where

- H is the inertia time constant
- f_0 is the nominal power system frequency
- P_m is the mechanical power
- P_e is the electromagnetic power

The value for ΔP_s represents the total active power imbalance. Eq. (2.1) shows that any active power imbalance (increase/decrease of load or generation) will cause a change in the grid frequency. Therefore, a governor controller will be needed to regulate for the speed (grid frequency) of the machine [42]. The proof of swing equation is available in Appendix C.

2.12.2 Grid frequency response during disturbances

As mentioned, sudden changes in wind power production might result in changes of grid frequency. Stability of the frequency indicates the balance between generation and consumption. Several reserves are activated in the power system if the frequency deviates from the allowed range in order to restore it back within the allowed ranges. In this study case, only single-area system is taken into consideration because a single area power system has been chosen in this study case, which will be explained in Chapter 3. Therefore, modes of operation of frequency control are divided into different responses:

- Inertial response (Inertia from rotating machine)
- Primary response (Droop control)
- Secondary response (Load Frequency Control)
- Tertiary response (controlled manually)

According to [43], large-scale penetration of wind power causes a decrease of inertia in the power system. This decrease has an impact in the power system. The increase of WPPs results in a reduction of conventional plants with high inertia in the power system [44]. This will result in a more fluctuation of grid frequency because the rate of change of the frequency depends on the total inertia in the grid. A higher amount of inertia in the power system, means that the frequency deviation from the nominal value will be less and also the controllers will act faster to restore the grid frequency [45]. However, the focus of this study case is based on primary and secondary response, where inertial and tertiary response will be neglected.

2.12.3 Primary frequency response

The primary controllers of all generating units will be activated within a time frame of 0 – 30 seconds in a power system. The purpose is to avoid frequency fluctuation and bring it back within the allowed limits. This is achieved with primary reserves in a power system. The frequency is brought back to a steady state level f_{ss} by the primary frequency controller. However, the restored frequency has a steady state error, which deviates from the reference frequency f_0 that is $\Delta f_{ss} = f_0 - f_{ss}$ [42]. The primary frequency controller uses droop control, which only reduces the deviation in frequency but is not able to bring it back within limits. To solve this problem, a secondary controller is needed. The response of the primary frequency controller depends on the frequency response characteristics of the power system, which is denoted by β . The grid frequency change after an imbalance of ΔP is given by (2.2) [46]

$$\Delta f_{ss} = -\frac{\Delta P}{\beta} \quad (2.2)$$

The frequency response characteristic β has a unit of MW/Hz. It is a constant which expresses how much the grid frequency will change for a given generation or consumption from the power system. The frequency response characteristic β is given by (2.3) [46]

$$\beta = \frac{P_{nom_{total}}}{f_0 * R_{total}} \quad (2.3)$$

, where P_{nom} is the total generation capacity, f_0 is the grid frequency and R droop of the generation unit. If the generation units share the same droop setting in the system, the total droop R will be equal to the one single droop setting.

2.12.4 Governor droop settings

The droop denoted as R in this case is the relation between the power, which can be produced by the generator and the grid frequency. The unit of the R is % and defines the power change required for a governor in order to change the frequency. According to [47], coal fired steam power plants have a R value of 4 % which means that 4 % of a frequency deviation results in a power change of 100 % [46]. Figure 2.4 shows a steady state droop characteristic. The generating units in a power system changes their power output back and forth according to this figure in order to ensure a stable frequency in the grid.

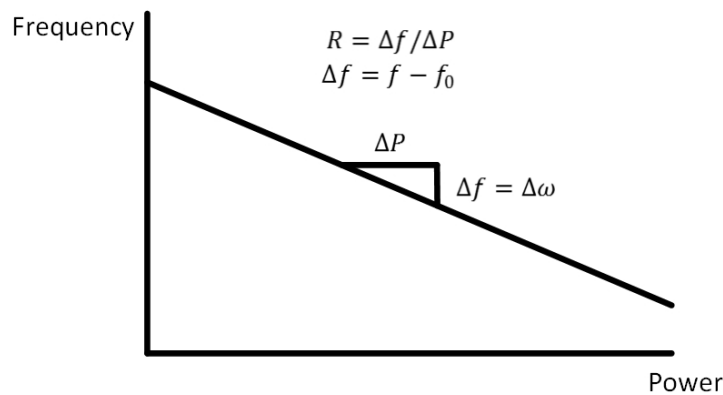


Figure 2.4 – Droop [46]

The change in power generation ΔP depends on the droop settings from the set point based on the frequency deviation from 50 Hz.

2.12.5 Secondary frequency response – Single area system

Secondary frequency control is provided by the secondary reserves within a time frame of 30 seconds to 15 minutes in a power system. The secondary frequency controller is activated in order to eliminate the steady state error Δf_{ss} by regulating the power set points of the generators in order to bring the grid frequency to its nominal level 50 Hz. This control method is called Load Frequency Control (LFC). As it is mentioned in section 2.7, secondary controller is much slower than the primary controller and continuously responds to the power imbalance. The LFC reduces the power imbalance using the control error P_{error} as input signal, which is given in (2.4)

$$P_{error} = -\Delta f * B \quad (2.4)$$

, where B is the frequency control error. The bias B is not the same thing as frequency response characteristic β , even though both are in MW/Hz. Since β is a characteristic for frequency and power mismatch for the primary controller, the frequency error B approximates β , and is also a value for mismatch between frequency and power for the secondary controller [42]. The desired behavior of LFC can be obtained by introducing an PI controller to act on the power reference setting in order to change the speed reference. The system type will be increased by one, which results in a frequency deviation of zero [42]. The PI controller is shown in (2.5)

$$K_P + \frac{K_I}{s} \quad (2.5)$$

The parameters K_P and K_I are needed for the secondary controller to bring the grid frequency to its set point.

2.13 Summary

According to the introduced growing wind power penetration in Denmark, several challenges will appear in the power system. Therefore, Smart Grid comes into minds as a solution to these challenges. These challenges can be dealt with intelligent control of flexible loads by proving primary and secondary reserves in the power system. It is seen that both the end-user and the power system owner will benefit by controlling the flexible loads.

Regarding the technology behind P2G, the Alkaline Electrolyzer is well known as a mature technology and it is available in the market. It has a lifetime of 15 years and the efficiency can be brought up to 82 % depending on the usage. Therefore, AE is chosen to be included in this project.

In the future, the end-user is expected to install an average sized HP. According to the presented HP technologies, Danfoss HP has an average capacity among all three technologies. Therefore, the Danfoss HP is chosen to be included in this project. Regarding the EVs, pure EVs will be considered in this study case. It is assumed that no end-user wants their EV to be 100 % charged in this study case. Therefore, the EVs will be controlled with a margin of $70\% \pm 20\%$. The control of the EVs will be on stand-by mode, if the SOC exceeds this range.

The flexible loads can hereby be integrated with the so-called Load Frequency Control strategy in order to perform frequency regulation. The next chapter will introduce the modelling of the LFC controller integrated with flexible loads.

3 Load Frequency Control

Increasing wind power affects the power system operation, especially the active power balancing control. The fluctuation of wind and the technical limitations of the generators in the power system makes it difficult to achieve a proper active power balancing control. Therefore, power system studies should be carried out in order to investigate the frequency stability.

According to [48], more than 50% of the power demand in the Western Danish Power system is supplied by wind turbines and decentralized CHPs. The decentralized CHPs mostly produce heat to the consumers. The wind turbines produce power whenever the wind is blowing. The unpredictability of the wind power generation results in a difficult task to match the consumption in the power system. In order to maintain the power balance in the power system, the CHPs and DCHPs could be grouped into an aggregated and controlled as a single unit. Here, the flexible loads has very high potential, because they can act as an aggregated storage as a solution to the power balancing challenges in the power system.

This case study deals with an integrated energy system, which incorporates electricity, gas, heat and transport systems. The aggregated models are directly connected to the power balancing control and therefore the effects for elements such as transformers, lines or converters are not investigated.

This chapter models the 9-bus network and an LFC system with large-scale wind power integration for controlling the flexible loads and CHPs in the power system and contributes with presentation of the 9-bus network and LFC system with regard to power balancing control. First, the case study with the 9-bus network is explained and discussed. Then, the LFC system is explained with the control principles. Finally, the winter and summer profiles used in the study case is presented.

3.1 Case study description

The simulations are performed in a wind dominated 9-bus network. The 9-bus network is considered operating in a single power system in order to evaluate the flexibility of the flexible loads and CHPs in regulating the grid frequency in a single control area. As it is shown in Figure 3.1, wind farms and CHP plants are the main power supply of the transmission system in Denmark. Therefore, the 9-bus network will be modelled based on the Danish power system case. The Alkaline Electrolyzer is connected to the Medium Voltage (MV) level where the HP and EV are connected to the Low Voltage System (LV) in real life. Although, in this study case, only aggregated models and their flexibility are investigated. Therefore, all the models will be directly connected to the transmission level as lumped models.

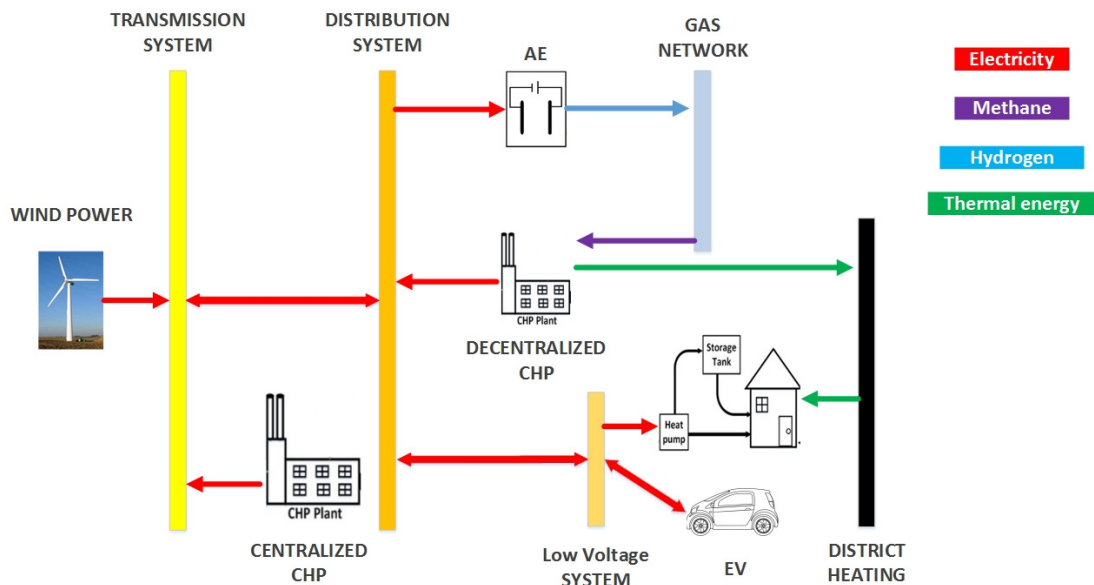


Figure 3.1 - Integrated system

It is worth to mention that the 9-bus network is modified according to requirements of the project. The power generating units in the 9-bus network includes lumped models of CHPs, DCHPs and Wind Farms. The loads in the 9-bus network includes the base loads and flexible loads. For CHPs and DCHPs, the primary control is included in the model. The total network is expected to be used to evaluate the need of LFC with flexible loads during winter and summer cases. The interesting topic in this study case is the impact of large-scale wind power integration in the power system and secondary control of flexible loads and CHPs to reduce the power imbalances caused by wind farms.

The power imbalances in the network can be defined as given in (3.1)

$$P_{dev} = P_{Wind} + (P_{CHP} - P_{BaseLoad}) \quad (3.1)$$

, where P_{dev} is the deviation of power in the system, P_{Wind} is the power generated by the wind farm model, P_{CHP} is sum of the power generated by CHP models and $P_{BaseLoad}$ is the power consumption of the base loads. The simulation concept can be seen in Figure 3.2.

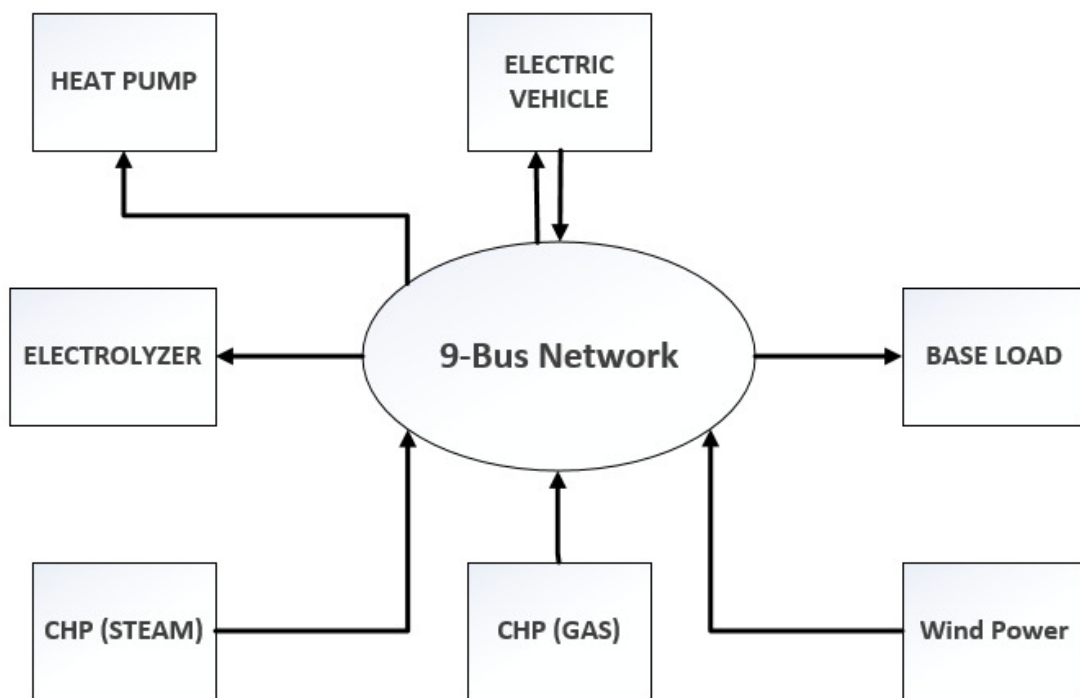


Figure 3.2 - 9-bus network simulation concept

The detailed overview of the 9-bus network is shown in Figure 3.3, where the power system is islanded by two lumped CHPs and a lumped wind farm. The generation units are connected to a transmission level of 230kV with step-up transformers. The CHPs are based on steam (G1) and gas (G3) turbine units. The installed capacities are of the CHPs are 287.5 MW (G1) and 212.5 MW (G3) respectively. A wind farm model is connected at busbar 2 (B2) with the capacity of 250MW.

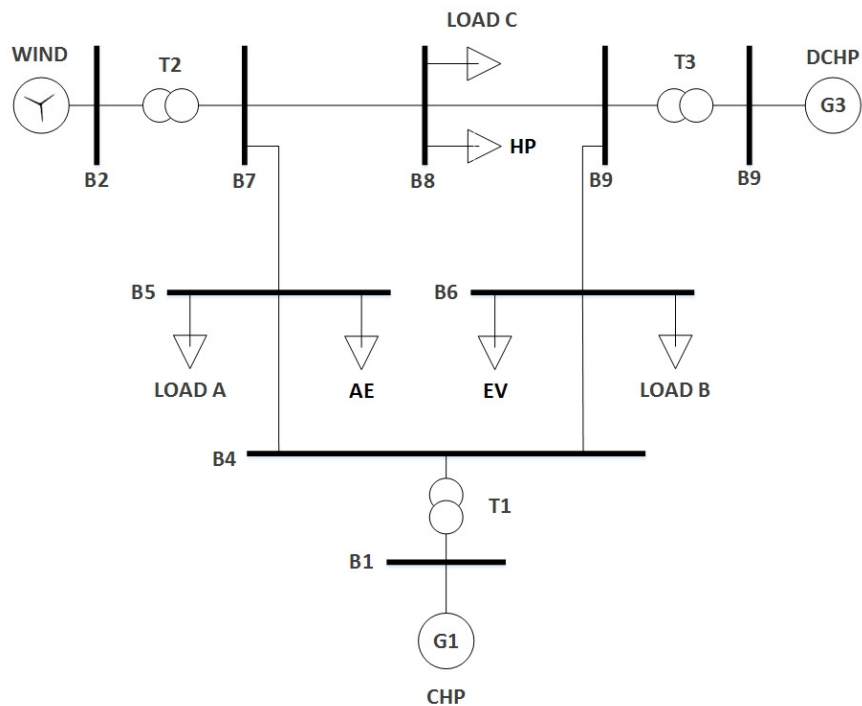


Figure 3.3 – Single line diagram of the modified 9-bus network (Test grid)

The wind turbine model is assumed to operate at a unity power factor since the frequency is only dependent on active power imbalances. Since it is a single area power system, the flexible loads are distributed along the network, where the AEs are placed at B5, the HPs are placed at B8 and the EVs at B6. The parameters of this grid can be found in Appendix D for further detail.

3.2 Integration of flexible loads in LFC

The large-scale wind power penetration will increase the power regulation need in the power system, when additionally offshore wind farms are commissioned. This topic requires a solution. Therefore, the proposed LFC strategy with flexible loads is presented. The main objective of LFC is to balance the power generation and consumption in the power system, which will result in a stable frequency within the required ranges. An imbalance in the power generation and consumption in the power system will result in a frequency change. The LFC is an ancillary service, which helps to balance generation and consumption in a power system. The LFC performs an intelligent and automatic control, which is achieved by generation or load changes in a power system by sending a control signal directly to the participating units in order to provide regulation. The TSO sends a real time signal to the units whenever there is a need for ancillary services in the grid [49].

The system frequency will increase above 50 Hz, if the power generation is higher than the load demand and decrease under 50 Hz, if the power generation is lower than the load demand. The major understanding of frequency stability is to keep it at 50 Hz at every instant. The synchronous generators in the power system, which is equipped speed governors, provide frequency support by releasing primary control if the frequency deviates from its nominal value, which is 50 Hz beyond a dead band of 10 mHz. The response of primary control depends on the frequency characteristic β of the power system, which is explained in Chapter 2. The primary controller will be change the power set point by ΔP to the turbine in order to reduce the power imbalance, if the frequency deviates from the nominal value, as given in (3.2)

$$\Delta P = -\beta * \Delta f \quad (3.2)$$

, where β is frequency response characteristics of the power system which is a sum of all the primary responses in the power system. Primary control is performed by speed governors of the CHPs and activated when the frequency deviates from the nominal value which results in a change of the power set point of the turbine. The primary controller brings the frequency to a new value with a steady state error. The secondary controller is then required to restore the frequency to its nominal value and this is generally done by LFC. The main idea with the LFC strategy is to manage the response of the available flexible loads by performing up and down regulation in order to minimize the imbalances. The proposed LFC strategy, which is implemented in this study case, is sketched in Figure 3.4.

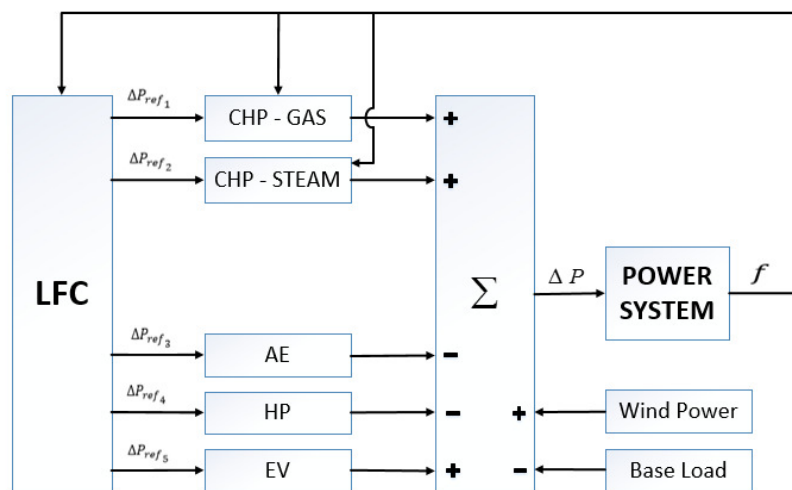


Figure 3.4 - LFC strategy with flexible loads

The LFC block is shown in details in Figure 3.5. As an input signal, the speed of the machine is used, where the speed error is calculated by subtracting it from the nominal speed. Since the error in the generator speed equals the error measured in the grid frequency, the generator speed is directly feedback from the output of the CHPs as it is shown in Figure 3.6.

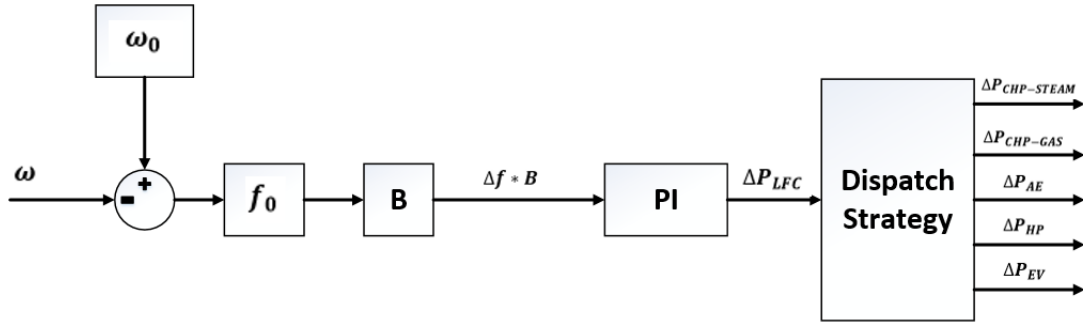


Figure 3.5 - LFC controller

The frequency control error $\Delta f * B$ is calculated by multiplying the frequency error and the frequency bias factor **B**. The LFC deals with any imbalance in the signal ΔP_{LFC} , which is a measure of power deviation in the system. The power-frequency characteristic of the generating units is dynamic because it depends on a droop characteristic and generation capacity. In this study case, the frequency bias factor **B** [46] is calculated as given in (3.3)

$$B = \beta_{CHP-STEAM} + \beta_{CHP-GAS} \quad (3.3)$$

The ideal function of LFC is to maintain balance in the power system by keeping the frequency error and power error at zero. Although, this is not the case in real life due to the delays between the power system units and the output power limitations of the generation units. The LFC dispatches the power error to the different units in the power system, which are participating in secondary control. Therefore, the gains of the PI controller affects the performance of the participating units in the secondary control. The dynamic of the CHPs and flexible loads differ. This is due to their constraints with regard to responses and delays. The CHP plants response in couple of minutes where the flexible loads such as HPs, in couple of seconds.

It is decided that the most suited PI response will be a smooth control with an overdamped characteristic with no overshoot. The behavior of the controller will be obtained by following relation given in (3.4)

$$\Delta P_{secondary} = K * P_{ACE} + \frac{K}{T} \int P_{ACE} dt \quad (3.4)$$

, where $\Delta P_{secondary}$ is the set point for the units, which are providing LFC response. The value K is the proportional gain and T is the integration time constant of the LFC controller, where P_{ACE} is the imbalance in the power system. It is a difficult task to properly match the generation and consumption in a real system, although appreciate values are needed for the PI controller. The PI values are obtained from [50]. According to the UCTE guidelines, the typical values for the controller gain is 0 – 0.5 and the time constant within 50-200 seconds. A higher time constant will give a more smooth secondary control operation, but also slow down the operation respectively. The chosen PI value for the LFC controller is provided in Appendix E.

3.3 Centralized combined heat and power plant

According to [51], the most common type of centralized CHPs in Denmark is the coal-fired steam plants. The centralized CHPs are required to produce power at minimum 20% of their rated power output. However, in this study case a minimum production of 10 % has been chosen. The CHP must have a ramping rate of the full load per minute at different operating stages. In study case, a ramping rate of 4%/minute has been chosen [51]. It is assumed that all the centralized CHPs are based on a steam turbine technology. The aggregated CHP model might affect the system due to the slow response. This subsection introduces the aggregated centralized CHP model.

3.3.1 Aggregated steam turbine model

For this study case, it is desired to analyze at the dynamic characteristic of the CHPs that can affect the LFC operation in the power system during frequency fluctuations. Therefore, the modelling of the CHPs is based on this. The diagram of the generic CHP model is shown in Figure 3.6. The model is used considering primary and secondary control capabilities along the dynamic limitations. The performance of the CHP depends mostly on the type of plant, which is used, controller dynamics and the steam turbine power ramp rate. However, in this study case, the steam turbine is a built-in model named IEEEG1 in DIgSILENT with modifications. Although, there is an automatic voltage controller (AVR) connected to the generator. The AVR model, which is chosen in this study case, is IEEE1.

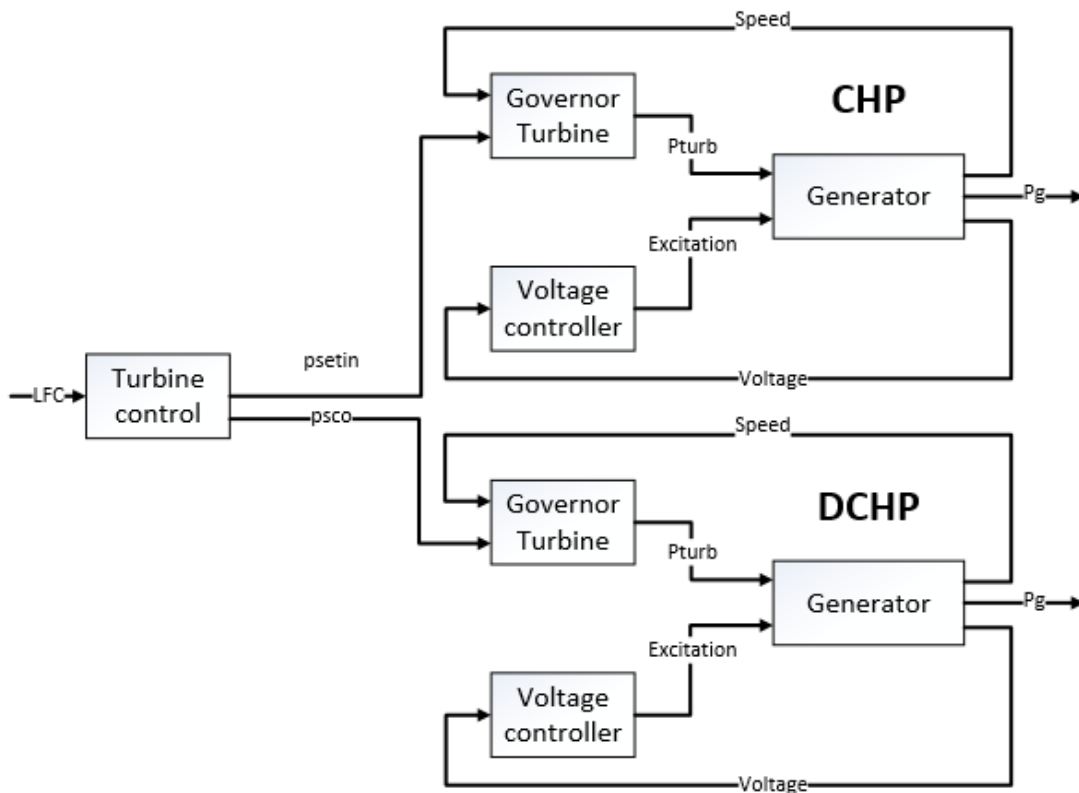


Figure 3.6 - Aggregated steam turbine and gas turbine model for LFC

I. Turbine control

The turbine control block, shown in Figure 3.7, controls the power set point sent to the steam turbine. In DigSILENT, turbine control block is built together with the participation block in order to simplify the modelling. The output of the turbine is limited due to thermal and mechanical constraints [51]. The turbine control is both used for centralized and decentralized CHP models.

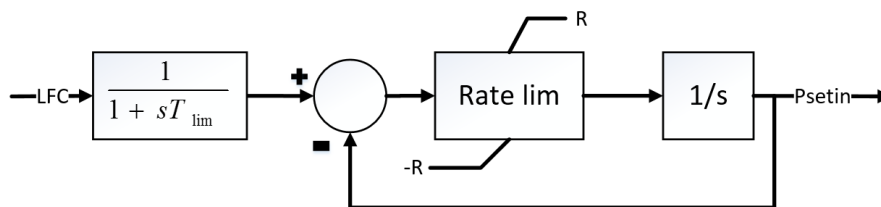


Figure 3.7 - Turbine control

The LFC signal is delayed by few seconds as an estimation of a realistic time delay in real life. If these constraints were not added, it would result in an unrealistic action of the steam turbine. The parameters of the turbine control model is provided in Appendix E.

II. Speed governor

The speed governor model can be seen in Figure 3.8. The speed governor of the steam turbine unit ensures to provide primary response when the frequency deviates from nominal value. The frequency deviation is measured as a change in the generator speed. Any speed deviation of the generators is converted to a power deviation and sent to the power set point of the turbine through the droop.

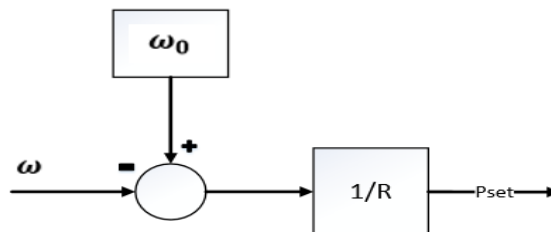


Figure 3.8 - Speed governor for steam turbine and gas turbine

The governor control is both used for centralized and decentralized CHPs. The parameters of the speed governor model is provided in Appendix E.

III. Steam turbine

The purpose of the steam turbine is to convert the energy in the high-pressure steam into mechanical energy. In real life, the steam turbine consists of blades connected to the rotor of the generator. The high-pressured steam creates a torque on the shaft and moves the blades. The amount of steam flow is controlled by the governor, which regulates the valves to the turbine. The delays through this process are accounted in the DigSILENT model for a steam turbine, which is shown in Figure 3.9.

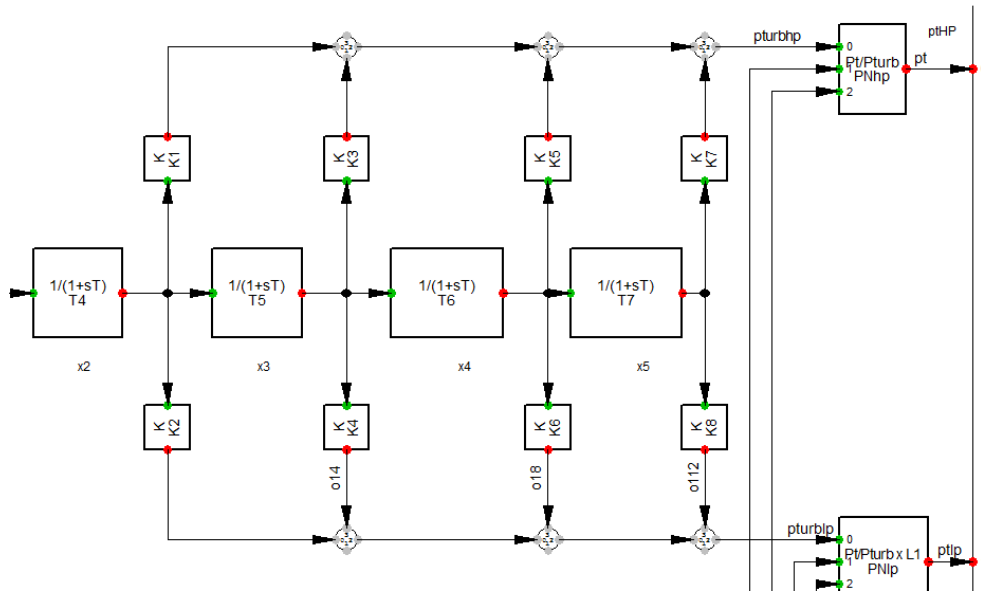


Figure 3.9 - Steam turbine model IEEEG1

As it is shown in Figure 3.9, the response of the steam turbine depends on the time constants, which are used in the model. The parameters of the steam turbine model is provided in Appendix F.

3.4 Decentralized combined heat and power plant

According to [52], the most common type of decentralized CHPs in Denmark is the gas turbine based power plants. The decentralized CHP must also have a ramping rate of the full load per minute. In study case, a ramping rate of 10 %/minute has been chosen [51]. It is assumed that all the decentralized CHPs are based on the GAS turbine technology. This subsection introduces the aggregated decentralized CHP model.

3.4.1 Aggregated gas turbine model

The diagram of the generic DCHP model is shown in Figure 3.6. The model is used considering primary and secondary control capabilities along the dynamic limitations. In this study case, the gas turbine is a built-in model named IEEEGAST in DIgSILENT with modifications. Again, there is also an automatic voltage controller (AVR) connected to the gas turbine generator. The AVR model that is chosen in this study case is IEEE1.

The detailed turbine block is shown in Figure 3.10 and consists of a simple frequency and temperature loop [52]. The gas turbine has a droop R/proportional gain to perform frequency regulation, where P_{ref} is the power reference. The temperature of the turbine is assumed to be constant during simulations [53].

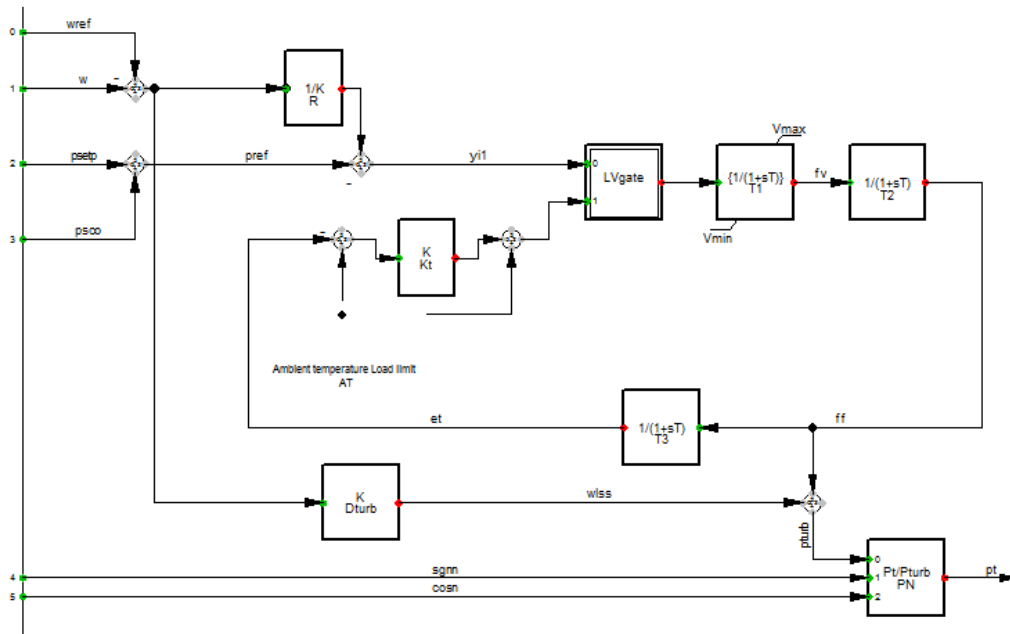


Figure 3.10 - Detailed Gas Turbine model IEEE GAST

The parameters of the gas turbine model is provided in Appendix G.

3.5 Wind power generation

The type of selected wind turbine in this study case is a 6 MW Siemens Offshore Wind Turbine. The equation to calculate the active power output of Siemens Offshore Wind Turbine is given in (3.5)

$$P_{wind} = 0.5 \cdot \rho \cdot \pi \cdot R^2 \cdot v^3 \cdot C_p \quad (3.5)$$

, where ρ is the air density which is assumed to be 1.225 kg/m^3 . R is the radius of the rotor in meters and v is the wind speed in m/s. The efficiency coefficient C_p is assumed to be at Betz limit, which is 0.59 [54]. During high wind speed, the pitch angle will be increased in order to prevent overloading of the wind turbine.

The power generation of the wind turbine is obtained through a measurement file (*ElmFile) in DlgSILENT. The values for this power output is obtained through wind speed data, which is provided by the Department of Energy technology, Aalborg University. The data has been analysed in MATLAB and the active power is calculated as shown in Figure 3.11. The power output is multiplied with the selected number of wind turbines in order to obtain the total generation for the aggregated wind farm. The profile is prepared for both winter and summer scenarios. The units are in MW.

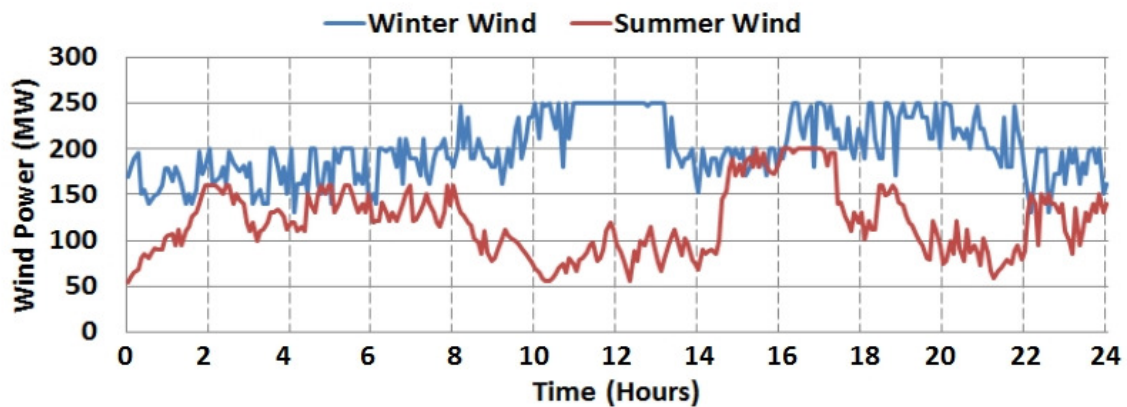


Figure 3.11 - Wind generation profile

3.6 Passive load

The base loads are the passive elements in the power system, which are not actively controlled. They will represent the total base consumption in the power system. The base consumption profiles for both winter and summer cases are shown in Figure 3.12. The consumption data is provided by [55]. The units are in MW.

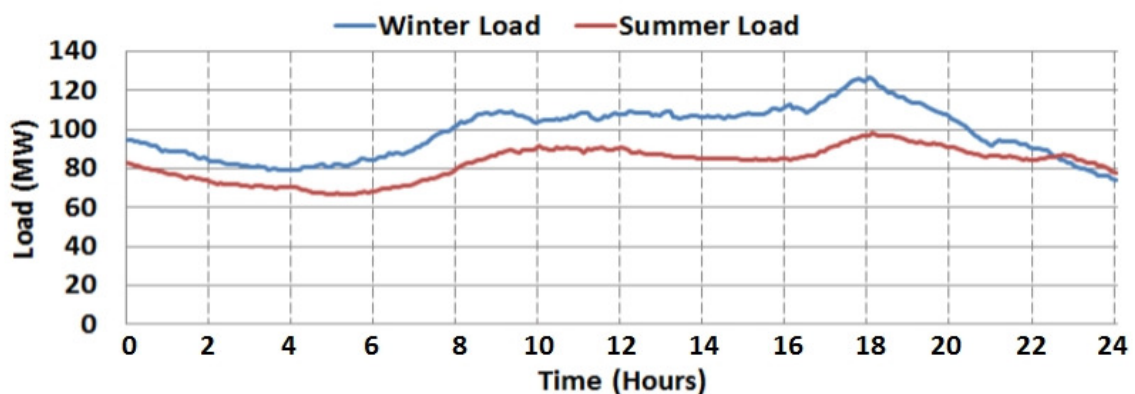


Figure 3.12 – Base consumption profile

3.7 Load model

In order to account for the voltage and frequency dependency of the loads in the power system, a simplified load model is introduced as shown in (3.6)

$$P = P_0(1 + k_{pf}\Delta f + k_{pv}\Delta V) \quad (3.6)$$

, where P is the resultant power and P_0 is the initial power. The gains k_{pf} and k_{pv} are frequency and voltage dependant coefficients. The values set to be 0.5 in this study case. Finally, Δf and ΔV are the frequency and voltage deviations [56].

3.8 Simulation results

Various test have been made in this subsection to observe the frequency behaviour of the 9-bus network, which are presented in the following section.

3.8.1 Primary response

In order to analyse the power system frequency response of the 9-bus network, a step increase of the load is simulated. It is expected that the frequency will drop below 50Hz, when the load increases. This demand of power from the load has to be met by the generators participating in the primary response. This scenario is with wind power supply of 62 % of the system load. CHPs and DCHPs are in droop mode. As initial operating conditions, the CHP is 19% loaded and generates 36.9 MW, where the DCHP is 34.11 % loaded and generates 85 MW. A step load of 18MW is applied at time, $t = 5$ sec on the system load B. The primary response is provided by the speed governor and depends on the droop characteristic of the generating unit. The 18MW load step will change the frequency of the power system depending characteristics of the CHPs as given in (3.7)

$$\beta_{9bus} = \beta_{CHP} + \beta_{DCHP} \quad (3.7)$$

, where

$$\beta_{9bus} = \frac{P_{CHP}}{R * f} + \frac{P_{DCHP}}{R * f} = \frac{287.5 \text{ MW}}{0.04 * 50 \text{ Hz}} + \frac{212.5 \text{ MW}}{0.1 * 50 \text{ Hz}} = 186.25 \frac{\text{MW}}{\text{Hz}} \quad (3.8)$$

The steady state frequency can be calculated as shown in (3.9)

$$f_{ss} = f_0 - \frac{\Delta P_{load}}{\beta_{9bus}} = 50 \text{ Hz} - \frac{18 \text{ MW}}{186.25 \frac{\text{MW}}{\text{Hz}}} = 49.904 \text{ Hz} \quad (3.9)$$

The speed governor will detect this change as a change in the generator speed and will start to release the primary reserves. The steady state primary response from the CHPs and DCHPs in the 9-bus network is calculated as given in (3.10) and (3.11)

$$\Delta P_{CHP} = \Delta f * \beta_{CHP} = (50\text{Hz} - 49,904\text{Hz}) * \frac{287.5 \text{ MW}}{0.04 * 50 \text{ Hz}} = 13,8\text{MW} \quad (3.10)$$

$$\Delta P_{DCHP} = \Delta f * \beta_{DCHP} = (50\text{Hz} - 49,904\text{Hz}) * \frac{212.5 \text{ MW}}{0.1 * 50 \text{ Hz}} = 4,08\text{MW} \quad (3.11)$$

The frequency response and the dynamic response of the CHP and DCHP to the load step change is shown in Figure 3.13 and Figure 3.14.

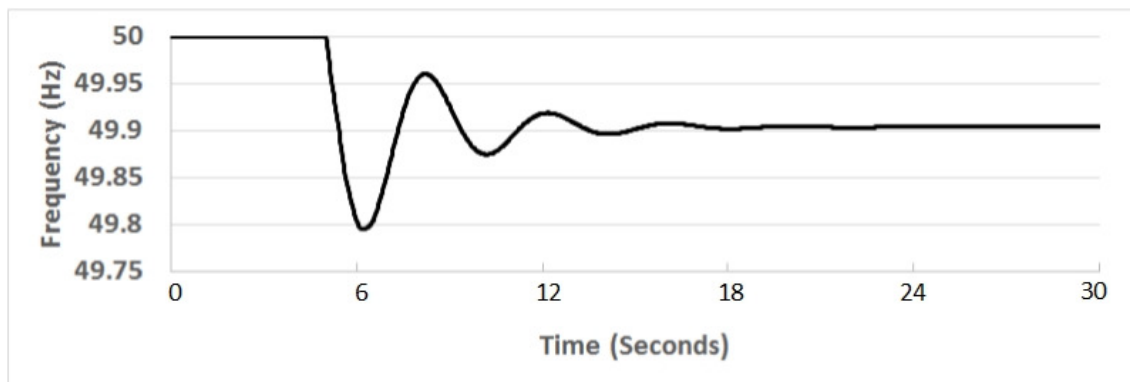


Figure 3.13 - Frequency response for step load increase

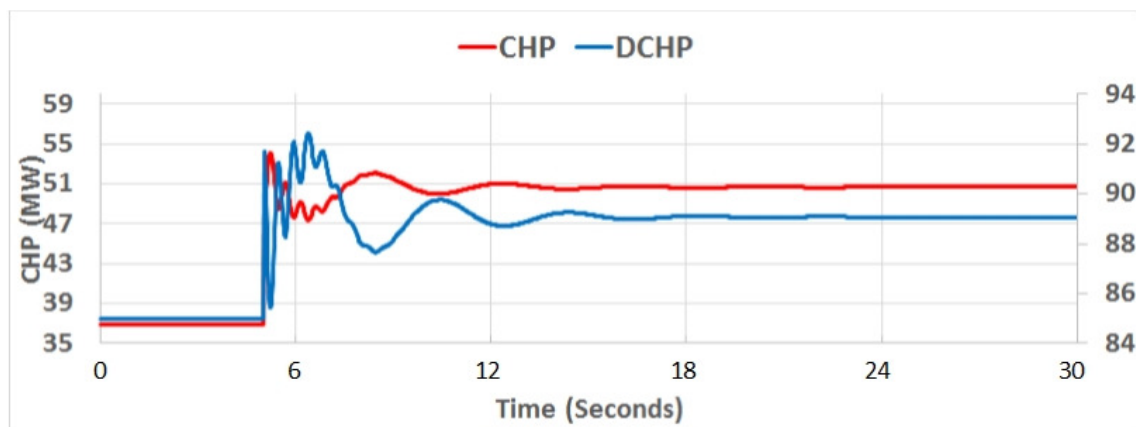


Figure 3.14 - Primary response of the CHP and DCHP

It is observed that the governor response is very fast to any frequency change in the system. It is also indicated that the calculations stated above matches the result of the load step change. Therefore, the behavior of the primary controller can be verified. It is seen that the frequency change is limited due to the droops of the generating units. Another fact that limits the frequency change is the total inertia of the power system. A power system with higher inertia will give a less frequency drop for a load change and vice versa.

3.8.2 Step reference power

The response of the CHPs and DCHPs has been tested for a positive step in the LFC signal. The step signal is stepped by 0.1 p.u after 50 seconds. The response will mainly depend on ramp rate limitations, which are added in the Steam turbine and Gas turbine models in DigSILENT. The LFC step signal is shown in Figure 3.15.

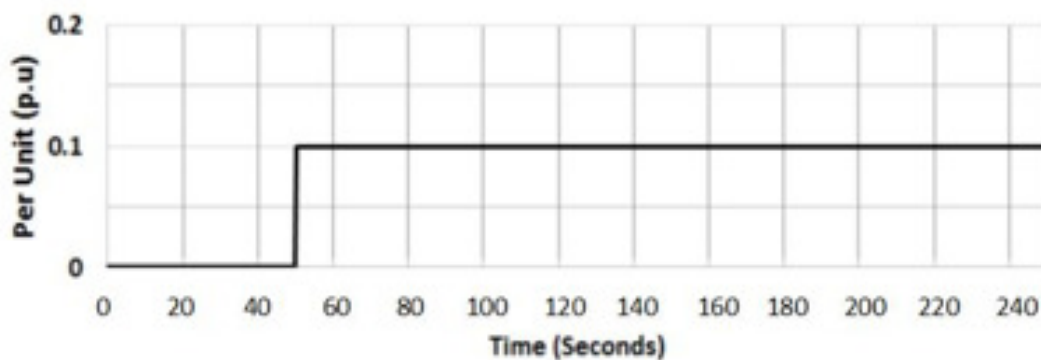


Figure 3.15 - LFC step signal

From Figure 3.16, it can be observed that the dynamic behavior of the CHP depends on the ramp rate limiter. The CHPs gets a step response of 0.1 p.u at $t = 50$, where it can be seen that the turbine power output increases from 0.128 p.u to 0.228 p.u within 150 seconds.

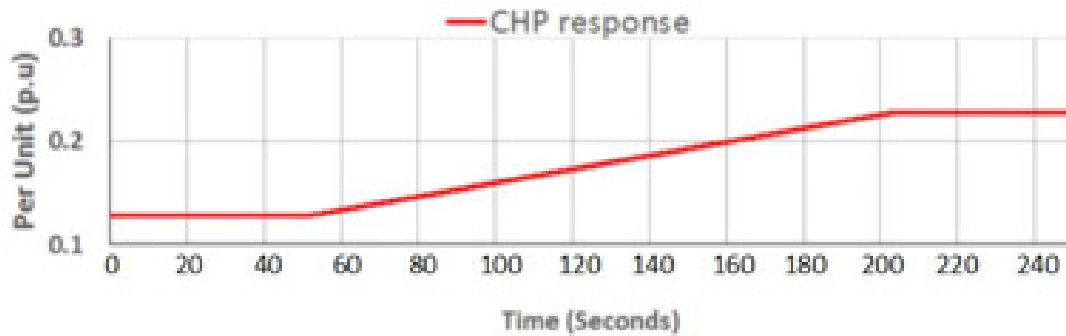


Figure 3.16 - CHP dynamic response to a LFC step signal

From Figure 3.17, it can be seen that the turbine output of the DCHPs increases from 0.4 p.u to 0.5 p.u within 63 seconds. The ramping time of the DCHPs are faster than the CHPs due to the ramping limits, which are 4%/min for the CHPs and 10%/min for the DCHPs.

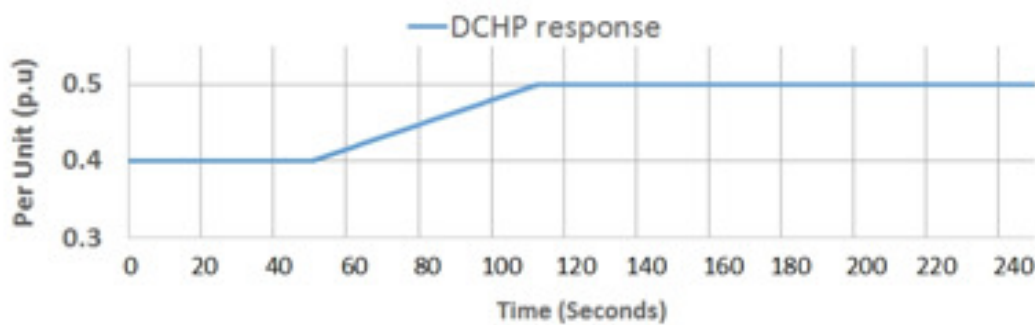


Figure 3.17 - DCHP dynamic response to a LFC step signal

3.8.3 Secondary response

The LFC controller introduced in this chapter provides secondary response to help the primary response in order to restore the frequency back to the nominal level. The LFC calculates the power using the Bias setting **B** of the LFC, which equals to the total power frequency of the power system β_{bus} . The PI in the LFC controller will provide the required secondary response to the power system. The secondary response has been tested with an 18 MW load step increase at system load B. The frequency response is shown in Figure 3.18. The regulation power from the LFC controller is shown in Figure 3.19.

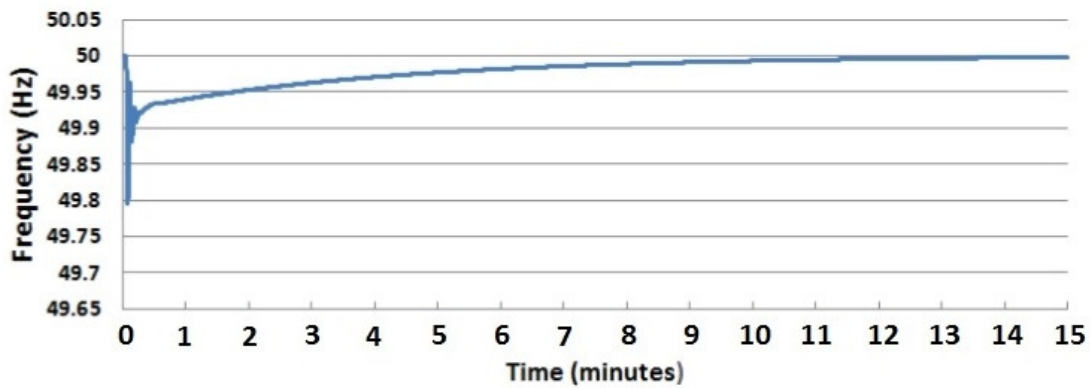


Figure 3.18 - Secondary frequency response in the 9-bus network

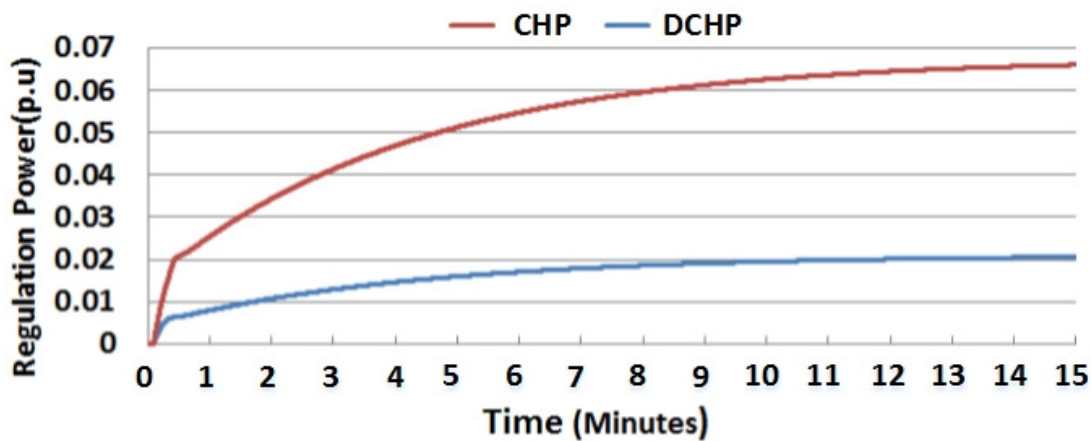


Figure 3.19 - Regulation Power

The primary response starts immediately and the reserve is activated, while the secondary reserve is provided within 14 mins to restore the power system frequency. The primary and secondary responses depends on the delays in the system, the introduced ramping rates of the CHPs and DCHPs and the total inertia of the generating units in the power system. The participation factor has been set as 0.75 for the CHPs and 0.25 for the DCHPs. The dispatch of the participation factor for the CHPs and DCHPs is explained in the following subsection.

3.8.4 Base Case

In this subsection, the 9-bus network is analyzed without the influence of flexible loads. The base case considers a single area power system, where the CHPs and DCHPs provide LFC control with fluctuations in wind power generation.

Winter scenario

The dynamic behavior is analyzed using the winter profiles of the base loads and wind farms. Figure 3.21 shows the obtained results from the wind power, CHPs, frequency situation of the grid during a winter day with high wind. Figure 3.20 shows the share of the wind power that supplies the load in the 9-bus network in percentage. It is observed that the highest point of share is 75 % and the lowest is approx. 40 %.

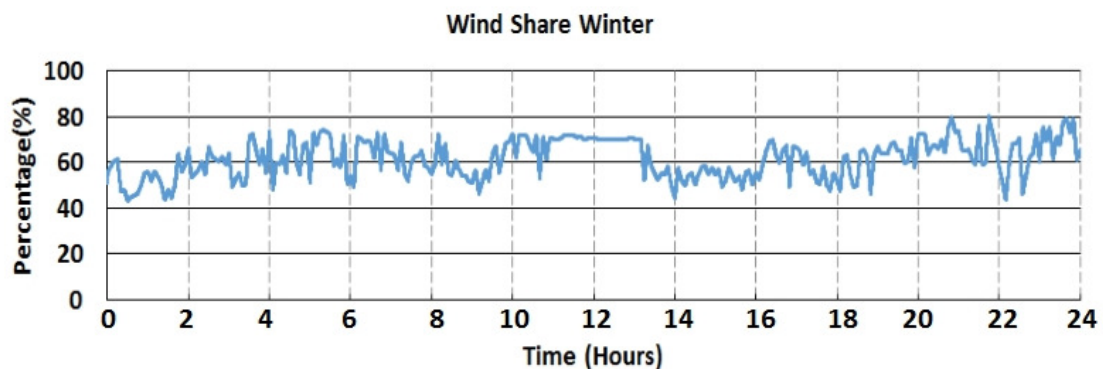


Figure 3.20 - Wind share of the winter scenario

Figure 3.21 shows the obtained results from the winter scenario. The wind power production of the aggregated wind farm is plotted in plot b). During the winter scenario, the wind power fluctuates 100 MW – 250 MW within 5-10 mins. This huge amount of fluctuation in the wind production creates frequency problems in the power system as observed in plot a), which shows the frequency of the 9-bus network. The LFC controlled power output of CHPs is shown in plot b). The centralized CHPs (CHP) has a participation factor of 75 % and the decentralized CHPs (DCHP) have a participation factor of 25 %. The reason behind a higher participation factor for the centralized CHPs is that they consist of larger power plants which quiet often produces reserves. The centralized CHPs have a bigger size to big and provide reserves in the market. The decentralized CHPs are smaller sized and they mostly cover the heat demand in the power system. Therefore, they might have a limited availability of reserve power in the market and power system operation for reserves. The set point of frequency is set as 50 Hz. The maximum frequency fluctuation is detected to be 50.5 Hz, where the minimum fluctuation is at 49.5 Hz.

It is seen that the CHP hit the lower limit, which is set as 10% of the rated power, when the wind power production is high and the total load is low. The wind power production is too high during certain hours that the CHPs, which is the main regulating unit, has no regulation possible as it is hitting its minimum generation limits. The non-regulation of the DCHPs is due to the facts that they have less participation factor compared to the CHPs. Furthermore, the CHPs and DCHPs have a ramping rate of 4%/min and 10%/min, which results in an extra power error in the system due to a slow response.

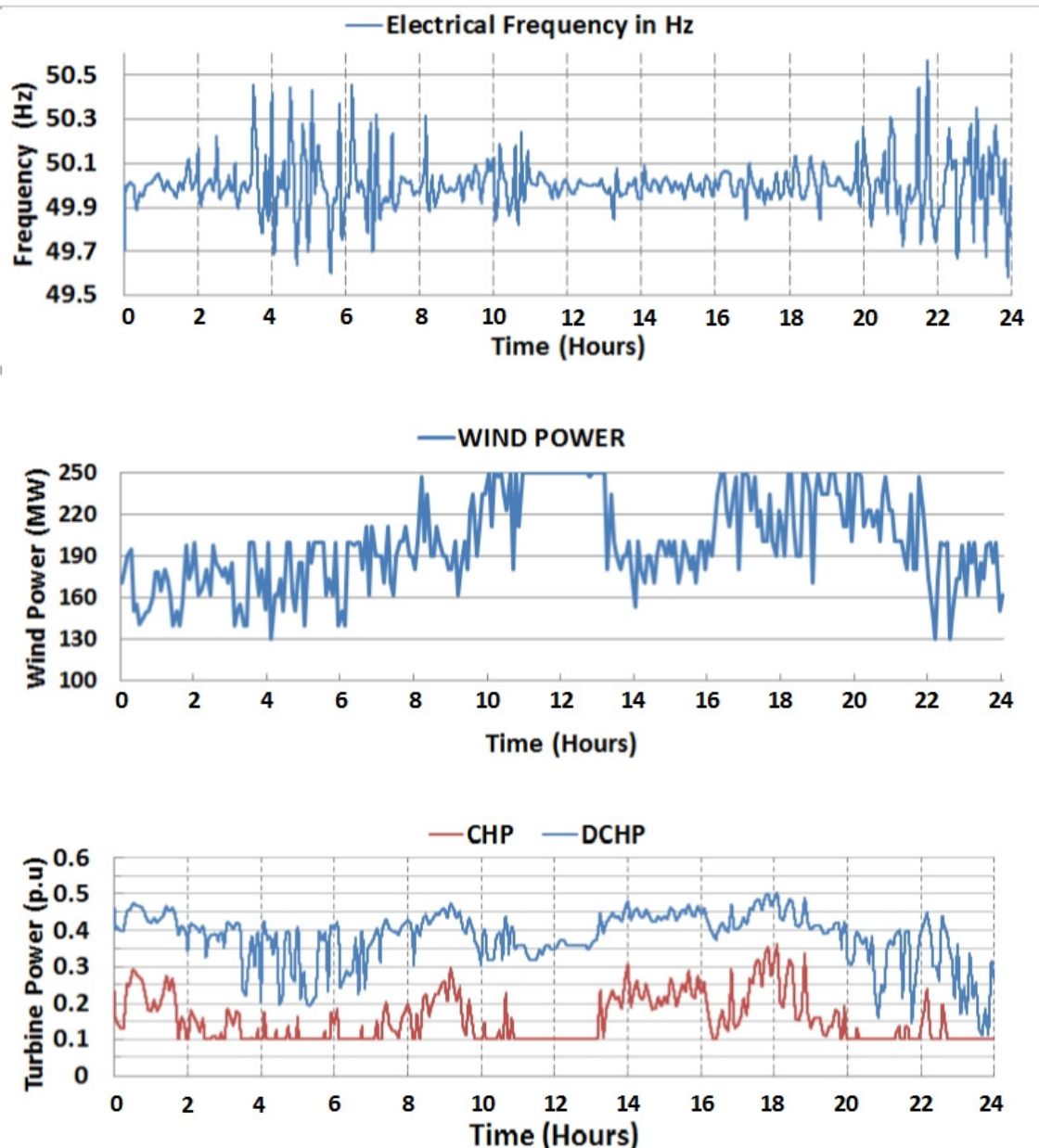


Figure 3.21 - Results during winter scenarios

Summer scenario

In this scenario, the 9-bus network is analyzed with summer profiles of aggregated wind farms and base loads. Figure 3.23 shows the obtained results from the summer scenario from the wind power, CHPs, frequency situation of the grid during a summer day. Figure 3.22 shows the share of wind power, which supplies the total loads in 9-bus network. It is observed that the highest point is 72 % and the lowest is 18 %.

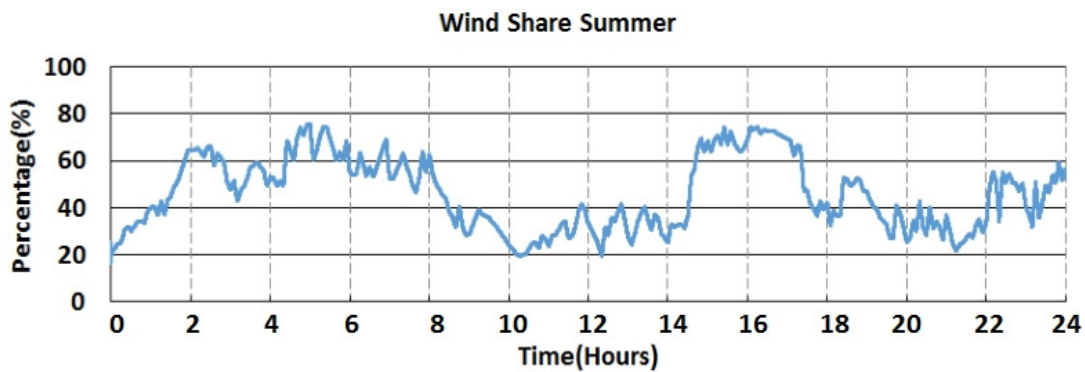


Figure 3.22 - Wind share of the summer scenario

Plot a) shows the frequency fluctuation in the 9-bus network during a sunny day. It is observed that the frequency fluctuation is less than the windy day due to a lower generation of wind power production. The maximum frequency is 50.4 Hz and the minimum is approx. 49.65 Hz.

Plot b) shows the wind power fluctuation in the 9-bus network during a sunny day. The output of the aggregated wind farm is fluctuation between 40MW – 160MW within 5-10 minutes. Therefore, the wind power production is slightly lower during the summer scenario compared to the winter scenario.

The participation factor for the CHPs and DCHPs is the same as in winter scenario. It can be seen that the power error in the system will keep growing unless the wind power production stays unchanged for a longer time. After several tests, it is observed that the power error in the power system will mostly depend on the chosen PI values implemented in the LFC controller and the chosen participation factor excluding the inertia of the power system.

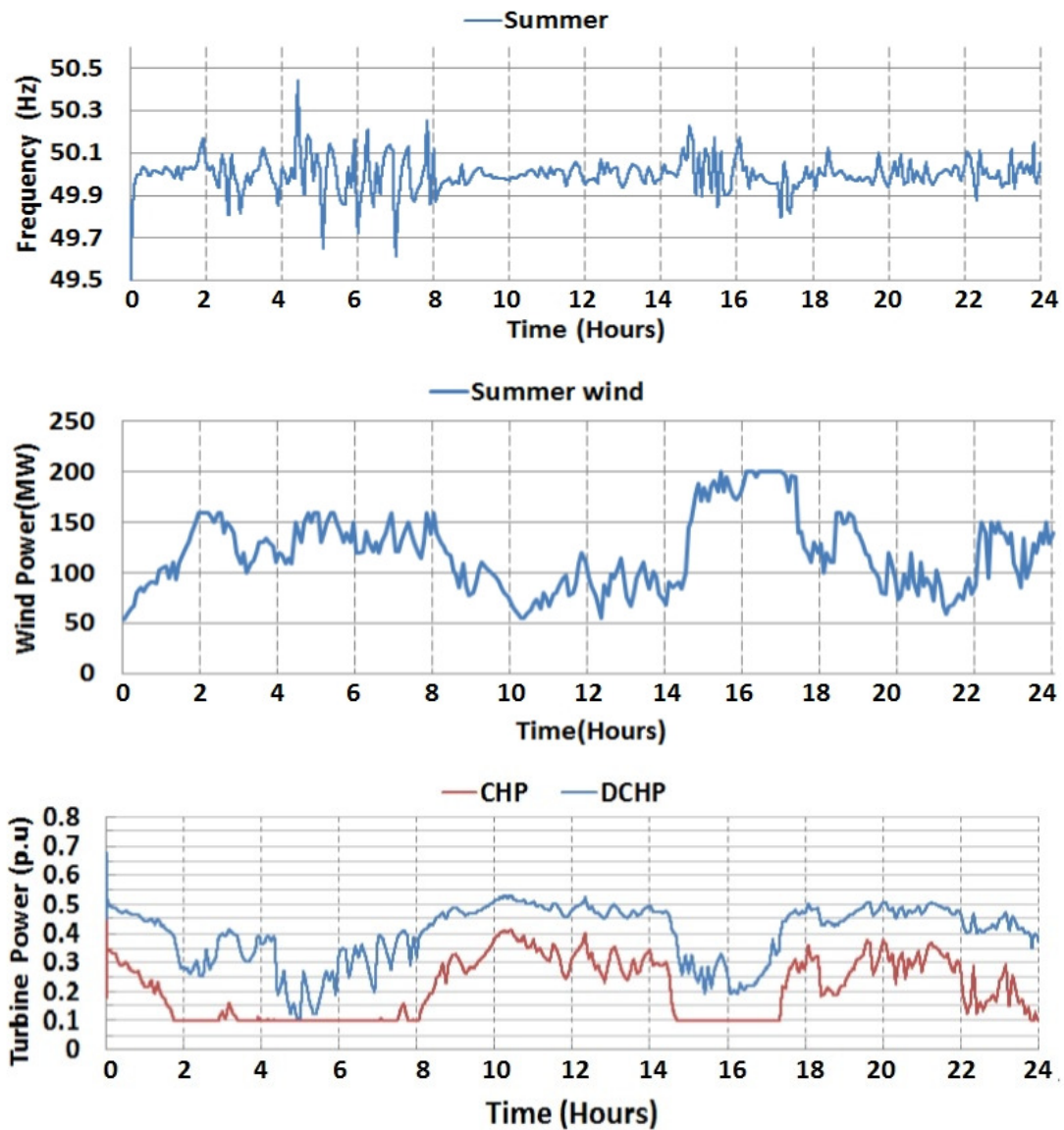


Figure 3.23 - Results during summer scenario

In both of the cases the regulation capability of CHPs are not sufficient to meet the high wind penetration in the system. This is a reality in the future when big power plant who are the main source of frequency reserves are decommissioned. Therefore, new and fast regulation reserves in the form of flexible units are required in the power system.

4 Dynamic modelling of Flexible Loads in DlgSILENT PowerFactory

In this section, the dynamic behaviour of the different flexible loads, which are participating in the frequency regulation, is modelled. The models will be tested and simulated in MATLAB/SIMULINK and hereafter implemented in DlgSILENT PowerFactory. There are three active controllable loads in this study case: Alkaline Electrolyzer, Heat pumps and Electrical Vehicles.

Table 4 shows the owners and control margins of the dynamic elements in this study case. As the HP and EV are owned by private owners, the TSO is only able to control them within a certain amount of range if there is any frequency imbalance in the system. However, their active power output depends on different criterias: Capacity, availability and demand. Nevertheless, the operation of the flexible loads might be constrained by their dynamic characteristics.

It is common for DSOs to own a part of the distribution network. This means that the owner of the electrolyzer farm can make benefit of the produced hydrogen, and provide frequency regulation to the power system at the same time.

The HPs and EVs are owned by private owners. This means that the HP and EVs might be desired to be fully controlled. The availability of HP and EVs will be dependent on the time of the day. The TSO will not be able to have 100% control because of the end-user convenience. Therefore, a control range is needed which can be seen in Table 4.

Table 4 - Owners and control availability of the different flexible loads in the grid

	AE	HP	EV
Owner	Private/DSO	Private	Private
TSO Control	Full	40% of Rated Power	50-90% SOC

The dynamic behaviour explained in this chapter will help the reader to understand the dynamic constraints of each model and hereby observe how these constraints will affect the frequency regulation during the interactions with CHPs, wind farm fluctuations and base consumptions in the grid.

4.1 Implementation of Alkaline Electrolyzer

In order to integrate the P2G technology in this case study, the modelling of the AE is needed. This subsection introduces the modelling of the AE. The model is based on [57] and [58]. First, the overall scenario for the AE will be presented and hereby the modelling of the AE module will be introduced. Finally, the test of the AE model will be presented.

The purpose of the AEs in this study case is to consume the excess of power caused by the wind fluctuation in the power system. It is expected that the electrolyzer farm will only be available for frequency regulation and the TSO will be able to fully control all the AE units whenever it is needed. Depending on the frequency in the grid, the AE model will change the consumption. If the frequency is higher than the nominal value, which is 50Hz, the AE model will increase the consumption in order to keep the frequency within the allowed limits explained in Chapter 2 by providing down-regulation. If the frequency is below the nominal value, which is 50 Hz, the AE will start to decrease the consumption in order to provide up-regulation.

As explained in Chapter 2, many electrolyzer farms are being built worldwide. According to [59], a 6MW electrolyzer farm is built in Mainz, Germany. Therefore, it is assumed that the electrolyzer farm sizes will increase in the future. In this study case, an aggregated electrolyzer farm of 29.75 MW is considered for both winter and summer cases.

The aggregators will make sure that the AE farm is always available for frequency regulation if requested by the TSO. The flexibility of the AE model could be sold in the balancing market, where both the TSO and aggregators even end-users could get benefits from providing ancillary services by controlling the AE units. It is assumed that the TSO and the aggregator of the AE farm have a monthly contract, where the aggregator makes sure that the AE farm is always available whenever it is needed and can be fully controlled to provide frequency regulation. Therefore, it is assumed that the storage is always and 100% available.

4.1.1 Modelling of Alkaline Electrolyzer

The LFC input is going to be the power set point to the AE model. The AE is set to increase the consumption for a negative signal, which means down regulation. By doing this, it is ensured that the AE will consume more power if there is an over frequency and decrease the consumption if there is an under frequency situation in the power system. The LFC signal will determine the set point for each electrolyzer modules and hereby calculate the voltage for the cells in the electrolyzer model U_e and mass flow rate m_e . The AE has an output power of 355kW P_e , where a compressor with 70 kW size is included, P_{com} .

The final consumption output will be a sum of these two values, P_{sys} which is multiplied with the number of AEs in the system. The AE model is shown in Figure 4.1.

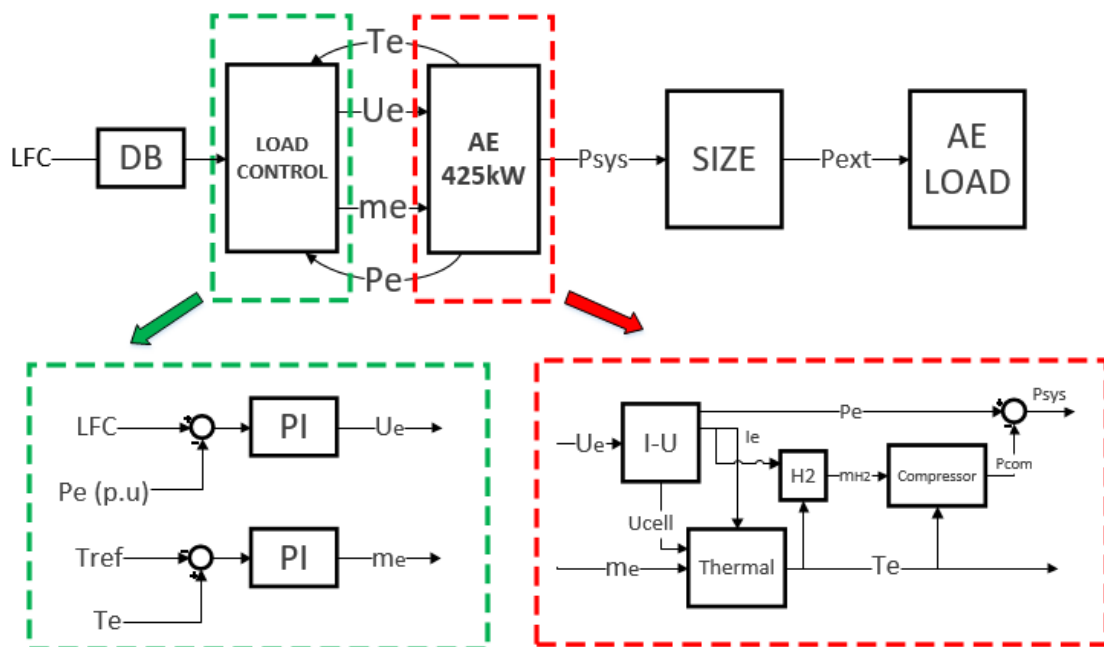


Figure 4.1 - AE model

The LFC received by the model must be in per unit, therefore the LFC signal received by the participation block in Chapter 3 is divided by the total capacity of the AE model. A dead band is set in front of the model in order to avoid unnecessary use of the AE. The AE model will only provide regulation if the LFC signal is more than a certain amount. The AE 425kW module consists of four submodels. The parameters for AE model can be found in Appendix H.

Load Control

Load control block includes two PI controllers, which controls the electrolyzer cell voltage U_e and mass flow rate m_e . The PI values are chosen according to [57]. The first part of the controller receives the power set point from the LFC signal, where it is compared to the actual power set point of the AEs. The PI will change the set point to the AE cell voltages in order to increase or decrease the power consumption of the AE module to ensure that the consumption follows the LFC power set point.

The second part of the controller controls the temperature of the AE module. The nominal level of the temperature is set to be 80°C during dynamic simulations. The temperature set point is compared with the initial temperature of the AE module. The error in the temperature is sent to a PI controller, which ensures the needed electrolyte mass flow in order to maintain the temperature within the limits.

425kW AE plant model

In this section, the four different sub-models of AE 355kW block is described. The detailed parametrization of these models are based on [57] and [58].

I-U: In this sub-model, the relation between current and voltage can be found. The relation is used to determine the behaviour of the electrolyzer at different temperatures.

The I-U relation is shown in Figure 4.2.

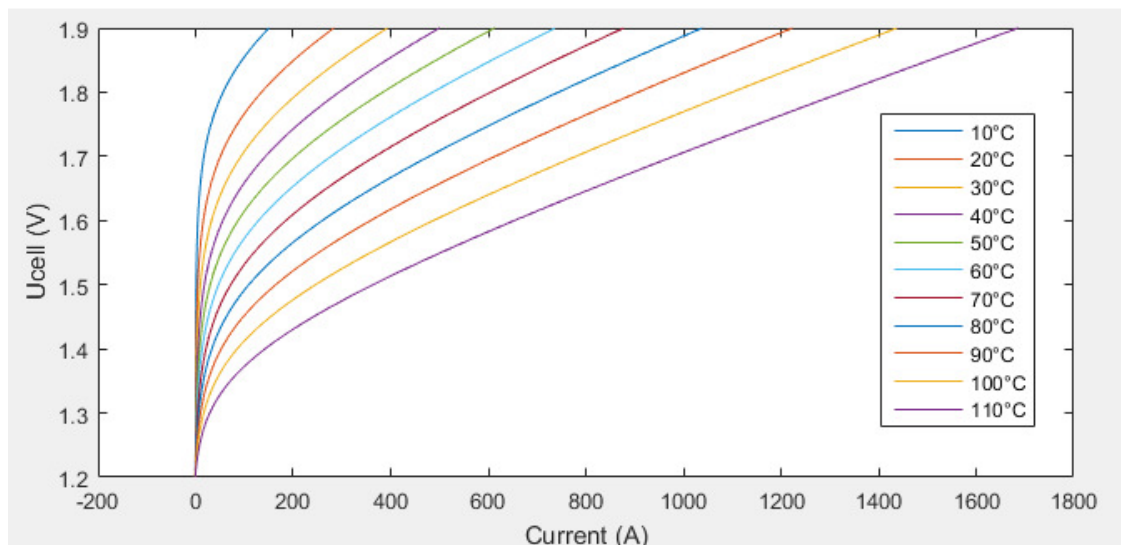


Figure 4.2 - I-U relation

The power consumption without the compressor is given in (4.1)

$$P_e = U_e \cdot I_e \quad (4.1)$$

Thermal: The thermal model calculates the temperature change in the AE. It is based on the formula given in (4.2)

$$C_t \cdot \frac{dT_e}{dt} = Q_{gen} - Q_{loss} - Q_{cool} \quad (4.2)$$

, where C_t is the thermal capacity. Q_{gen} is the internal heat generation, Q_{loss} is the heat loss and Q_{cool} is the cooling demand by the AE.

H2: The production rate of hydrogen is calculated in this sub-model. It is based on Faradays electrolysis law, which is given in (4.3):

$$n_{H_2} = n_F \cdot \frac{n_C \cdot I_e}{zF} \quad (4.3)$$

, where F is 96485 C/mol, z is 2 and n_F is the efficiency. In order to calculate the production rate (kg/s), the molecular mass of hydrogen gas is multiplied, as shown in (4.4)

$$m_{H_2} = n_{H_2} \cdot M_{H_2} \quad (4.4)$$

Compressor: The power consumption of the compressor is calculated in this submodel. The compressor compresses hydrogen up to 150 bar and this happens in two stages. It is assumed that 10% of the hydrogen volume is stored in the gas network, where the rest is converted into methane before storing it in the gas network. However, the methanization process is not considered in this project. The active power consumption of the compressor is given in (4.5)

$$P_{com} = m_{H_2} \cdot (W_1 + W_2) \quad (4.5)$$

, where P_{com} is the compressor power and m_{H_2} is the hydrogen mass flow rate (kg/s).

4.1.2 Test of the Alkaline Electrolyzer

The proposed aggregated AE model has been tested in MATLAB and then implemented in DigSILENT. The power consumption and temperature response of the AE has been tested for 24 hours with an initial temperature of 20 °C. The behaviour of the AE is shown in Figure 4.3. It is observed that the response is very slow in the beginning during start-up. The active power consumption response is limited by the temperature of the AE. The response is very fast during normal operation when the temperature is at nominal value.

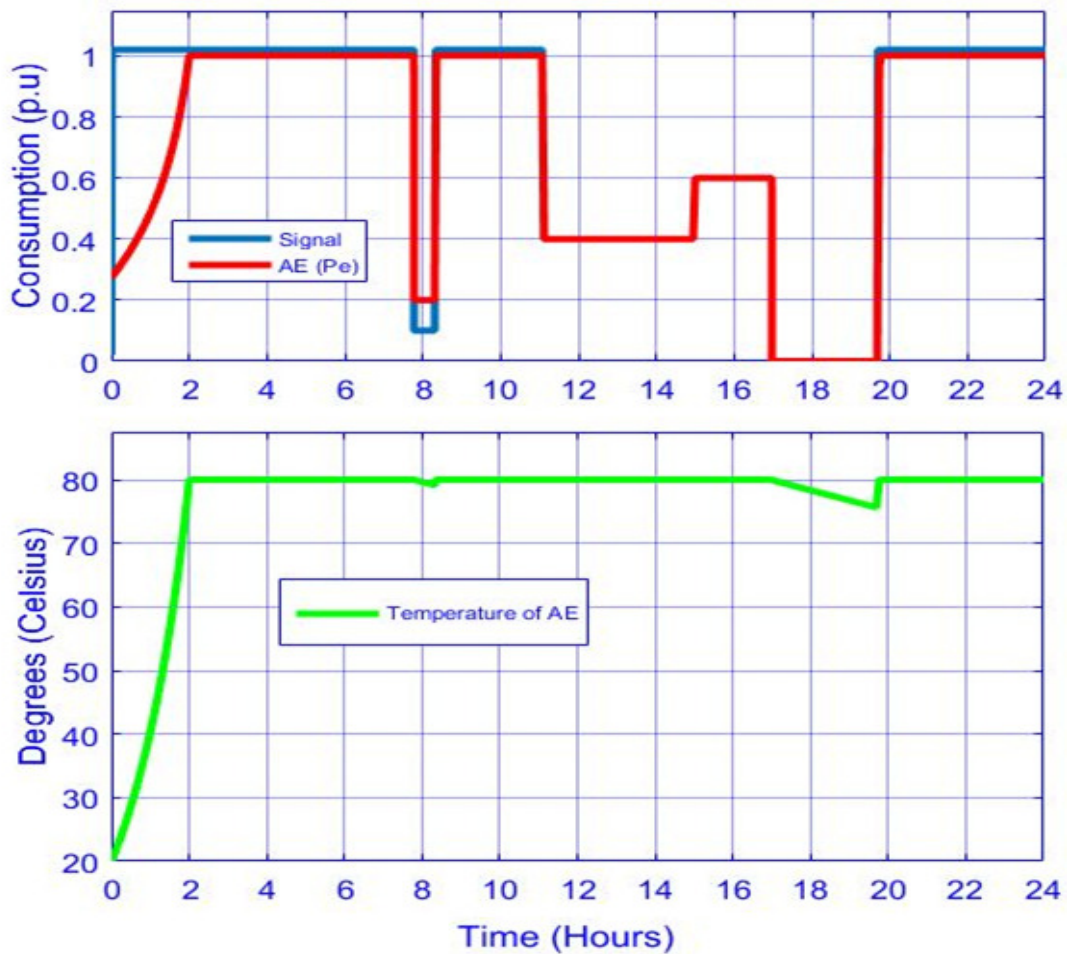


Figure 4.3 - Test of AE

The consumption is limited at 20% when the set point is between 0 – 0.2 p.u due to the purity of hydrogen [58] and 0% consumption when the set point is exactly 0 p.u. A huge drop in temperature is observed when AE is set into standby mode. This adds another slow response to the upstart of AE in terms of few minutes. Therefore, it is assumed that the AE module will never be set on standby in the power system and will always consume 20% of its rated power to slow down the temperature drop. Due to the temperature limitation on the consumption response, the initial temperature is set to 80 °C during the LFC integration to provide fast regulating services.

4.2 Implementation of Heat Pump

In order to integrate the heating demand in this case study, the modelling of the HP is needed. This subsection introduces the modelling of HP. The model is based on [60]. First, the scenario for HPs will be explained and heat demand data will be introduced. Hereafter, the modelling of HP will be presented. Finally, the test of the HP model will be discussed.

The purpose of the HP is the same as AE, to consume the excess of power caused by the wind fluctuation in the system. It is assumed that only 40% of the total HPs will be controlled by the TSO during the day due to the end-user convenience and availability. Depending on the frequency in the grid, the HP model will change the consumption. If the frequency is higher than the nominal value, which is 50Hz, the HP model will increase the consumption in order to keep the frequency within allowed limits by providing down-regulation. If the frequency drops below 50Hz, the HP model will decrease the consumption and ensure that the frequency will be kept within the allowed limits by providing up-regulation.

According to [61], there are currently 80000 heat pumps in Denmark. The test grid 9-bus network is a smaller power system than the Danish power system. Therefore, less number of heat pumps is needed in order to achieve a realistic case. Therefore, it is assumed that 30000 heat pumps are installed during the winter case. Regarding the summer case, it is assumed that the heat demand and number of HPs during summer is much less than during winter. As a result, it is assumed that the heat demand during summer is chosen the July from the data and the number of the heat pump is 67 % of the winter case.

The aggregators again will have to ensure that a certain amount of HPs will always be available for frequency regulation if it requested by the TSO. As in case of AE, the HP flexibility should be available in the balancing market. It is assumed that the TSO can only control a certain amount of the rated power of the HPs since the HPs are owned by private owners. Therefore, a limit of 40% of the rated power of HPs has been set to the

LFC control signal. It is assumed that the HPs cannot be controlled during their storage time, which is 45 minutes. Therefore, the HPs are only available after the storage operation and limited with a 40 % control margin. It is desired to have a base consumption, which is calculated by the formula (4.8) in order to resemble the real life case. However, there might also be a need for heating during low wind conditions in the grid. Therefore a minimum power consumption of 5% has been added to the model.

4.2.1 Heat demand

In this section, the chosen heat pump and heat demand for winter and summer cases are presented. The residential heat demand data for a winter and summer month is used in order make the model more realistic. An aggregated model for HPs with integrated hot water storage is considered in this study case. Danfoss 1,71kW HPs are chosen for integration in the power system. The parameters of the chosen HP can be seen in Table 5.

Table 5 - Danfoss 1.71 kW heat pump [62]

Rated power consumption, kW	1.71
COP	3.61
Rated thermal output, kW	6.17

The heat demand for this study case is obtained from Prof. Mads Pagh Nielsen in Department of Energy Technology, Aalborg University. The data is collected from four different types of houses every 15 minutes for one year. The obtained data is available in Appendix I. Data from February and August are chosen where a random percentage of each house type is used. The averaged heat demand is shown in Table 6.

Table 6 – Heat demand for four types of households

	House type1	House type2	House type3	House type4
Heat demand, E_{demand} (kWh/day) – Winter	63.4	57.1	56.14	26.3
Heat demand, E_{demand} (kWh/day) – Summer	22.16	23.25	20.52	15
Household percentage	30%	20%	10%	40%

4.2.2 Modelling of Heat Pump

The model consists of 30000 HPs which equals 51.3MW rated power output during the winter case and 20000 HPs during the summer case which equals 34.2 MW. It is assumed that the model has a constant COP. The LFC signal is received from the participation block, where it is given as a set point for the HP model. The HP will change its consumption according to the set point given from the LFC signal. The HP is set to increase the consumption for a negative signal, which means down regulations is needed in the power system. This will ensure that the HP will provide down-regulation during an over frequency case and up-regulation during an under frequency case in the power system. The LFC signal to the HP model must also be in per unit and therefore the LFC signal is divided by the total capacity of the HPs. A dead band is again used in this model to avoid unnecessary use of the HPs. The HP model will only provide regulation if the LFC signal is more than a certain amount. The common model of the HP composite frame is shown in Figure 4.4.

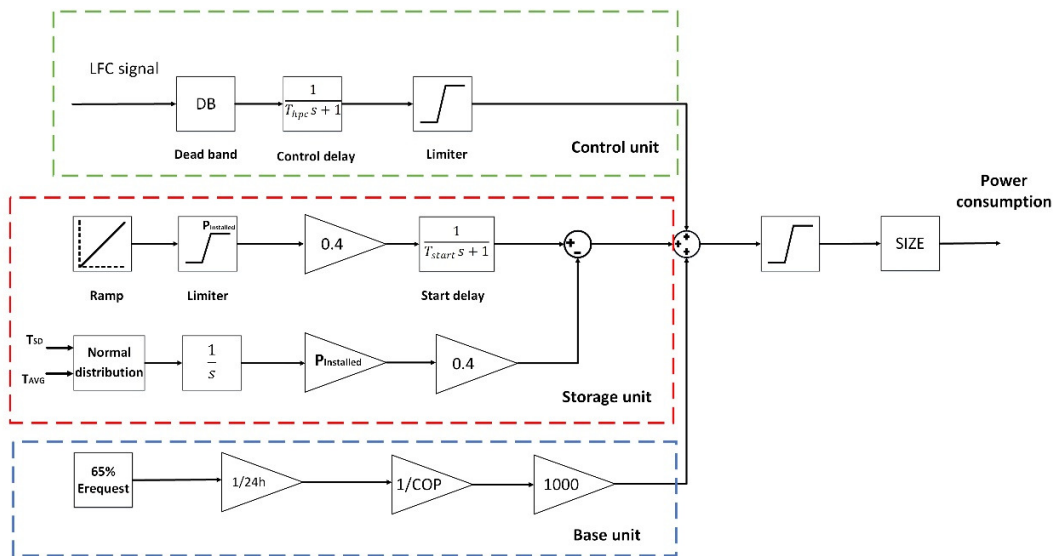


Figure 4.4 – Common model of the HP block

The strategy of the HP is based on a two-staged operation. The control center predicts the total demand of heat in the area, where planning and operation is performed for storage and normal operation.

Storage operation

It is assumed that 35 % of the heat demand is stored at the hot water tank at 40 % of the rated capacity in the beginning of the day. The other 60 % of the rated capacity is reserved for frequency regulation and normal operation. The average time for heat demand is calculated from the values in Table 6 by (4.6)

$$T_{HEAT}^i = \frac{0.35 * E_{demand}^i}{0.4 * P_{HP} * COP} \quad (4.6)$$

The change of total power consumption is estimated according to [60] by a normal distribution. The average and standard deviation is calculated by the formulas in (4.7)

$$T_{AVG} = \frac{\sum_{i=1}^{N_{HP}} T_{HEAT}^i}{N_{HP}} \quad T_{SD} = \sqrt{\frac{\sum_{i=1}^{N_{HP}} (T_{HEAT}^i - T_{AVG})^2}{N_{HP}}} \quad (4.7)$$

The total power consumption is modelled to reach 60 % of the rated capacity in 30 minutes. The model is assumed to start storing energy in the tank at hour 0 (beginning of the day). A normal distribution is used to model the end time for storage operation. When 35 % of the demand is reached, the storage operation ends.

Normal operation (Base unit)

The normal operation is expected to have a constant rate heat demand through the day with the remaining 65 %, which is the base unit. The base consumption is calculated as given in (4.8)

$$P_{base} = \frac{65\% * E_{demand}}{COP * 24h} \quad (4.8)$$

A base consumption has been added to the model in order to make it more realistic. It is assumed that the heat imbalance in the power system will be balanced by the storage system.

Control unit

The control unit has been added to the model to account for the changes in the LFC signal. The HP model will start to change the consumption if there is any change of set point from the LFC signal. For a negative LFC signal (down regulation), the given value for the control unit is a positive signal. A positive signal added to the summation point will increase the power consumption of the HP model. For a positive LFC signal (up regulation), a negative signal through the control unit is given to the summation point. Therefore, in this case, the HP model will start consuming less until it reaches the minimum consumption point, which is set as 5 % of the rated power output, if an up regulation is required in the power system.

Figure 4.5 shows the principle behind HP operation.

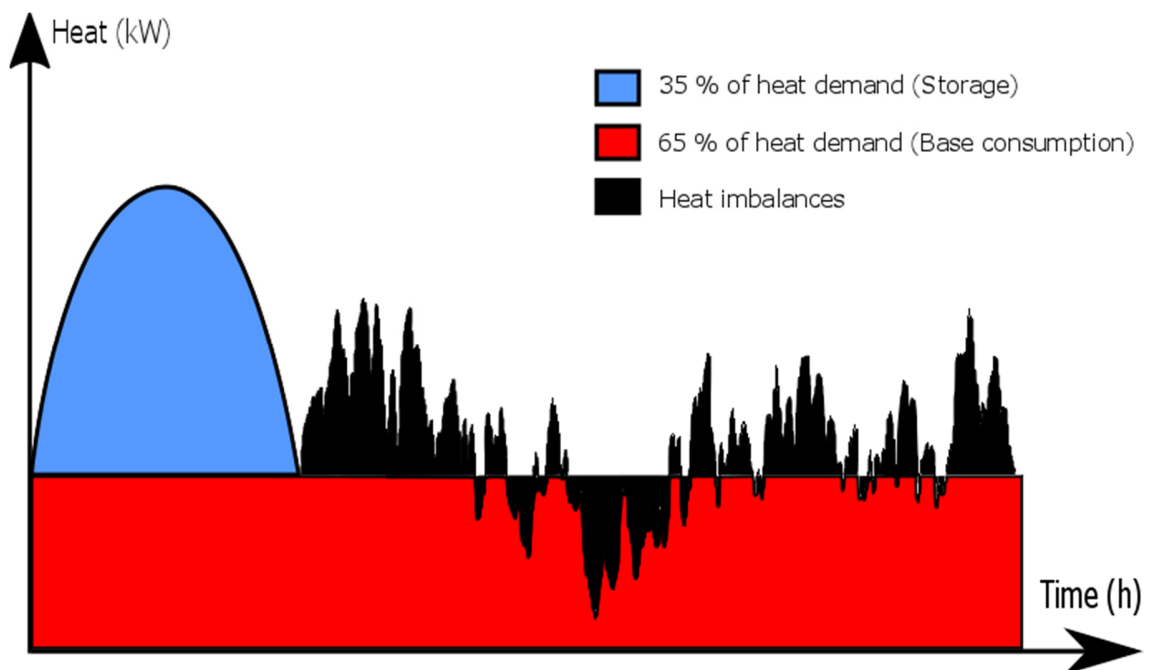


Figure 4.5 - HP heat demand operation

4.2.3 Test of the Heat Pump

The proposed aggregated HP model has been tested in MATLAB and hereafter implemented in DlgSILENT. The model has been tested for 24 hours with the winter demand. The behavior of the aggregated model is tested with control signals and presented in Figure 4.6.

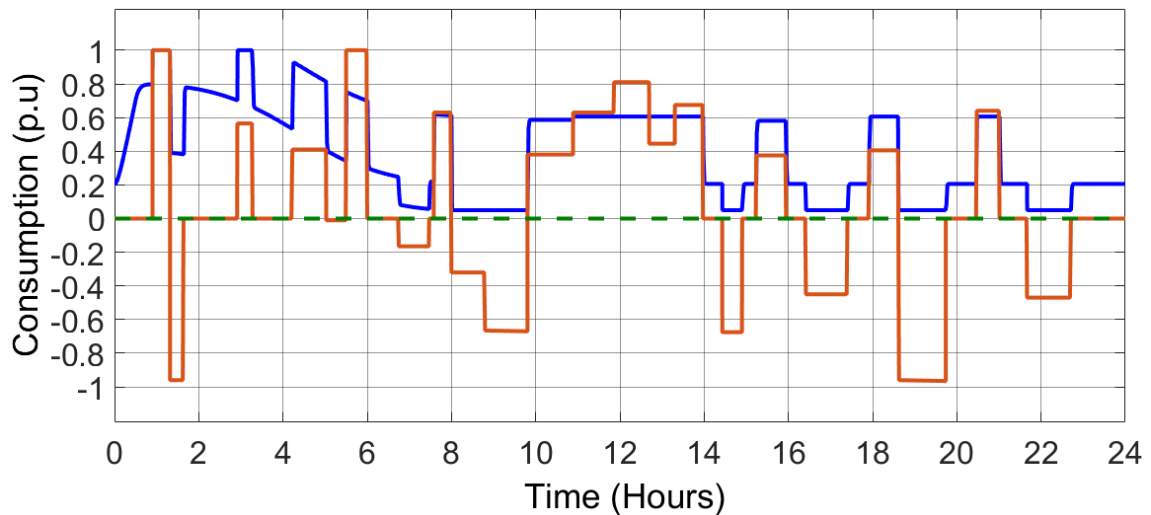


Figure 4.6 – Test of HP during winter

It is observed that the power consumption is between 5% to 40% of the rated capacity. This is due to the 5% of minimum consumption limit. Hence, the model already has a base consumption P_{base} of 20%. It is seen that the power consumption never exceeds 40% of the rated power output during the storage time and normal operation. It is seen that the storage operation ends after the 7th hour. The control signal limits are 1 and -1 which indicate the highest consumption of power. It is observed that the response according to the control signal is very fast in terms of seconds.

4.3 Electric vehicle (EV)

The integration of the EVs requires an aggregated EV model. This subsection presents the modelling of EVs. The aggregated model of EVs is based on the data from Danish driving pattern [63] and the detailed EV model in [60]. First, the participation scenario will be introduced in this subsection. And then the modelling of EVs will be presented. Finally, the test of the aggregated EV model will be investigated.

Unlike AEs and HPs, the EVs can both work as a load and a generator in the power system. This means that the EV can both be charged up and even discharged if needed. The main purpose of EVs is to consume the excess of power caused by the wind fluctuation in the power system. It is assumed that the EVs can only be controlled with a range of 50%-90% of the state of charge due to the end-user convenience and lifetime of the EVs as explained in Chapter 2. The control margin of 40% of the SOC has been set because the EVs are owned by private owners. The owners might want to still be able to use their cars outside in the regulation time. If the frequency is higher than the nominal value, the EVs will start to consume more in order to keep the frequency within allowed limits by providing down-regulation. If the frequency is below the nominal value, the EVs can consume less in order to keep the frequency within the allowed limits by providing up-regulation. In cases where the frequency is lowered too much, the EVs can start working like a generator and discharge their stored energy. In this case, the EV will start working like a generator and provide an extra capacity on up-regulation together with the CHPs in the power system.

According to the report made by Copenhagen Economics, CE [64], around 24000 EVs are expected to be sold in Denmark by 2020. Since the test grid, 9-bus network is on a smaller scale than the Danish power system. This number has been scaled down to 10000 EVs in this study case during winter. Regarding the summer case, it is assumed that only 70% of the 10000 EVs are available to control during summer due to summer vacations etc. The aggregators will have to make sure that there is always a certain amount of EV left for frequency regulation if the TSO requested. If the SOC of the aggregated model goes beyond 90% and less than 50%, the control of the EVs will not respond to the LFC signal and keep the output power within the limit. According to [63], the average daily driving distance of a normal passenger car is 42km. It is observed that there is a slightly difference between the weekend and weekdays, more than 70% cars per day are traveling less than 50km which means that the daily driving requirement can be satisfied by current EV technologies. It is assumed that the EVs are only charged at home. Figure 4.7 shows the driving distance in Denmark during weekdays and weekends.

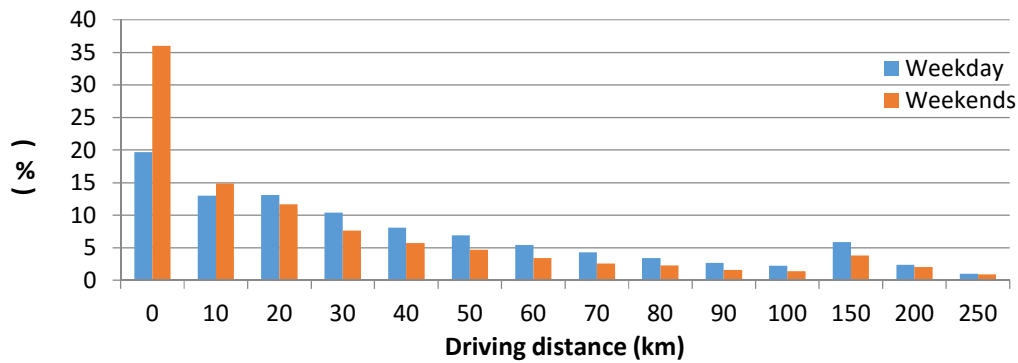


Figure 4.7 - EV driving distance in Denmark (Weekdays) [63]

The EV is fully controlled when the charge reaches 70% between the range 50% - 90%. This limit is determined by the Battery Efficiency Test, which is published in [65]. According to [65], the EV battery has higher efficiency and less heat generation when the SOC is within the range of 40% to 85%, which is shown in Figure 4.8. However, considered that SOC of the battery have to meet the daily travel requirement, the EVs, which participate in the LFC control, can be controlled in the range of 70% \pm 20% of the SOC.

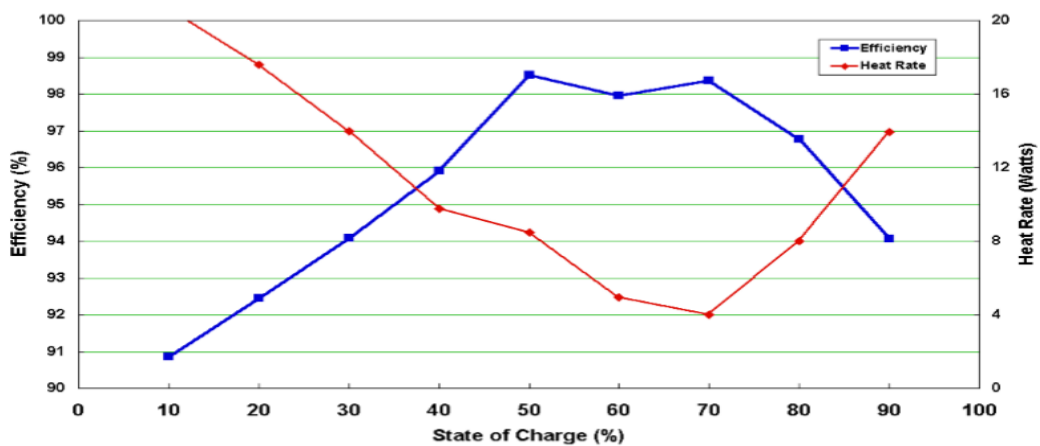


Figure 4.8 – Battery heat rate & efficiency as a function of SOC [65]

Many automobile manufacturers develop their own EV Technologies and launch their product into the market. The battery capacity is the one of most important factors to evaluate the EV performance. The battery capacity of the well-known Tesla model S can reach 90 kWh, which allows the car to travel 270 miles without recharging [66]. The advanced technology makes tesla a global leader within this area. However, Tesla S model is not considered in this study case due to its expensive price. It is assumed that the end-users buy less expensive EVs. Therefore, two popular plug-in electric cars are chosen,

produced by BYD and Chevrolet. The specifications of these two EV models are shown in Table 7.

Table 7 - EV specification [67] [68]

	Type A	Type B	Average
Brand	Chevrolet Bolt	BYD E6	
Inverter capacity [kW]	7.1	7	7
Battery capacity [kWh]	60	61.5	60.8
Installation rate [%]	50	50	

The installation rate has been set to be equal, 50 % for both EVs in order to give an equal distribution between the two kinds of EVs. Figure 4.9 shows the principle of EV participating in the LFC control. There are three states, which are the driving state, charging state and controllable state. The three transitions from one state to another are also considered in this study case.

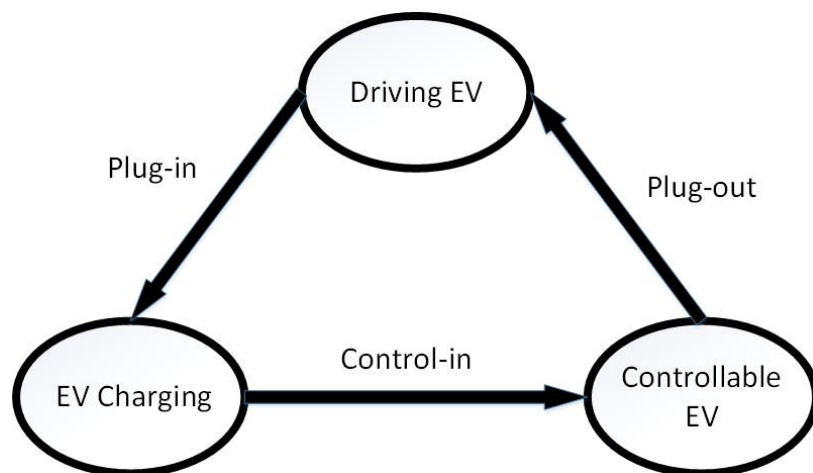


Figure 4.9 - State transition of EV

In the driving state, the EVs are plugged out from the system when driving is needed or the SOC is out of the controllable range. The EV state changes from the controllable state to driving state. In the next transition, the EVs enter the charging state to charge the battery with the charging station at home. The charging period depends on the battery capacity and the rated power of the charger. The EV changes to controllable EV state if the SOC hits 70%.

It is assumed that the EVs that are controlled can only repeat to change three states in a day. Figure 4.10 shows the changed of the number of controllable EVs and control-in and plug out rate in one-day simulation respectively. The data is normalized by the total number of controllable EVs. According to [69], the average daily trip with a passenger car in Demark is 1.5 times. Therefore, the total number of the control-In and plug-out rate is more than 100%.

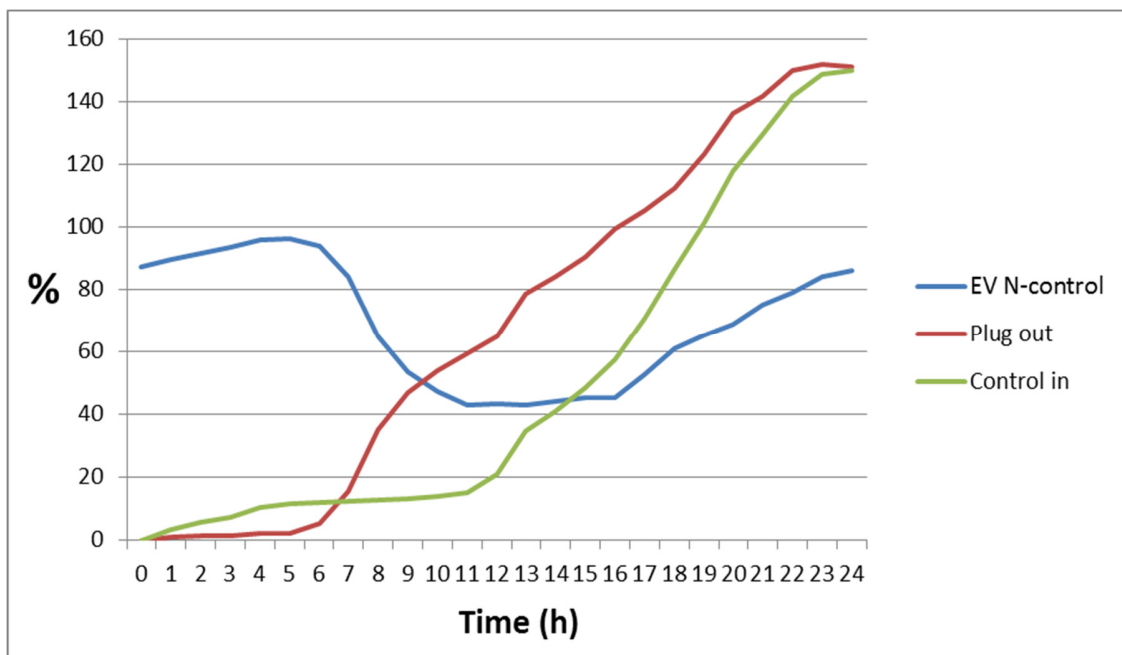


Figure 4.10 - Number of controllable EVs, control-in, and plug out rate in a day

4.3.1 Modelling of the EV

The EV model consists of 10000 EVs, which equals to 70MW of output power during the winter case. The LFC signal is the reference set point for the power consumption of the EV model. The EV will change the consumption depending on the LFC signal. Like the AE and HP, the EV model will be connected to a load in the power system. Therefore, the LFC input has to be inverted in order to perform up-regulation during low frequency conditions and down-regulation during over frequency conditions in the power system. The detailed EV block is shown in Figure 4.11.

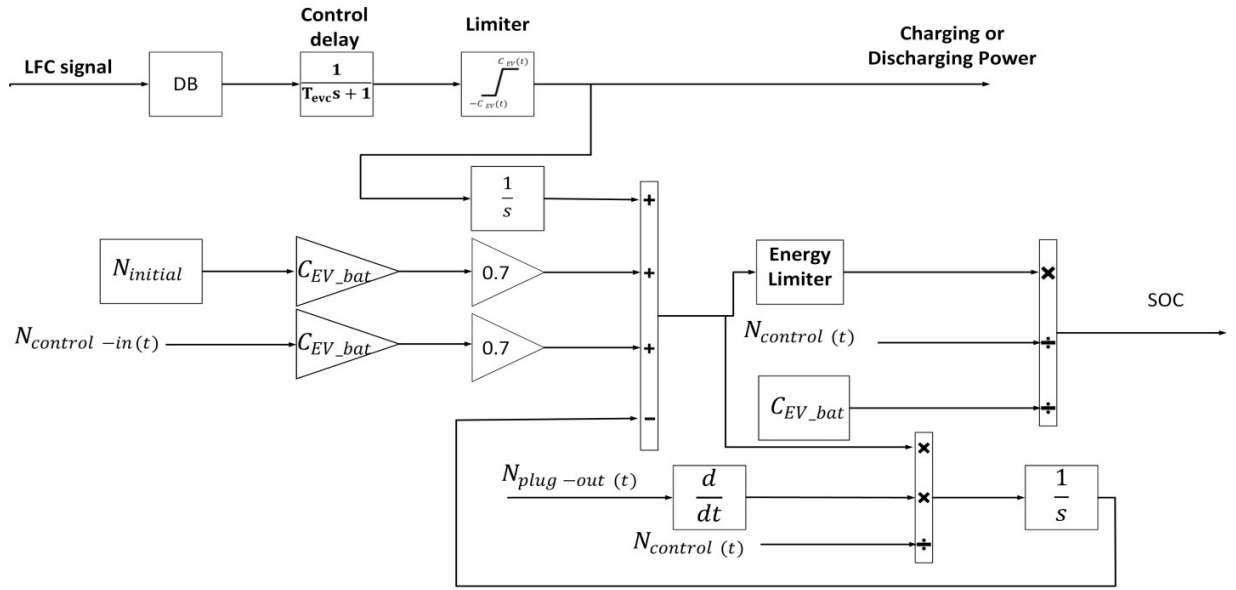


Figure 4.11 - Aggregated detailed EV model

The control delay is considered as a first order model with a delay of T_{evc} . The total inverter capacity of the EV model is calculated by (4.9)

$$C_{EV(t)} = N_{control(t)} * C_{EV_inv} \quad (4.9)$$

C_{EV_inv} is the average inverter capacity which is shown in Table 7 and the $N_{control(t)}$ is the number of controllable EV which is calculated by (4.10)

$$N_{control(t)} = N_{initial(t)} + N_{control-in(t)} - N_{plug-out(t)} \quad (4.10)$$

, where the $N_{initial(t)}$ is the initial number of the controllable EVs, $N_{control-in(t)}$ indicates how many times the cars are controlled-in, and $N_{plug-out(t)}$ indicates how many times the cars are plugged out. In order to calculate the SOC of the controllable EVs, some parameters have to be determined. $E_{control(t)}$ defines the total stored energy of the all controllable EVs, which is given by (4.11)

$$E_{control(t)} = E_{initial(t)} + E_{control-in(t)} + E_{LFC(t)} - E_{plug-out(t)} \quad (4.11)$$

However, due to the dynamic capacity of EVs, the model can only follow the LFC signal when the input energy within the energy capacity limit. As a result, the $E_{control(t)}$, has a constraint which is shown in (4.12)

$$E_{min_control(t)} \leq E_{control(t)} \leq E_{max_control(t)} \quad (4.12)$$

$E_{min_control(t)}$ and $E_{max_control(t)}$ are the lower limit and upper limit respectively, which can be calculated by (4.13) and (4.14)

$$E_{min_control(t)} = N_{control(t)} * C_{EV_bat} * \frac{50}{100} \quad (4.13)$$

$$E_{max_control(t)} = N_{control(t)} * C_{EV_bat} * \frac{90}{100} \quad (4.14)$$

$E_{initial(t)}$ is the initial energy of the controllable EVs, which is calculated by (4.15)

$$E_{initial(t)} = N_{initial(t)} * 0.7 * C_{EV_bat} \quad (4.15)$$

, where the C_{EV_bat} is the average battery capacity shown in Table 7. $E_{control-in(t)}$ is the incensement in the energy caused by the EV which changes the state from charging state into controllable state and is calculated by (4.16)

$$E_{control-in(t)} = N_{control-in(t)} * 0.7 * C_{EV_bat} \quad (4.16)$$

$E_{LFC(t)}$ is the total charging/discharging power of the EVs corresponding to the LFC control and given by (4.17)

$$E_{LFC(t)} = \int_0^t P_{EV(t)} dt \quad (4.17)$$

$E_{plug-out(t)}$ defines the decrease in the energy caused by the EV plug out and is given by (4.18)

$$E_{plug-out(t)} = \int_0^t R_{plug-out(t)} * \frac{E_{control(t)} dt}{N_{control(t)}} \quad (4.18)$$

Finally, the average SOC of the lumped EV model can be calculated by (4.19)

$$SOC_{AVG(t)} = 100 * \frac{E_{control(t)}}{N_{control(t)} * C_{EV_bat}} \quad (4.19)$$

Test of EV model

Figure 4.12 indicates the charging and discharging power of the EVs. It is seen that the output power is limited by the total inverter capacity of the controllable EVs. The total inverter capacity depends on the driving profile of the EVs. Besides, the output power is slightly shifted compared with the original input signal due to control delay. It is important to notice that the output power of EVs hit the upper limit during the 6:00 to 9:00. It is because the LFC signal is always positive during this period. The positive LFC signal causes the EVs to charge all the time. However, due to limited battery capacity, the EV model cannot handle more power after the battery is fully charged up to 90%. Similarly, the output power of EVs hit the lower limit during the 12:00 to 16:00 according to the continuous negative input signal. After hitting the limit, the EV model cannot be discharged for following the LFC signal.

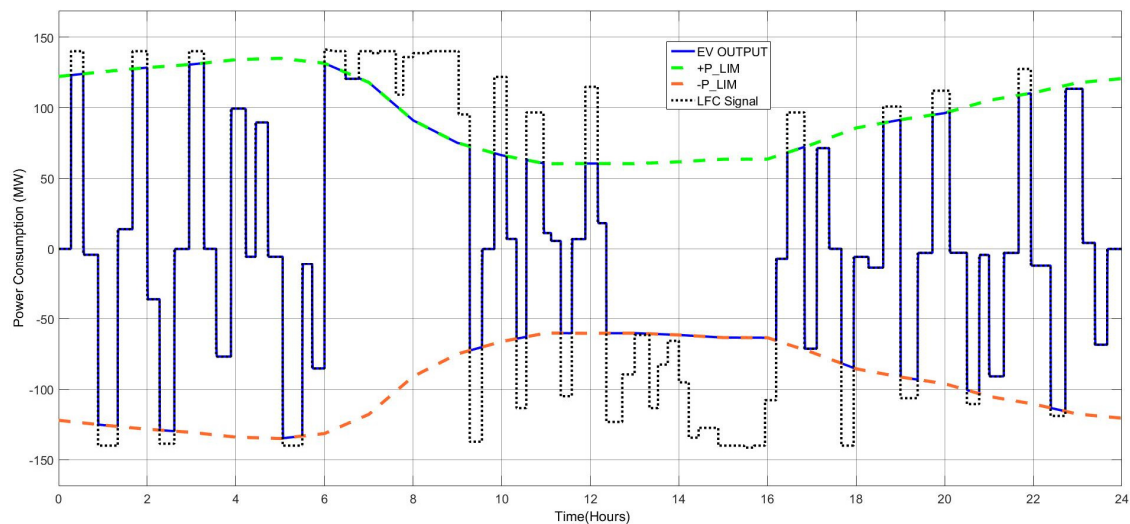


Figure 4.12 - Output power of the aggregated EV model

Figure 4.13 shows the average SOC of EVs. The initial value of SOC is set to be 70% in order to access the controllable state in the beginning of the day. As a result, the SOC fluctuates in the range of 70 % \pm 20 % as desired.

Moreover, as shown in both Figure 4.12 and Figure 4.13, it can be seen that the EVs are not controlled when the SOC hits the upper limit and the power output cannot response to LFC signal for charging at that time.

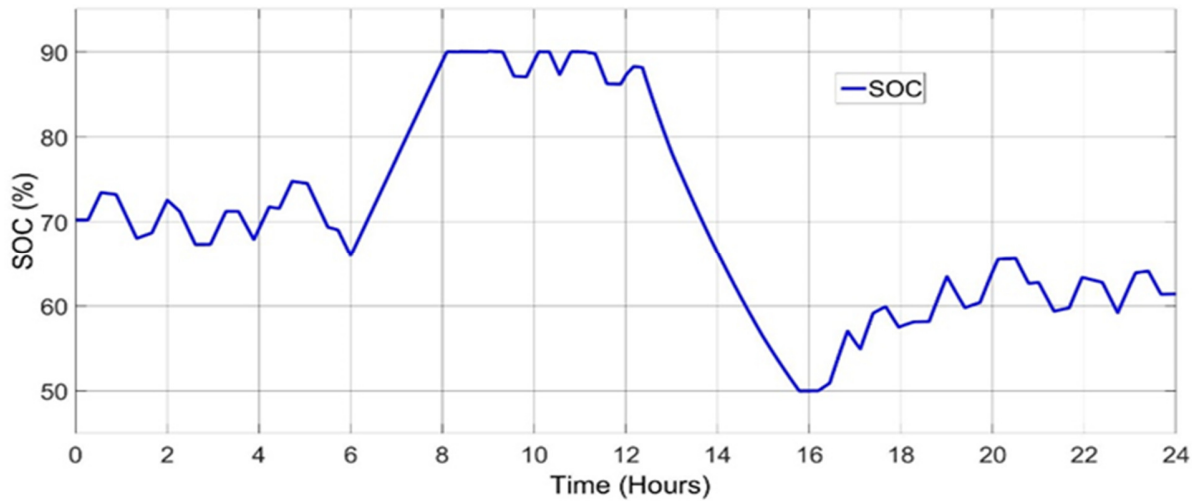


Figure 4.13 - SOC of the EV

5 Integration of Flexible Loads in a Wind Dominated Power System

In this chapter, the ability of the flexible loads to provide frequency regulation, is analyzed. First, the flexible loads have been added one by one to the power system in order to analyze the maximum capability of each flexible load to provide frequency regulation and their operating constraints. During the analysis, all the flexible loads are modelled as lumped models. The considered wind power profile and base consumption for the simulation scenarios are the same as the base cases used in section 3.8.4. As observed from the base case results, the biggest frequency fluctuation happens from $t = 3$ h to $t = 7$ h. Therefore, this time range will be the focus point in the analysis. The frequency values during this time range will be compared with the values from the base case, which had a maximum value of 50,455 Hz and minimum value of 49,6 Hz during these hours for the winter case. The maximum value for summer case is 50,446 Hz and minimum is 49,615 Hz.

Secondly, all three flexible load will be a part of the frequency control together in order to analyze the regulation affect from all of them. Finally, a statistical analysis of the results will be presented where the minimum, maximum and the standard deviation of the frequency will be compared.

5.1 Frequency support from AE

The aim of this section is to analyze the results of integrating the AE into the frequency regulation. This analysis is made in order to analyze the capability of the model and constraints while providing frequency regulation. The presented results include the frequency fluctuation in the power system and operation of the CHPs and DCHPs. However, the basic parameters of the AEs are also presented, such as active power consumption, operating temperature and hydrogen production.

5.1.1 Winter scenario

Figure 5.1 shows the results of the implementation of the P2G technology in the 9-bus network during the winter scenario. During the winter scenario, the AE model is connected to the LFC controller in order to provide secondary reserves. The AE model has a rated capacity of 29.75 MW, which equals to 70 AE units, where one single unit equals 0.425MW. The participation factor for the AEs is 0.20, which equals 20 % of participation. This value has been chosen after several tests due to the power consumption limitation

of the AE model. The participation factors given to the CHPs is 0.55 and 0.25 for the DCHPs, which equals to 55 % and 25 % of participation.

The highest and lowest value of the frequency fluctuation is reduced compared to the base case, as observed from the plot. During $t = 3$ h and $t = 7$ h, the maximum value of the frequency is 50,398 Hz and the minimum value of the frequency is 49,804 Hz. Therefore, an improvement of the frequency regulation is visible with AEs.

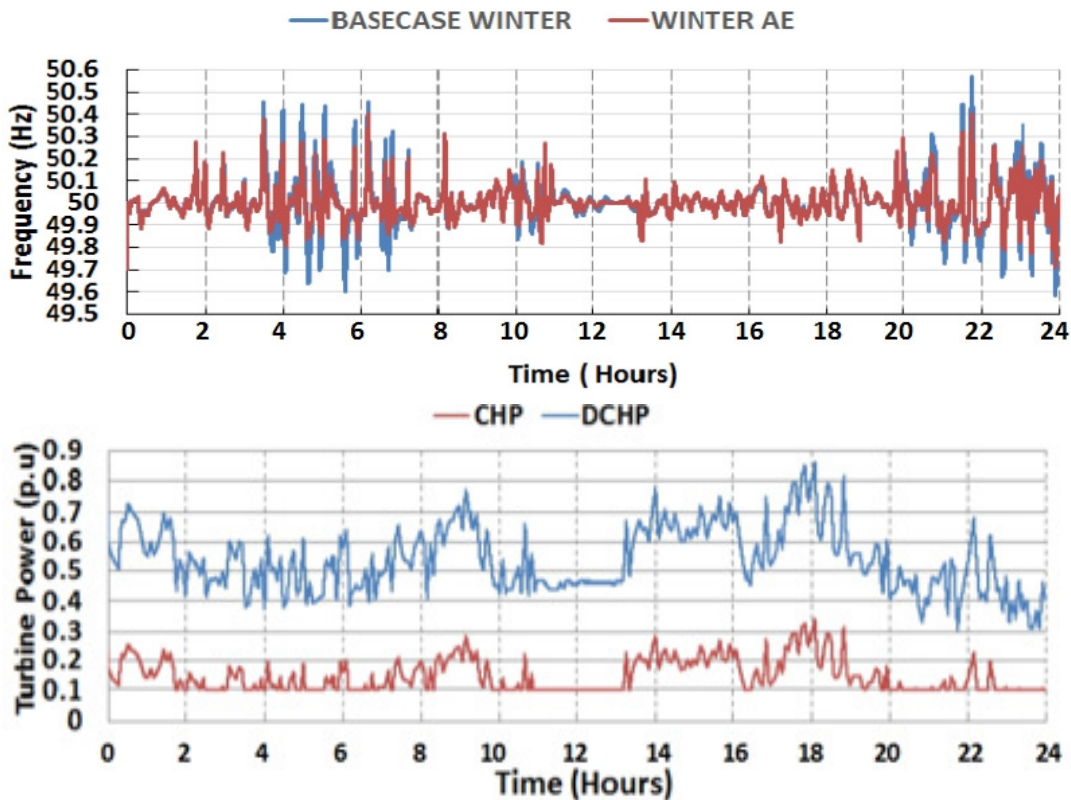


Figure 5.1 – Results of the power system with P2G integration, during a winter day

The figure shows the power production of CHPs and DCHPs. It can be seen that the power production of the CHP hits the lower limit during these 4 hours. Therefore, it has no more capacity to provide down regulation. A solution to this could be to use the AEs, especially during the hours where the CHPs hit the lower limit. It will be an advantage to use AEs due to their ability to perform both down and up regulation. The AE does the down regulation by increasing its consumption and up regulation by decreasing the consumption.

Figure 5.2 represents the parameters of the AEs. It can be seen that the AE starts increasing the consumption when down regulation is needed and decreases the consumption, whenever up regulation is needed in the power system. The AE increases the consumption when the CHPs and DCHPs decrease their generation and vice versa, which is desired. It is also observed that the total capacity of the AE farm is not always in use. The minimum consumption is approx. 6 MW, which equals to the 20 % base, as mentioned in section 4.1.2.

This minimum is set due to the I-U characteristic. The minimum cell voltage is set to be 1.2 V for each cell. When checking 1.22 V and 80°C in the table presented in section 4.1.2, the power consumption of the AEs is still positive due to a positive current. The consumption response of the AE farm is dependent on the temperature of the AEs. If the total AE farm consumes less, the temperature of AE units will start to decay down. A lower temperature means that the AE units will have difficulty in following the power set points due to the slow response because of the temperature drop. Although, the hydrogen consumption for other purposes such as heating or transportation could keep the temperature of AEs higher. However, other purposes than frequency regulation is not considered in the scope of this study case.

The temperature of the AEs is shown in Figure 5.2. The response of the AEs is very fast in terms of minutes due to the high temperature of the farm, as observed in plot c) because the temperature did not drop so much. As shown in the previous chapter, the response of AE is quiet fast when the temperature is around 80°C. It is seen that the nominal temperature is at 80°C. Therefore, the power set point is reached without any problem when the temperature is 80°C. As it can be seen in the temperature plot, when the electrolyzer drops below 70°C, the response becomes slower, which is shown in section 4.1.2. This is a negative impact of the AE units as a secondary reserve in the power system. A slow response might lead to a late release of secondary reserves, which would result in a wrong set point to the power system frequency. However, they are quiet fast and almost reacts like ON-OFF due to the high temperature. The AE increases the consumption when the CHPs and DCHPs decrease their generator and vice versa, which is desired as seen in the plot.

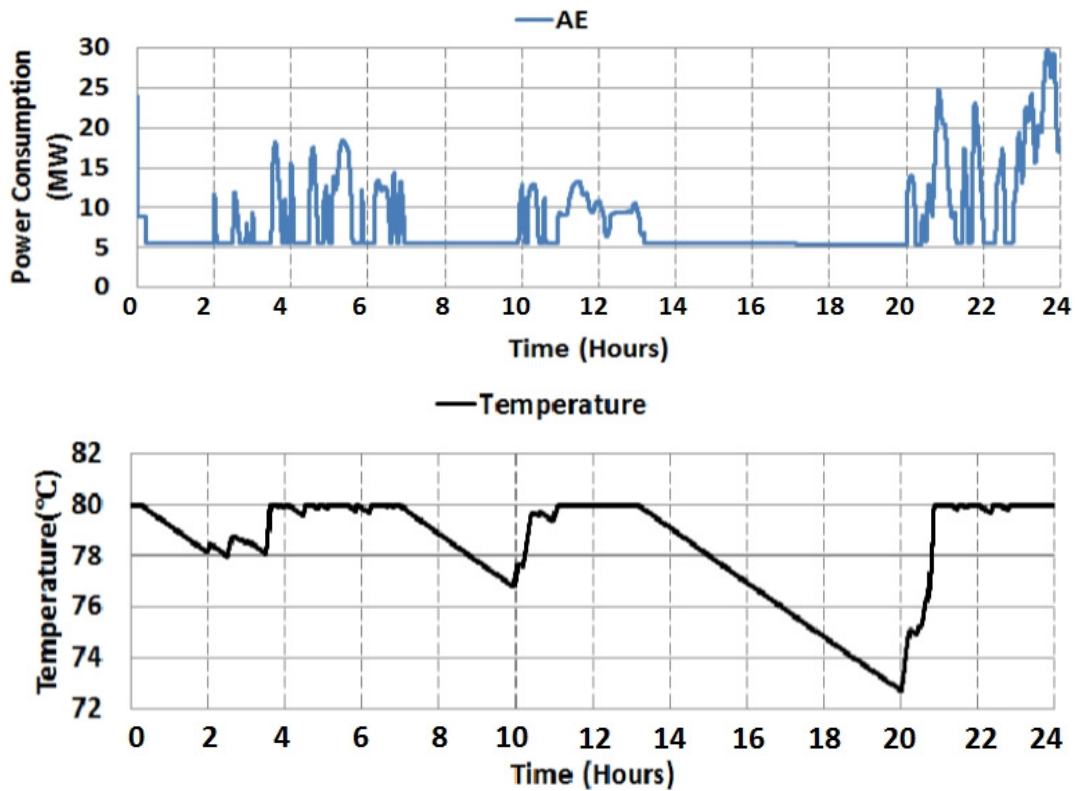


Figure 5.2 - AE parameters during a winter day

Additionally, the hydrogen production is analyzed, which is shown in Figure 5.3.

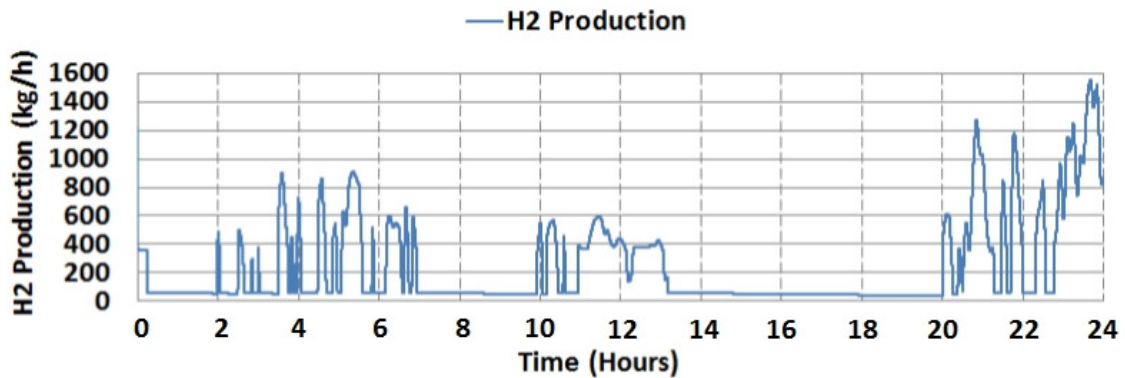


Figure 5.3 - Hydrogen production

The figure shows the hydrogen production in kg/h . It is seen that the peak production of hydrogen reaches approx. 1600 kg/h . Therefore, a consumption of the hydrogen is necessary. The analysis is made during a winter day, where the DCHP has to produce more heat, which means that the gas consumption will be higher than any other period of the year. Somehow, the excess of hydrogen must be utilized. The possible solutions to

consume this excess of hydrogen could be the following: fuel cells or direct injection to the gas network. However, these solutions are beyond the scope of this study case.

5.1.2 Summer scenario

Figure 5.4 shows the results of the implementation of the P2G technology in the 9-bus network during the summer scenario. The capacity of the AE model is unchanged, 70 AE units, which equals to 29.75 MW. The participation factor for the AEs is again considered as 0.20. The participation factors given to the CHPs is 0.55 and 0.25 for the DCHPs. A reduction of peaks can also be observed during the summer scenario. Therefore, an improvement of the power system frequency is visible. During the analyzed time range, the maximum value of the frequency is 49.754 Hz and the minimum value of the frequency is 49.754 Hz, which are lowered compared to the values from the base case.

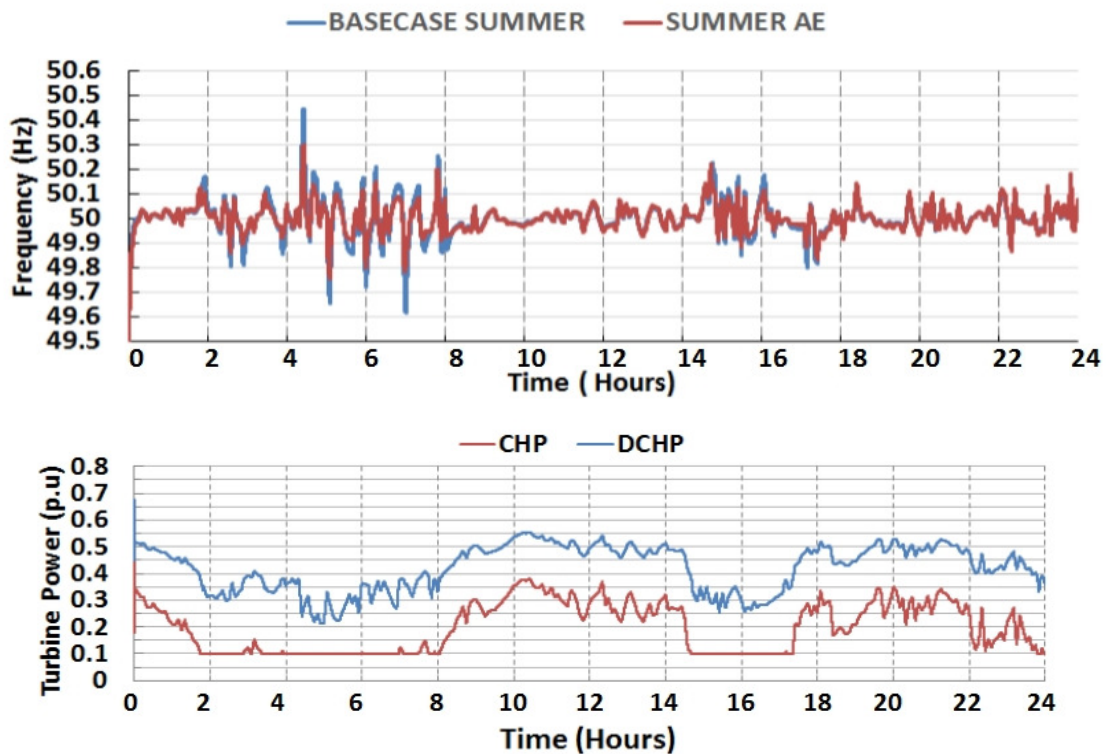


Figure 5.4 – Results of the power system with P2G integration, during a summer day

Figure 5.5 represents the parameters of the AEs. It can be seen that the total power consumption of the AE during summer is less than the winter scenario. This is due to less frequency fluctuations in the grid during summer, which also means that the produced hydrogen during summer will be less than the winter period. This is not a problem because the heat demand during summer from the DCHPs will be much less than the winter case.

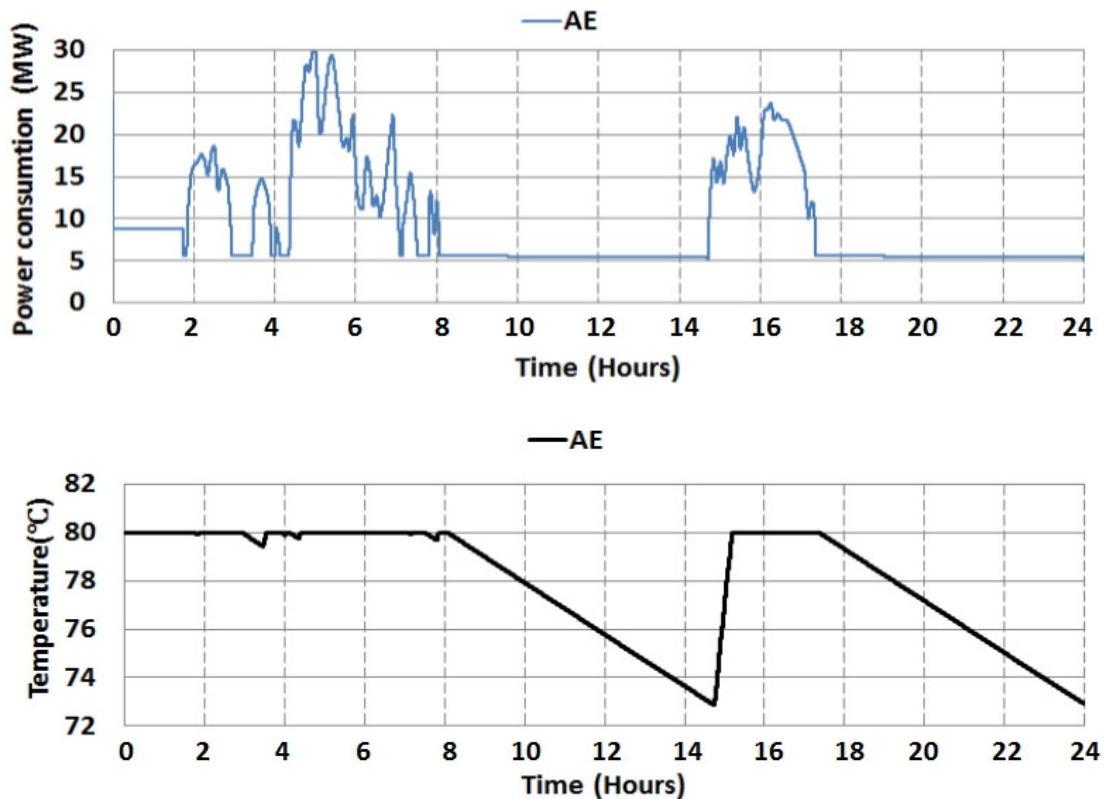


Figure 5.5 - AE parameters during a summer day

It is seen that the temperature from $t = 8$ h until $t = 15$ and from $t = 17$ h to $t = 24$ h keeps dropping due to less usage of the AEs. This slows down the response of the AE model to frequency regulation. Therefore, the power consumed from the power system will be delayed by a couple of minutes.

Additionally, the hydrogen production is analyzed, which is plotted in Figure 5.6.

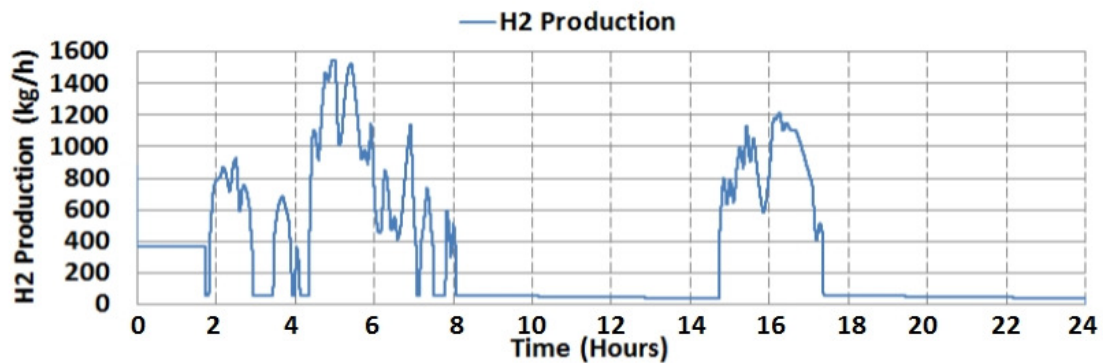


Figure 5.6 - Hydrogen production

The figure shows the hydrogen production in kg/h . It can be observed that peak production of hydrogen is approx. 1500 kg/h but the total generation of hydrogen is lower than the winter scenario. Therefore, less H₂ loads are needed to consume this amount of hydrogen production during the summer scenario.

5.2 Frequency support from HP

This section will introduce the results of integrating the HPs into the frequency regulation. This analysis will present the capability of the model and constraints during frequency regulation in the power system. The presented results include frequency fluctuation in the power system, operation of the CHPs and DCHPs. However, the basic parameters of the HP are also shown, such as active power consumption and the provided thermal energy.

5.2.1 Winter scenario

The results of implementing the HP technology in the 9-bus network is shown in Figure 5.7, during the winter scenario. The HP model is connected to the LFC controller in order to provide secondary reserves. The total amount of HPs are considered 30000 units, which equals to a size of 51.3 MW. It is also assumed that the control starts after the storage operation during the night, which takes 45 mins. The participation factor for the HPs is 30 %, which is chosen due to the power consumption limits of the HPs after several tests. The participation factors given to the CHPs is 0.45 and 0.25 for the DCHPs. As a result of this simulation, the frequency of the power system is shown in plot a). The maximum value of the frequency is 50.290 Hz and the minimum value of the frequency is 49.825 Hz during the analyzed time.

It is observed that the frequency fluctuation is slightly reduced compared to the base case. Therefore, an improvement on the frequency due to the integration of the HPs is visible. Therefore, the HPs are very controllable with a faster response time compared to CHPs.

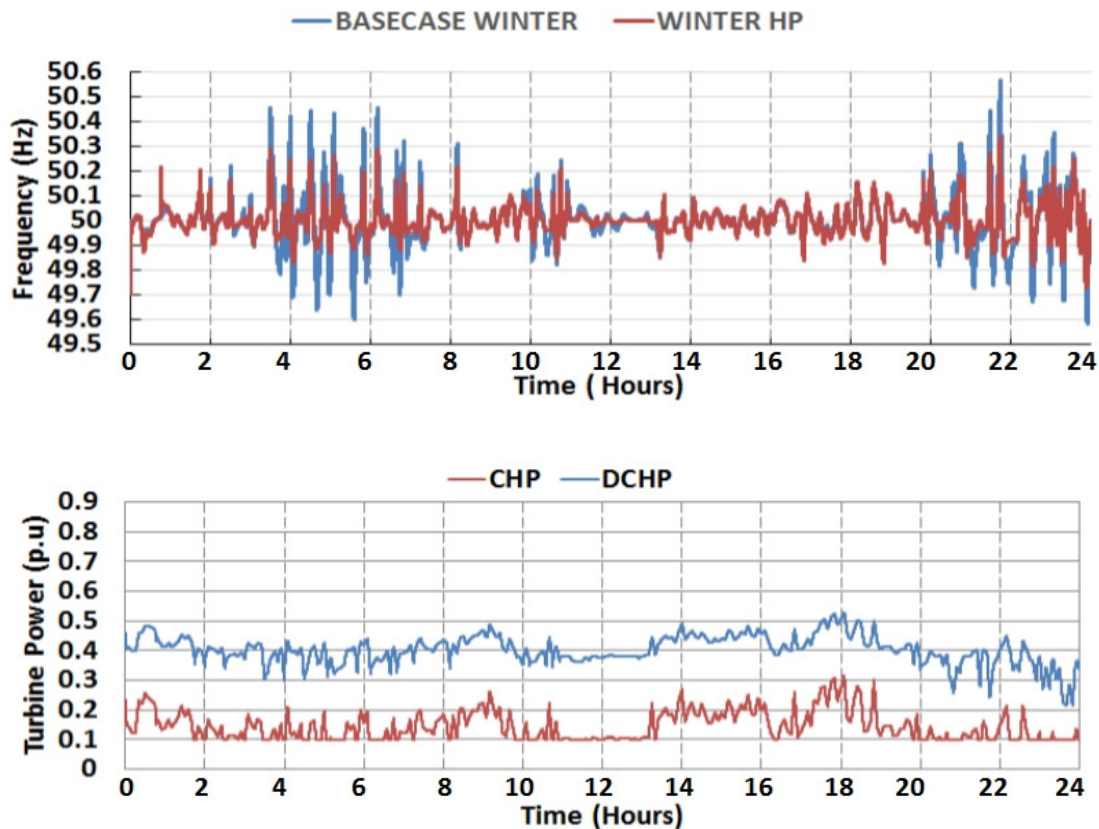


Figure 5.7 - Results of the power system with HP integration, during a winter day

Figure 5.8 represents the parameters of the HPs. During $t = 3$ h to $t = 7$ h, the HPs can also be used to perform down regulation and up regulation especially when the CHPs hit the lower limit. The HPs can provide down regulation by consuming more from the system and up regulation by decreasing the consumption from the power system as observed. The base consumption is approx. 10 MW and minimum consumption is approx. 2.6 MW in the figure, which equals to 5 % of the total capacity of the HPs. This minimum is set to not cut off the heating totally, which would be unrealistic. It is seen that the consumption goes up to the limit of 40 % on the control signal, where 40 % of the HPs are controllable due to the end-user convenience. The consumption of the HPs is very fast due to the ON-OFF operation. The highest delay which slows down the consumption is the built in induction motor in the HPs. The induction motor has a start up delay of 300 seconds, which might slow down the response of the HPs.

Like the AEs, the HPs can also benefit during the time ranges where the CHPs hit the lower limit capacity, as from $t = 3$ h to $t = 7$ h. As seen in Figure 5.8, the HPs will provide the necessary down and upregulation in the power system. The HP increases the consumption when the CHPs and DCHPs decrease their generation and vice versa, which is desired.

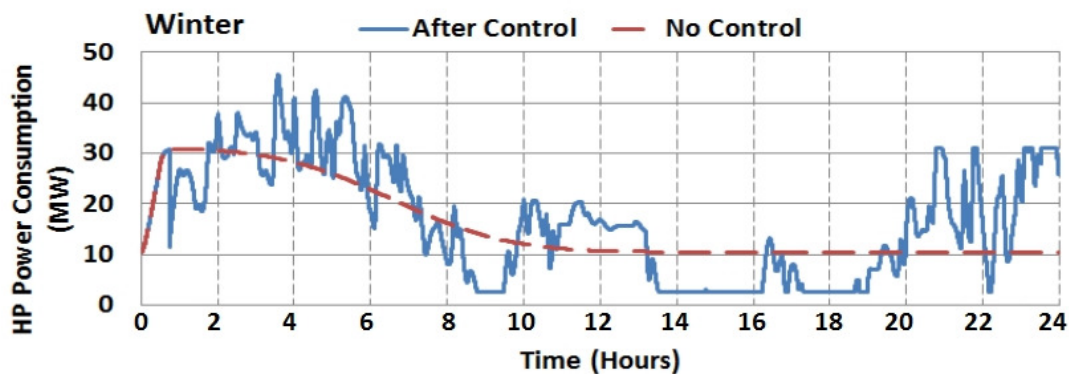


Figure 5.8 - HP parameters during a winter day

Additionally, the total generated heat by the HPs is shown in Figure 5.9.

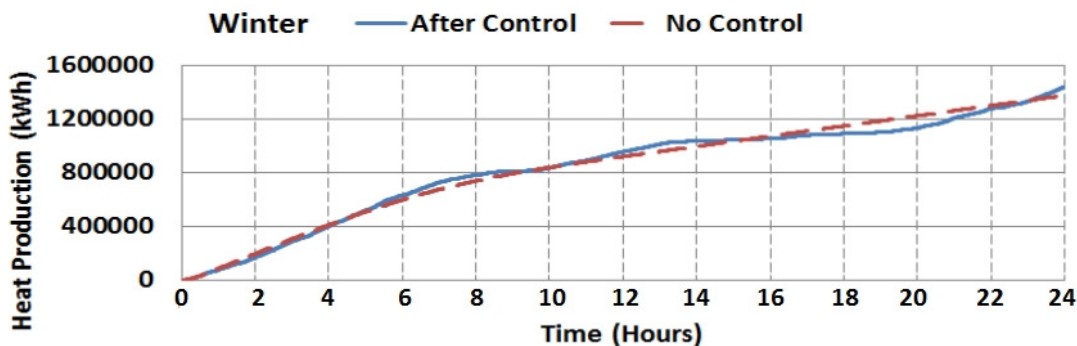


Figure 5.9 - Total generated heat

The heat demand during the winter scenario for all the HPs is 1397.2 MWh. The plot shows that the total generated heat demand through the day equals is 1438.8 MWh. It is observed that the total expected heat demand and generation almost matches with a small deviation. This actually shows how feasible it is to control HPs in order to provide frequency regulation. However, a limitation for the extra heat generation is needed. Somehow, the excess of heat must be consumed, which is out of the scope of this study case.

5.2.2 Summer scenario

The results of implementing the HP technology during the summer scenario is shown in Figure 5.10. The total amount of HPs are considered 20000 units, which equals to a size of 34.2 MW. The participation factor for the HPs is 10 %. This value has been chosen due to the capacity limits of the HPs during the summer scenario. The amount of HPs is slightly reduced compared to the winter scenario. The participation factors given to the CHPs is 0.65 and 0.25 for the DCHPs. It is observed that the fluctuation is reduced compared to the base case also in the summer period. Even though the capacity is less, the HPs are observed to be an advantage during the periods the CHPs hit the lower limit. Therefore, an improvement of the frequency fluctuation due to the integration of the HPs is still visible. The maximum value of the frequency is 50.686 Hz and the minimum value of the frequency is 49.356 Hz during the time range of $t = 3$ h and $t = 7$ h.

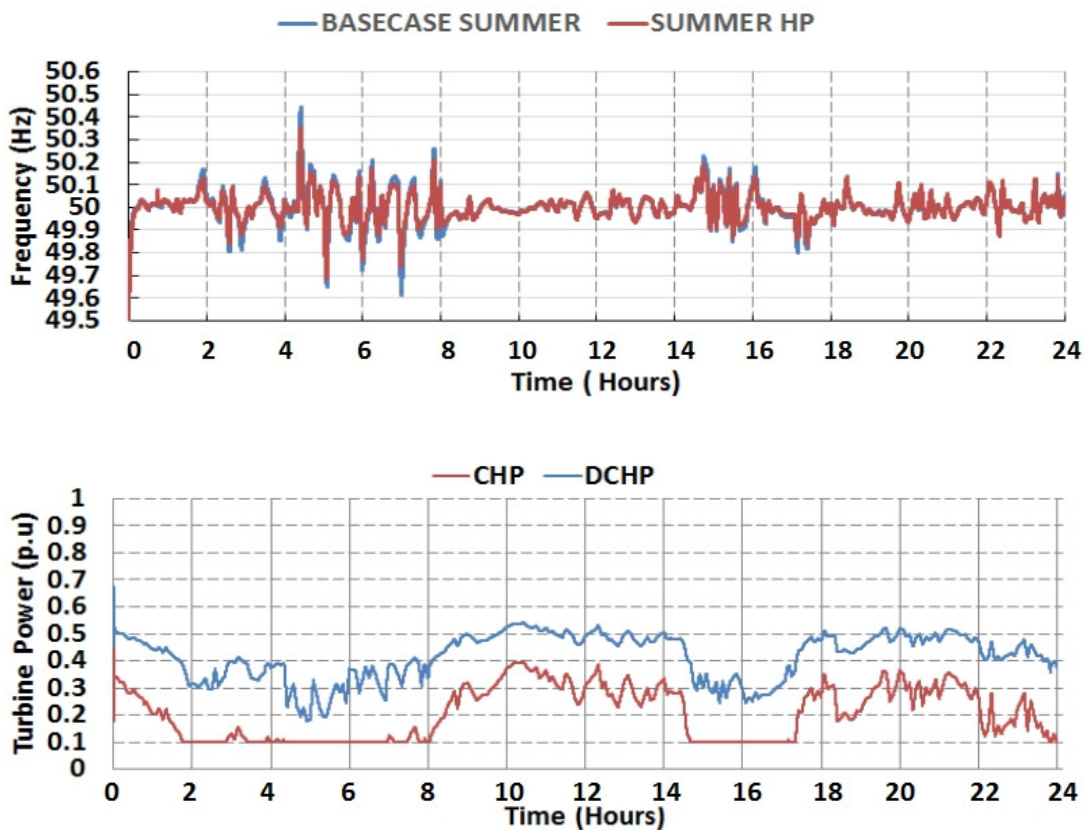


Figure 5.10 - Results of the power system with HP integration, during a summer day

Figure 5.11 represents the parameters of the HPs. It is seen that the HP increases the consumption when the CHPs and DCHPs decrease their generation and vice versa, which is desired. The total consumption of the HPs observed to be less than the winter scenario.

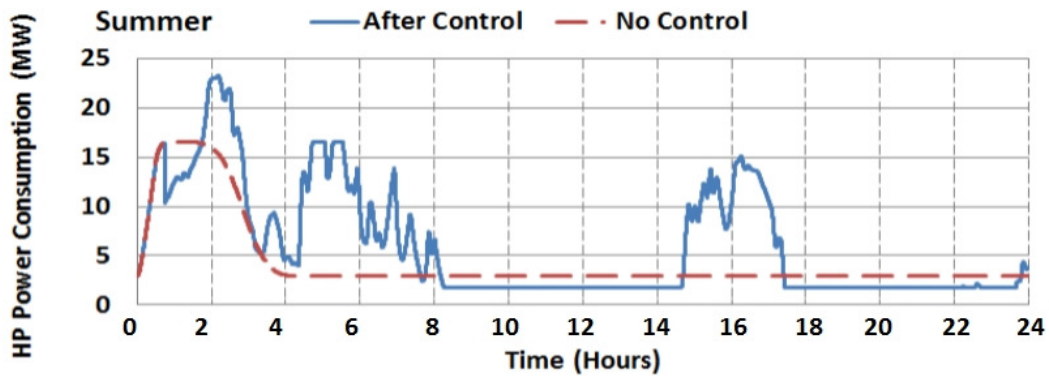


Figure 5.11 - HP parameters during a summer day

Additionally, the total generated heat by the HPs is shown in Figure 5.12.

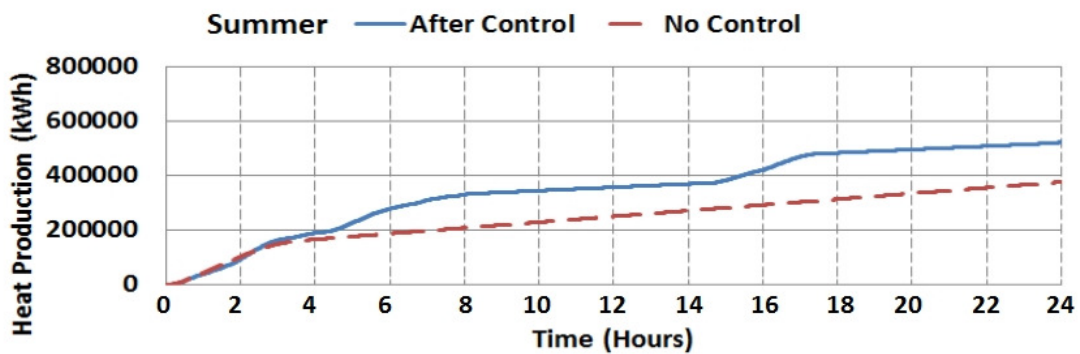


Figure 5.12 - Total generated heat

The heat demand during the summer scenario for all the HPs is 387 MWh. The total heat demand in the power system is much lower than the winter scenario, which is expected. The total generated heat demand through the day equals is 522 MWh. The produced heat is approx. 1.34 times higher than the demand. Therefore, possible solutions for the heat is needed in the power system.

5.3 Frequency support from EV

The section presents the results of integrating EVs into the frequency regulation. The capability and constraints of the model will be analyzed while providing secondary response. The EV model is a lumped model like the other flexible loads. The total size of the EVs is 70 MW. The results presented are the following: frequency fluctuation in the power system, wind power production, operation of the CHPs and DCHPs. The basic parameters of the EVs are also shown, such as active power consumption and the state of charge of the EVs.

5.3.1 Winter scenario

Figure 5.13 shows the results after implementing the EV technology in the 9-bus network during the winter scenario. The participation factor given to the CHPs is 0.45, 0.25 for the DCHPs and 0.30 for the EVs. The size of the total EVs in the winter scenario is 70 MW. The participation factor of the EVs is limited due to the SOC limits. As mentioned in section 4.3, it is assumed that the EVs can only be controlled between 50-90 % of the SOC due to the end-user convenience. If more than 30 % of participation is given, the EVs will hit the limit of SOC. Figure 5.13 shows the frequency fluctuation of the power system. During $t = 3$ h and $t = 7$ h, the maximum value is 50.279 Hz and minimum value is 49.831 Hz. It is hereby shown that the frequency fluctuations are even lowered with the flexibility of EVs. This shows the flexibility and fast response of the EVs as secondary reserves compared to HPs.

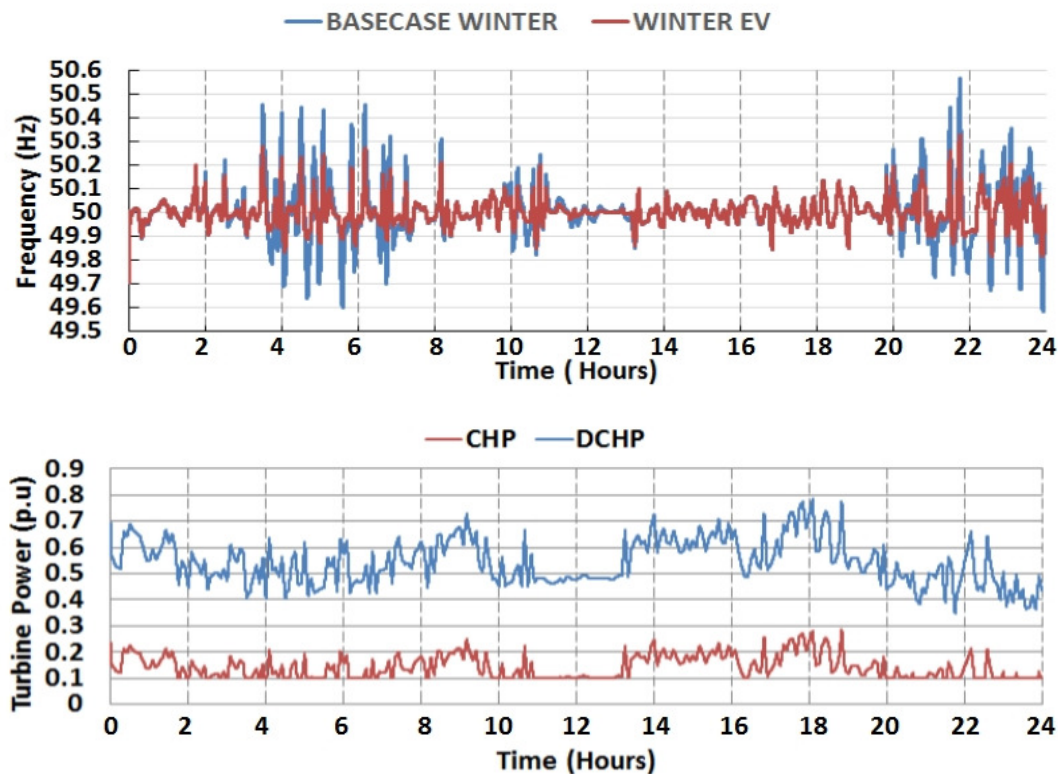


Figure 5.13 - Results of the power system with EV integration, during a winter day

Like the AE and HP, the EVs can also be used to both down and up regulation. The difference is that the EV can both act as a generator and a load. It is also able to provide V2G operation, which means generation of power into the grid as it can be seen in Figure 5.14. The active power consumption and generation of the EVs is shown in Figure 5.14.

It is seen that the EVs start to consume when down regulation is needed and act as a generator when up regulation is needed. A positive number above zero means that it acts like a load and consumes power from the grid in order to do down regulation. It can be seen that the consumption happens at the same time as the HPs and EVs, which verifies the operational condition. However, it starts going down to zero consumption when up regulation is needed and if the power system requires more power generated, it even acts like a generator and the values of the output power is now negative below the zero axis. In that case, the EVs has a V2G operation.

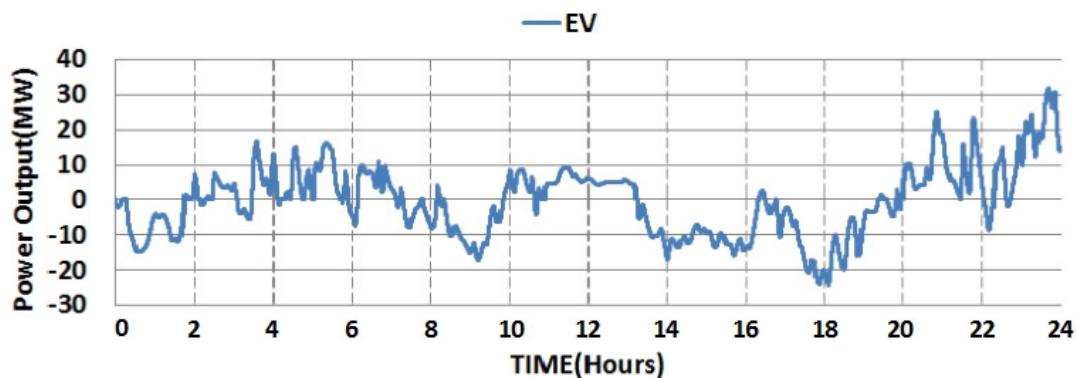


Figure 5.14 - EV parameters during a winter day

Additionally, the SOC of the EVs is shown in Figure 5.15.

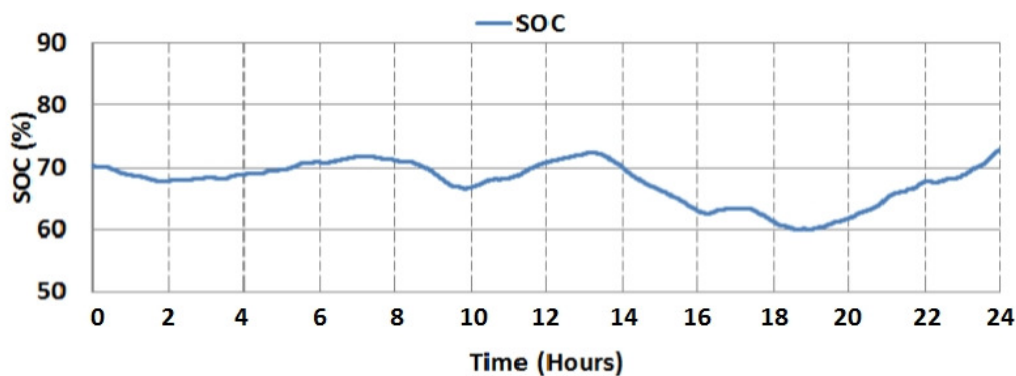


Figure 5.15 – State of Charge

It is seen that down regulation is needed between $t = 3$ h to $t = 7$ h and therefore, the EV starts increasing the consumption as seen in plot c. It is observed that the SOC increases when EVs act like a load with increasing consumption and decreases when the EVs acts like a generator, which is desired. The consumption is observed to increase during $t = 3$ h to $t = 7$ h due to the increasing consumption of the EVs.

5.3.2 Summer scenario

Figure 5.16 shows the results after implementing the EV technology during the summer scenario. The size of the EVs in the summer scenario is 49 MW, which equals to 7000 units that can be controlled. The participation factor of the EVs during the summer scenario decreased to 0.15 due to the SOC limits of the EVs. The participation factor given to the CHPs is 0.60, 0.25 for the DCHPs. Figure 5.16 shows the frequency fluctuation of the power system. During $t = 3$ h and $t = 7$ h, the maximum value is 50.317 Hz and minimum value is 49.750 Hz.

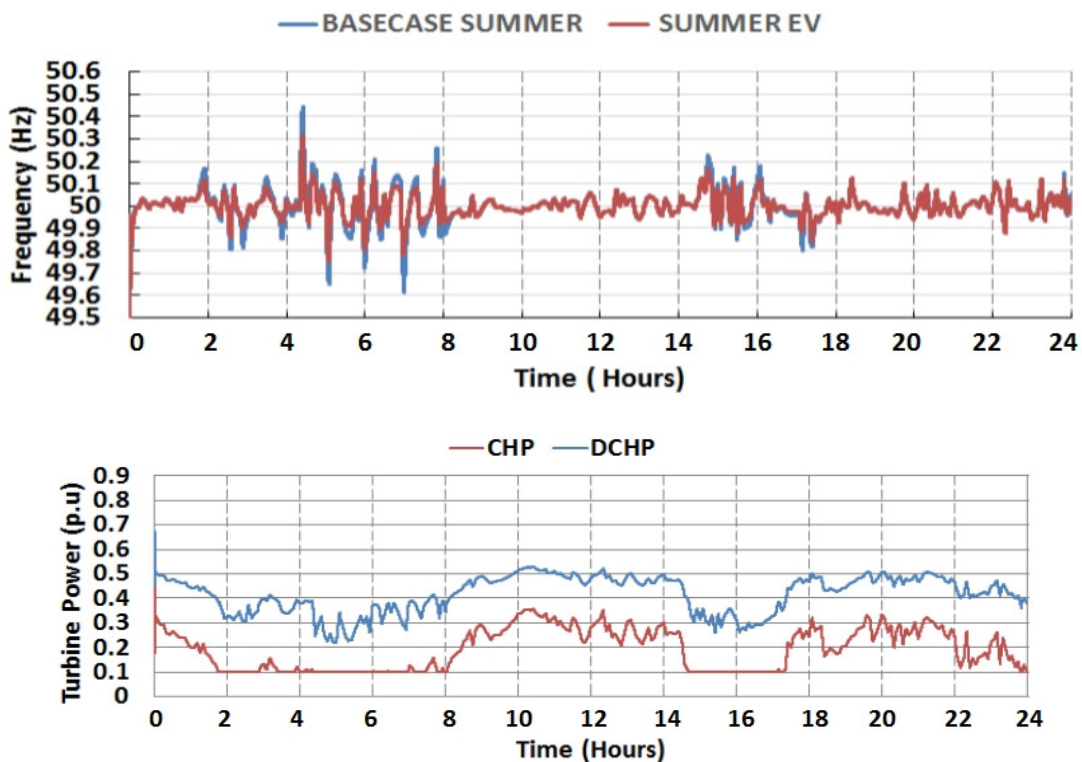


Figure 5.16 - Results of the power system with EV integration, during a summer day

Figure 5.17 represents the parameters of the EVs, which is the active power consumption.

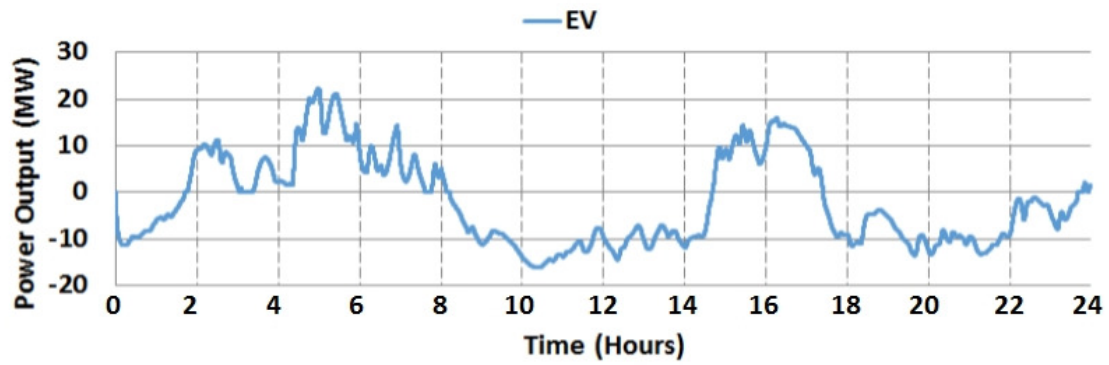


Figure 5.17 - EV parameters during a summer day

Additionally, the SOC of the EVs is shown in Figure 5.18.

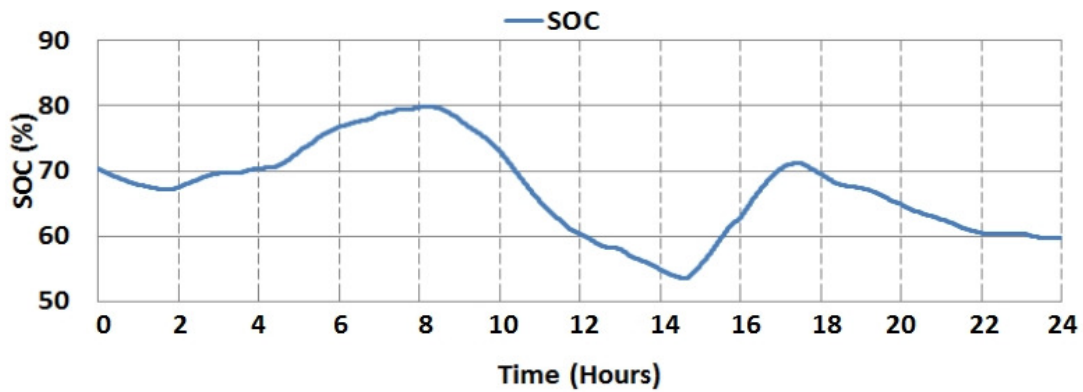


Figure 5.18 – State of Charge

It can be seen that the SOC is near the lower limit. Therefore, the participation is kept at 15 %.

5.4 Frequency support from all three Flexible Loads

In this section, the results of integration of all the flexible loads in the frequency regulation, is presented. In the following, the obtained results of this implementation is compared to the results obtained in the previous sections.

5.4.1 Winter scenario

Figure 5.19 shows the results of the implementation of all the flexible loads into the power system at the same time in order to provide frequency regulation with different units. During the scenario, all three flexible loads are connected to the LFC controller with different participation factors. The participation factor for the AEs is 0.20, 0.30 for the HPs and 0.30 for the EVs. The participation factors given to the CHPs is 0.15 and 0.05 for the DCHPs. It is in this scenario seen that the frequency peaks are slightly reduced compared to the cases with individual participation. The frequency is shown in Figure 5.19. The maximum value of the frequency is 50.282 Hz and the minimum value of the frequency is 49.832 Hz during $t = 3$ h and $t = 7$ h.

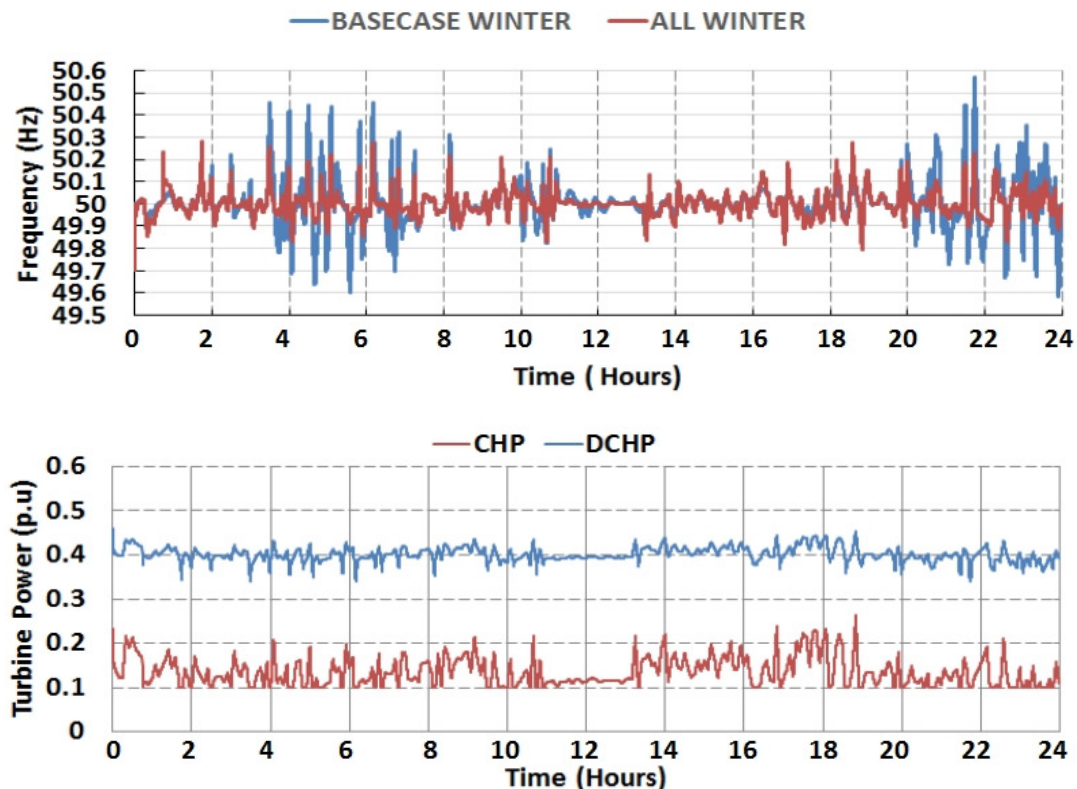


Figure 5.19 - Results of the power system with AE, HP, EV integration, during a winter day

The figure also shows the power production of CHPs and DCHPs. It is seen that the flexible loads provides a better frequency regulation compared to the base case due to their fast response. Figure 5.20 represents the parameters of the flexible loads. The figure shows the total active power consumption of the AEs, HPs and EVs. It is seen that the consumption of the AEs are less in this scenario. This is due to the extra addition of loads into the power system. The lower consumption of the flexible loads is due to the power set point. As seen in the figure, the consumption is almost near the base value and this is because the power set point sent to the AEs is lower than the base consumption most of the winter day. This proves that the base consumption can also provide frequency regulation in the power system. The power consumption of the HPs and EVs is also shown in Figure 5.20.

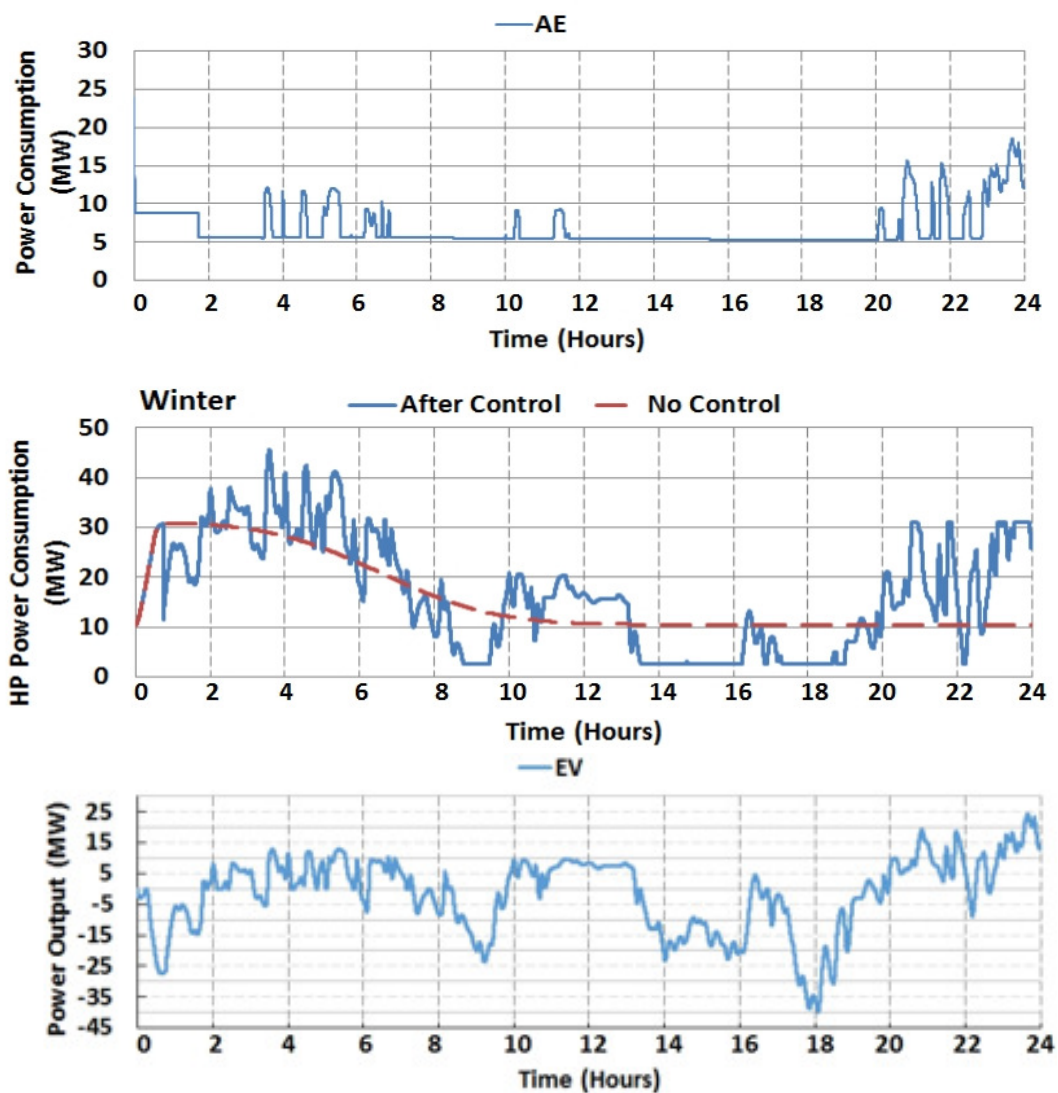
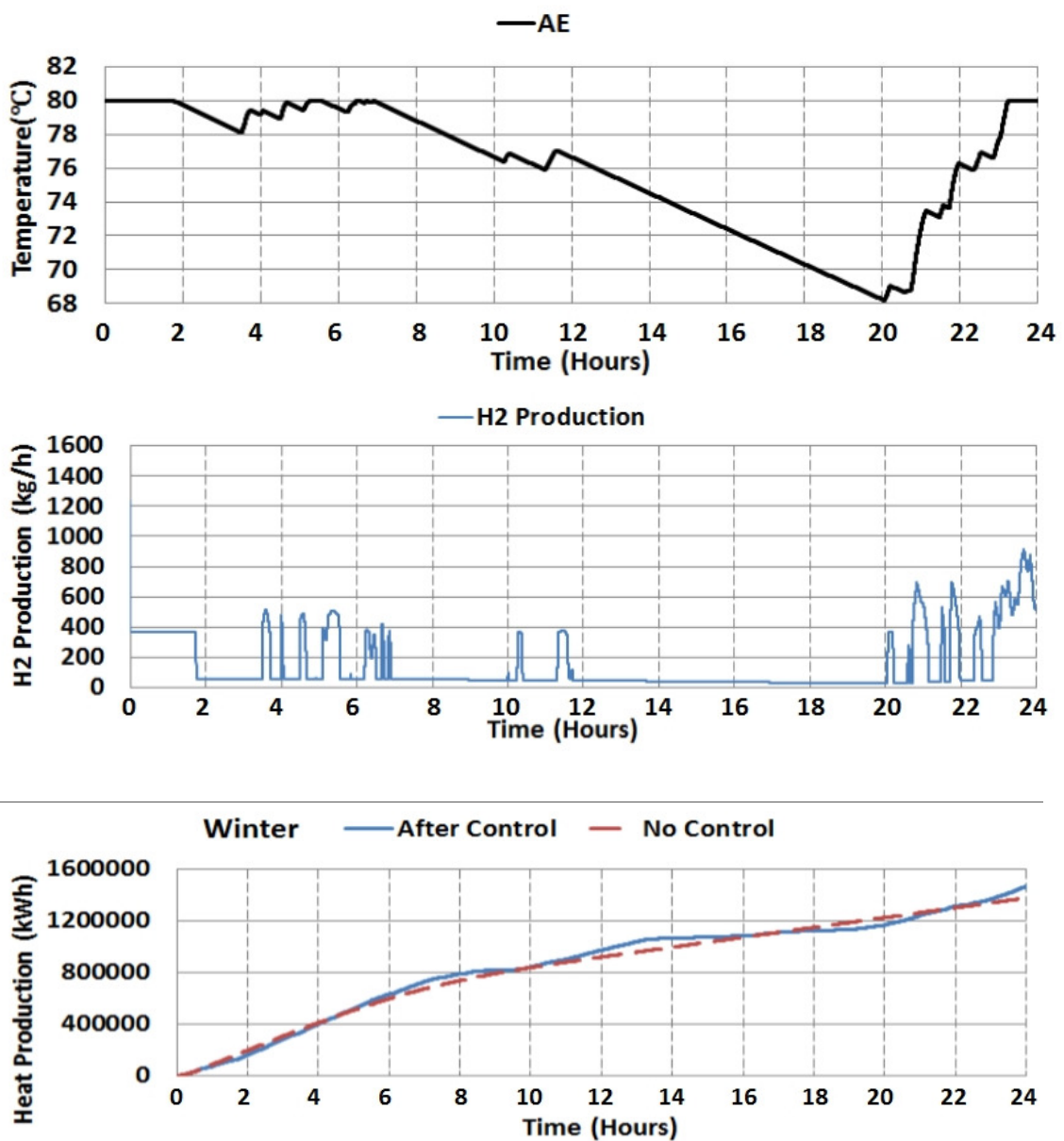


Figure 5.20 – AE, HP and EV parameters during a winter day

Figure 5.21 shows the constraints of the AEs, HPs and EVs. First, the temperature of the AE model is shown. It is seen that the temperature drops down to 68°C, due to the power set point to the AEs, which is mostly below the base consumption. Therefore, the temperature of the AE model keeps dropping. This results in a slow response of the AEs. Secondly, the H₂ production is shown in kg/h. It is seen that the peak production of hydrogen reaches approx. 800 kg/h due to the low operation of the AEs. Furthermore, the total heat production of the HPs is shown. The peak production is 1500 MWh, which almost matches the heat demand during the winter scenario. The SOC of the EVs is also shown in the figure.



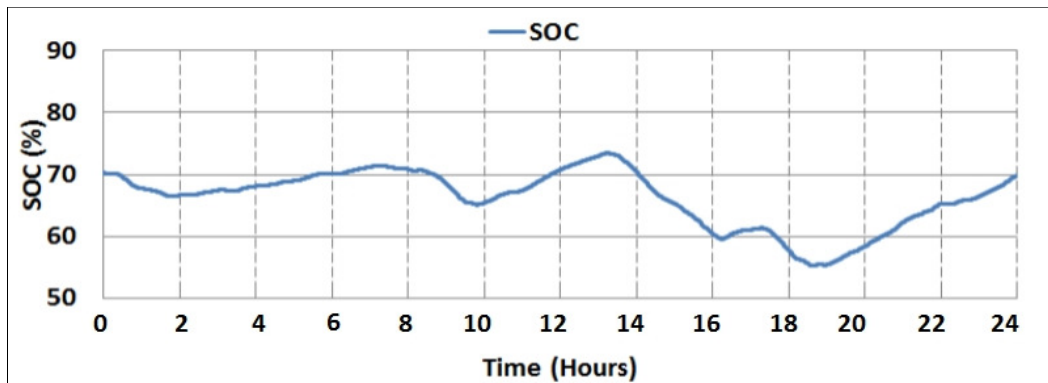


Figure 5.21 – AE, HP and EV constraints during a winter day

5.4.2 Summer scenario

Figure 5.22 shows the results of the implementation of all the flexible loads during the summer scenario. The participation factor for the AEs is 0.20, 0.15 for the HPs and 0.10 for the EVs. The participation factors given to the CHPs is 0.45 and 0.10 for the DCHPs. It is seen that the frequency peaks are reduced compared to the base case. The maximum value of the frequency is 50.248 Hz and the minimum value of the frequency is 49.790 Hz during $t = 3$ h and $t = 7$ h.

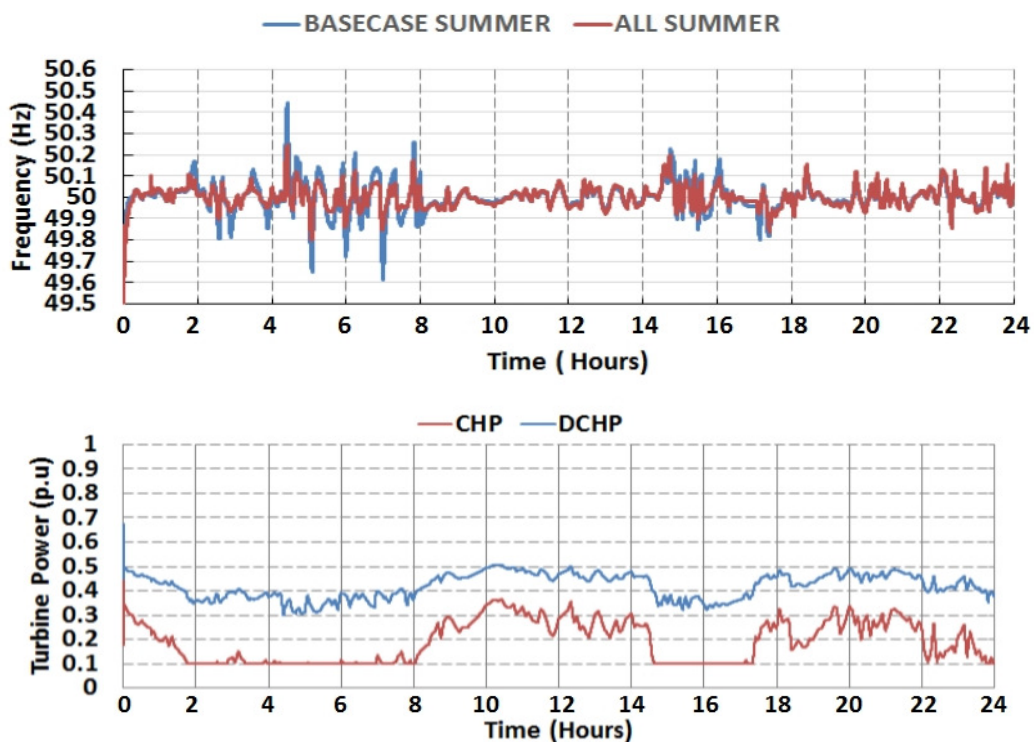


Figure 5.22 - Results of the power system with AE, HP and EV integration, during a summer day

Figure 5.23 represents the consumption and generation of the flexible loads.

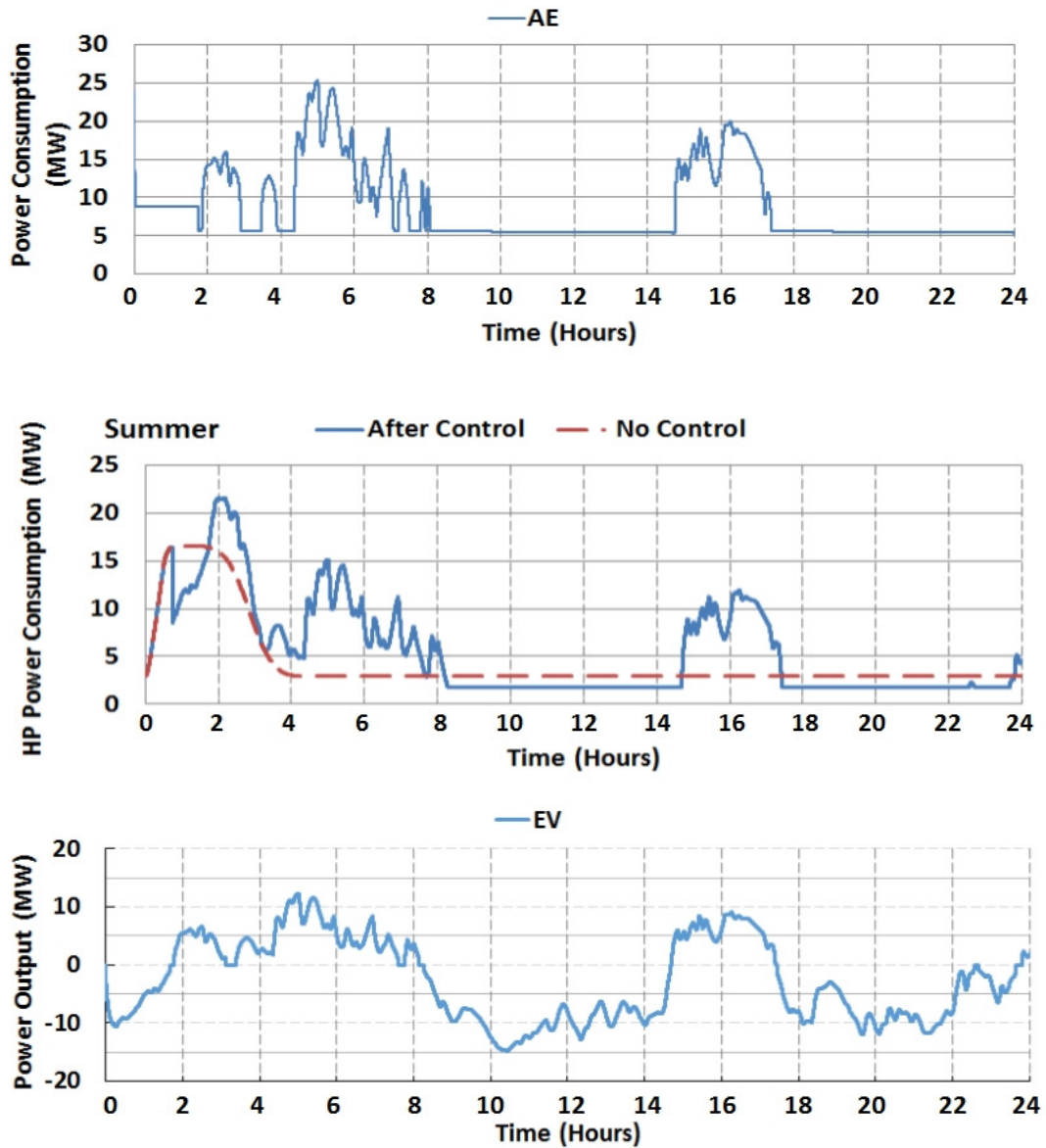


Figure 5.23 – AE, HP and EV parameters during a summer day

Figure 5.24 shows the constraints of the AEs, HPs and EVs. The temperature of the AE model is shown. It is seen that the temperature drops down to 73°C, due to higher usage of the AE model. If the consumption of the AE is higher, the temperature drop will be slower. Therefore, the response of the AE model is faster during this scenario. The hydrogen production is shown in kg/h . It is seen that the peak production of hydrogen reaches approx. 1200 kg/h . The total heat production of the HPs can be seen. It is seen that the peak production is 500 MWh. The SOC of the EVs is also shown in the figure.

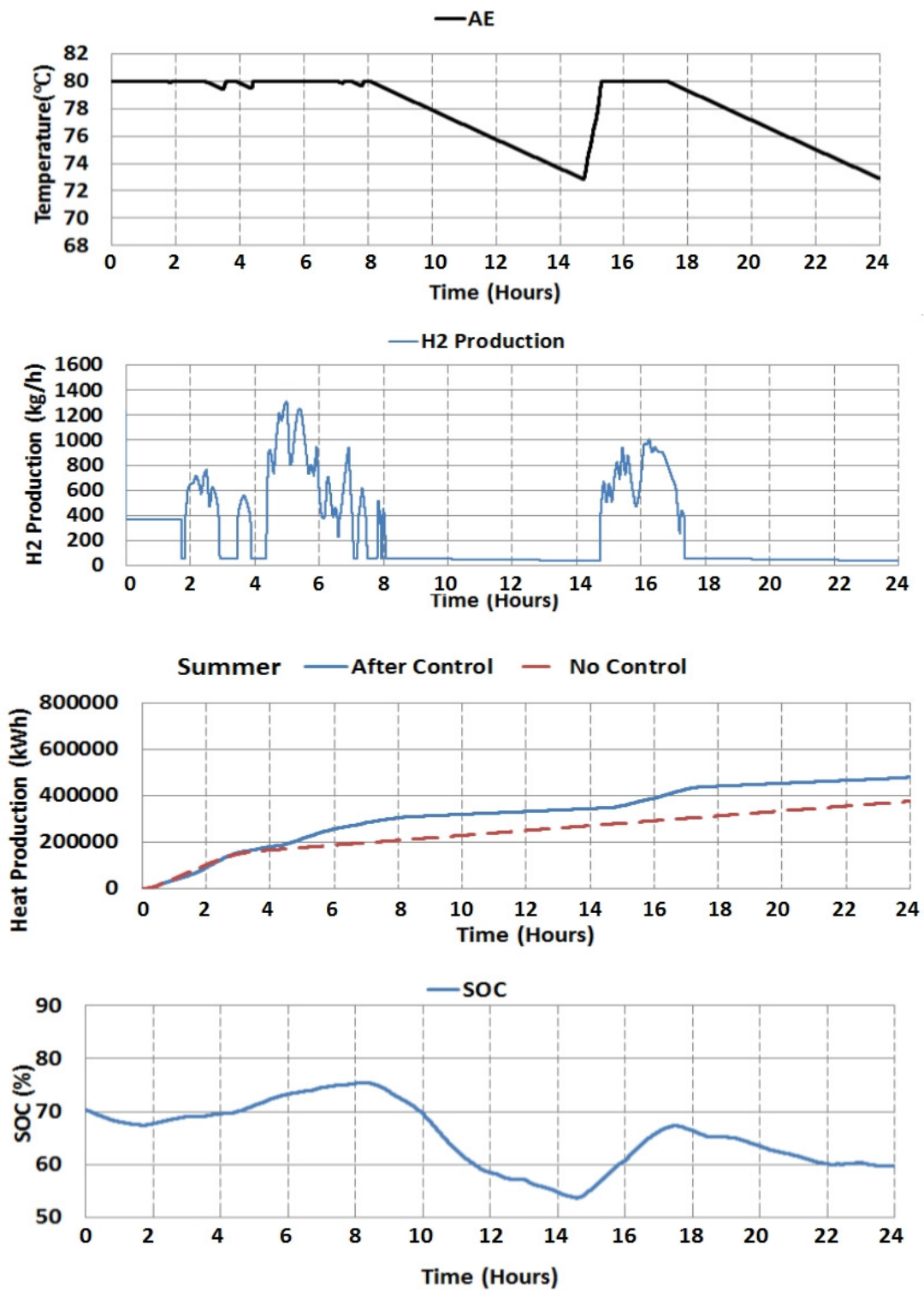


Figure 5.24 – AE, HP and EV constraints during a summer day

5.5 Statistical analysis

In the present chapter, four different frequency regulation cases have been tested and compared to the base case. Table 8 and Table 9 shows the values concerning the frequency deviations in the power system before and after regulation. First, the minimum values and maximum values of the frequencies fluctuations are picked out for 24 hours. Then, the standard deviation is calculated for the frequencies with N number of observations (depends on the chosen step size in DigSILENT). The standard deviation is calculated by the given formula in (5.1)

$$\sigma = \sqrt{\frac{1}{N-1} \sum_{i=1}^N |x_i - \mu|^2} \quad (5.1)$$

, where μ is the mean of x as given in (5.2)

$$\mu = \frac{1}{N} \sum_{i=1}^N A_i \quad (5.2)$$

The parameters are calculated in MATLAB for the whole simulation (24 hours).

Table 8 - Frequency deviation during winter and summer cases (One by One)

	Base Case		Integrating AE		Integrating HP		Integrating EV	
	Winter	Summer	Winter	Summer	Winter	Summer	Winter	Summer
f_{min}	49,5842	49,6158	49,7127	49,75	49,7288	49,6856	49,8155	49,7503
f_{max}	50,567	50,4464	50,4001	50,2967	50,3386	50,3564	50,3248	50,3173
f_{STD}	0,1043	0,0689	0,0776	0,0539	0,0656	0,0578	0,0595	0,0512

Table 9 - Frequency deviation during winter and summer cases (All Flexible Loads)

	Integrating all flexible loads	
	Winter	Summer
f_{min}	49,7964	49,8033
f_{max}	50,2821	50,2481
f_{STD}	0,0507	0,0495

The standard deviations are shown and compared in Figure 5.25.

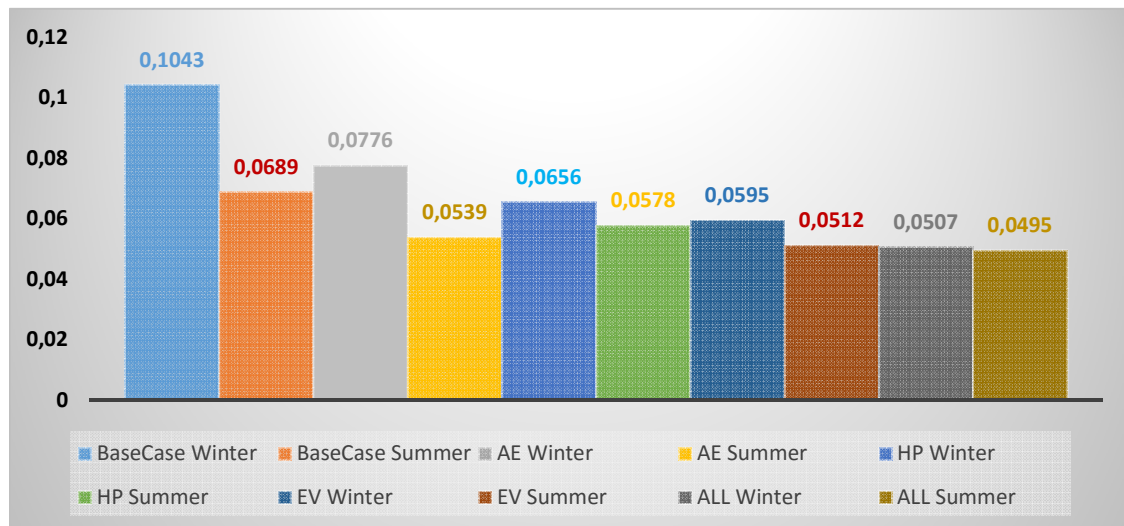


Figure 5.25 - Comparison of standard deviations

The base case presents a frequency profile, which is undesired in a real power system. The first improvement is made by integrating the AEs in the power system, which made a significant peak reduction of the frequency. However, the values are still high, which is due to the power capacity limits. The introduction of the HPs and EVs also drastically decreased the fluctuation of frequency of the power system. Especially, the response of EVs are the fastest among all the flexible loads. Therefore, the EVs might be more attractive as secondary reserve if the fast response is considered. If the consideration is availability, both HPs and EVs seems to be less feasible as secondary reserves.

In a real power system, the availability of the EVs and HPs is unpredictable. Especially during the summer scenario, less HPs will be used in households and more people will be driving the EVs. Therefore, HPs and EVs it might be infeasible to use these two flexible

loads as secondary reserves in the power system. Therefore, in this case the AE will be the most beneficial secondary reserve due to the unchanged size. Opposite, the AEs in the power system might also be used for other purposes, like H2 support to the gas network etc. Even though it is assumed that AEs will only be used to provide frequency regulation and keep the unchanged size, they might still have less availability in a real power system. This is of course only valid with limited sizes of HPs and EVs. The total amount of HPs and EVs in a power system might make a final decision for their availability and usage as secondary reserves because higher numbers of HPs and EVs might maybe not even give capacity and availability problems at all. Depending on the numbers of the flexible loads, which are available, the participation factor can be increased for an increasing amount of AEs, HPs and EVs. Higher numbers of flexible loads in a power system means that the aggregators will be able to control more of them to provide frequency regulation and therefore the availability will also increase proportionally. In a real power system, the participation factor could increase with the number of controllable units. If there were too much availability of flexible loads, it would even be possible to let the flexible loads handle the frequency regulation in the power system as secondary reserves. In this way, the TSO will get much more benefit of using the flexible loads as secondary reserves instead of the conventional power plants. However, this is not a part of this study case and therefore it will be a future work.

As it can be seen in Table 8, the standard deviations are lower with integration of flexible loads. This means that the deviation from mean are less in those cases with a controllable load added to the power system. This proves the fact that the flexible loads have a faster response than the CHPs and DCHPs and are highly controllable in the power system. It is seen that the standard deviation is lowest with the control of EVs. This is due to the high size of the controllable units and the fast response.

Table 9 shows the minimum, maximum and standard deviation of the power system frequency when all three flexible loads are integrated together. It shows that this case performs an even better frequency regulation due to the difference in control margins and availability of the flexible loads. When one of the flexible loads are less available or has less capacity, the other one can contribute with frequency regulation, which is an advantage in a real power system. The standard deviation is less with control of all three flexible loads in the power system, which was expected. In order to simplify comparison, Figure 5.25 shows the standard deviations for all the scenarios.

The following chapter will finalize the analysis with a conclusion to this study case.

6 Conclusion

This study case dealt with different scenarios analyzed in a 9-bus network, which had a high penetration with high wind power generation. The uncertain power generation from the wind turbines is challenging for the stable and reliable operation of the power system. The high penetration of wind power plants replacing the conventional power plants in Denmark requires new solutions for the large imminent power generation. In order to integrate the high share of wind power, the electrical power system must be more flexible and intelligent.

The flexible grid can have a more efficient use of the distributed energy sources. The flexible consumption, generation units and storage systems can be utilized across the different sectors such as electricity, heat and transport through the local control centers with smart controls.

In this study case, the role of the flexible loads to support large-scale wind power is verified through the test grid 9-bus network in both winter and summer scenarios. Different scenarios are analyzed in order to different the flexibility of the different flexible loads over the conventional power plants in providing secondary reserves. Aggregated AE, HP and EV models are modelled in DigSILENT representing the storages in the power system. The HPs are modelled according to different heat demand during winter and summer scenarios control limits. The EV model has the capability to represent the SOC limits. The conventional Load Frequency Control model is modified to integrate with AEs, HPs and EVs. The CHPs and DCHPs are modified to have a generation rate limits in the LFC model.

The results of the individual participation has shown that the flexible loads gives a better performance as secondary reserves compared to the conventional generation units. The application of flexible loads as secondary reserves were analyzed for both winter and summer scenarios with higher and lower availability of HPs and EVs. The scenarios were set up with continuous up and down regulation requirements throughout the day. First, the flexible loads were added one by one in order to analyze the operational constraints of each model. The integration of flexible loads into the power system has shown that it can minimize the frequency fluctuation in the 9-bus network when compared to the base with CHPs and DCHPs alone. It is also observed that the regulation from CHPs and DCHPs reduces after the integration of flexible loads in Load Frequency Control.

The results demonstrate that the fast operation of AEs, HPs and EVs provides a better performance than the CHPs and DCHPs as ancillary services. The AE provides a faster and more flexible smooth regulation service, as long as the operational temperature is high enough. It is seen that it can be both used for down regulation by increasing the consumption and up regulation by decreasing the consumption in the power system. However, H2 loads are required in order to consume the excess of H2 generation.

The same goes for HPs, which fast responding due to the ON-OFF operational conditions. The HPs can also both down and up regulate as AEs as observed from the results. Hence, the heat demand has to be met in all the scenarios. If the heat generation is higher than the demand, heat loads are required. If the generation is less than the demand, another solution for supplying heat to the area is required which is out of the scope of this study case.

The EVs are observed to operate both as a flexible load and a flexible generator depending on the power regulation requirement, which could be an interesting solution for replacing the conventional power reserves. The scenarios and control strategies used in this study case can easily be tested in other power systems, where large scale wind power penetration is considered. The regulation ability of the EVs depend pretty much on the SOC limits and the availability for control operation as observed. Therefore, the driving pattern of the EVs, storage capacity and charging/discharging patterns need a detailed study on different networks. The operation as a load or a generator depends also on the stiffness of the grid. In a weak network, too many EVs connected at once will cause voltage problems. On the other hand, the generation and load changes in a too strong network will have less effect. This is valid for all the flexible loads in the grid.

The integration of all the flexible loads in the power system at the same time has shown that the standard deviation of the power system frequency were reduced from 0,1043 to 0,0595 during the winter scenario and from 0,0689 to 0,0512 during the summer scenario. This shows that the frequency deviation from the mean value (50 Hz) is less with the cases where flexible loads are integrated and intelligently controlled in the power system. As an outcome of this, it can be concluded that the flexible loads has more potential as secondary responses than the CHPs and DCHPs.

6.1 Future work

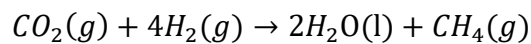
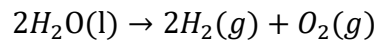
Although some results presented in this report to demonstrate how the flexible loads help the load frequency control in power system, this project can also be improved in the future. The following ideas could be explored in the future:

- The control strategy could be tested with different grids.
- Stability issues could be considered.
- Wind lull uncertainties can be analyzed.
- A forecast model could be integrated with LFC to utilize flexible loads better to reduce their uncertainties.
- The heat demand data should be collected from different areas in order to have a more realistic data.
- A limitation for the energy outputs might be considered.
- An advanced participation factor calculation method based on smart flexible market concepts & economic dispatch.
- The LFC operation could be tested with different sizes of flexible loads (bigger or smaller)
- Studies of economic benefits to the flexible demand and generation owners participating in the LFC strategy.
- IEEE 39 or real large power systems with generators and loads distributed in different control areas. Hereby, tie line bias control is also analyzed.

Appendix A

Theory and topologies of water electrolysis

Electrolysis is referred to generate hydrogen and oxygen by decomposition the water molecule. Methanation is a chemical process of generating methane from hydrogen and carbon dioxide synthesis reaction [70]



Over the decades, water electrolysis was a common way to produce hydrogen for industrial processes. Nowadays, it is attracting much interest for energy applications. In water electrolysis, water can be decomposed into hydrogen and oxygen by applying an electric current. When the electrolyzer is supplied by an external DC power, the current will flow between the anode and cathode which are separated and placed in electrolyte. Electrolyte is a chemical substance in order to raise the ionic conductivity, which could be different depending on the choice of technologies. But in general, hydrogen is generated at the cathode and the oxygen is generated at the anode in the electrolysis process. Nowadays, there are three main technologies named alkaline electrolysis, proton exchange membrane electrolysis and solid oxide electrolysis, which have different advantages and drawbacks [70].

Those technologies will be introduced in details as following:

Alkaline Electrolysis (AE)

The Alkaline electrolyzer has a long history for commercial applications. The electrolyte commonly used potassium hydroxide (KOH) and sodium hydroxide (NaOH) as an aqueous alkaline solution and nickel-coated steel is usually used to manufacture electrodes.

Reliability is the most attractive feature of Alkaline Electrolyzer. The lifetime of Alkaline Electrolyzer normally can approximately reach 15 years and the efficiency varies from 47% to 82% depending on the operation condition. Another advantage is that it is also suitable for massive production due to large stack size. Besides, from the commercial point of view, another obvious advantage of alkaline electrolyzer is that the cost is much cheaper than other technologies [70].

Proton exchange membrane electrolysis (PEM)

The first prototype of proton exchange membrane electrolyzer was established in 1960s. As the name implied, a proton exchange membrane or polymer membrane is used for electrolyte. The efficiency of this type is similar with AE, which is around 48% - 65%. It has good flexibility to response fluctuations in electrical input, which is important consideration when electrolyzer integrated with wind farm [70].

Solid oxide electrolysis (SOE)

The operation temperature of solid oxide electrolyzer usually is around 500°C to 1000°C. The boiling water turns it into vapor at the high temperature and the steam can be easily dissociated into hydrogen and oxide ions. The oxide ions pass through the solid oxide electrolyte to the anode and recombine to oxygen molecules. The solid oxide electrolyzer has higher efficiency compared with other type electrolyzer, which even can reach 85%. However due to the extreme reaction conditions, the solid oxide electrolyzer is still under research stage [70].

Appendix B

EV battery technologies

NiMH battery

NiMH battery is composed of a positive electrode which made by metal hydride and a negative electrode which made by Ni(OH)_2 with electrolyte in between. During the charge, water is decomposed into protons and hydroxide ions. The proton combines with electron which is provide by voltage source and enter the negative electrode. The hydroxide ions will enter the negative electrode. Meanwhile, some hydroxide ions will recombine with protons which is provide the Ni(OH)_2 and form water molecules on the surface of positive electrode. Nickel oxyhydroxide (NiOOH) is formed during the process. The whole process is reversed during discharge [37].

Li-ion battery

In the Li-ion battery, the negative electrode is most commonly made of graphite and the positive electrode is made of Li-containing metal oxide. During the charge, the Li ions are hops onto the surface of positive electrode and driven by the potential difference finally arrived at negative electrode. During the process, the oxidation state of the host metal will increase at positive electrode and LiC_6 is form at the negative electrode [37].

Appendix C

Technical requirements for frequency control

The grid code is a technical specification, which defines all the rules in order to ensure a stable electrical power system. Grid codes are full of requirements, which the TSO must follow. Therefore, it is important that the requirements for the frequency fluctuation in this study case are well known.

Swing equation

One of the main parameters in a power system is frequency. It is necessary to keep the frequency within the allowable range in order to maintain a stable power system. It is assumed that a synchronous generator developing a torque T_e running at a synchronous speed ω_{ss} under steady state. The mechanical torque T_m without losses in the system would be given by (6.1) [42]

$$T_m = T_e \quad (6.1)$$

If there is a disturbance included during the steady state, the torque will be accelerating or deaccelerating which given by (6.2) [42]

$$T_a = T_m - T_e \quad (6.2)$$

The losses are neglected under the steady state operation. Let's assume that the three phase generator is driven by a prime mover, from the laws of rotation the equation for the rotor is given by (6.3) [42]

$$J \frac{d^2 \theta_m}{dt^2} = T_a = T_m - T_e \quad (6.3)$$

, where

- J – Moment of inertia of the rotor
- θ_m – The angular position of the rotor
- T_a – Accelerating torque
- T_m – Mechanical torque of the prime mover
- T_e – Electrical torque

The angular position is measured with respect to the stationary reference frame. To represent it with the synchronously rotating frame, it is given by (6.4) [42]

$$\theta_m = \omega_s t + \delta_m \quad (6.4)$$

, where δ_m is the rotor position right before the time of disturbance. Defining the angular speed as seen in (6.5) [42]

$$\omega_m = \frac{d\theta_m}{dt} = \omega_{ms} + \frac{d\delta_m}{dt} \quad (6.5)$$

Eq. (6.5) can now be rewritten into (6.6) [42]

$$J \frac{d^2\delta}{dt^2} = T_a = T_m - T_e \quad (6.6)$$

If we multiply both sides by the angular rotor speed, we will get Eq. (6.7) [42]

$$J\omega_m \frac{d^2\delta}{dt^2} = \omega_m T_a = \omega_m T_m - \omega_m T_e \quad (6.7)$$

, where $\omega_m T_a$ is the accelerating power, $\omega_m T_m$ is the mechanical power and $\omega_m T_e$ is the electrical power. Eq. (6.7) can be rewritten into (6.8) [42]

$$J\omega_m \frac{d^2\delta}{dt^2} = P_a = P_m - P_e \quad (6.8)$$

The term $J\omega_m$ is defined as the inertia constant and denoted by M. The kinetic energy of the rotating mass is given by (6.9) [42]

$$W = \frac{1}{2} J \omega_m^2 \quad (6.9)$$

, where normalized the inertia constant is given by (6.10) [42]

$$M = \frac{2W}{\omega_m} \quad (6.10)$$

Therefore, the swing equation is given by (6.11) [42]

$$M \frac{d^2\delta}{dt^2} = P_m - P_e \quad (6.11)$$

It is known that electrical angular velocity and mechanical angular velocity is given by (6.12) [42]

$$\omega_s = \frac{2}{p} \omega_m \quad (6.12)$$

An important quantity as H constant is defined in seconds in (6.13) [42]

$$H = \frac{\textit{kinetic energy at rated speed}}{\textit{machine rating}} = \frac{W}{S_{base}} \quad (6.13)$$

Substituting (6.9), (6.10), (6.11), (6.12) ad (6.13), we get (2.1) [42]

$$\frac{2H}{\omega_s} \frac{d^2 \delta}{dt^2} = P_m - P_e \quad (6.14)$$

Eq. (2.1) shows that the difference between generation and demand power will cause a change in the rotational speed of the generator, which will result a change in in the grid frequency [42].

Appendix D

The parameters of the grid lines are stated in Table 10.

Table 10 - 9-bus OHL parameters

Element no	From bus	To bus	R	X
1	7	8	4,4965	38,088
2	8	9	6,2951	53,3232
3	5	7	16,928	85,169
4	6	9	20.631	89,83
5	4	5	5,29	44,965
6	4	6	8,993	48,668

The parameters of the transformers are stated in Table 11.

Table 11 - 9-bus transformer parameters

Element no	Size	LV kV	HV kV	SR voltage uk
T1	400MVA	16,5	230	8,79
T2	250MVA	13,8	230	8,79
T3	250MVA	18	230	12,5

The parameters of the generation units are stated in Table 12.

Table 12 - Generator parameters

Element no	Size	N. Voltage kV	xd	xq
G1	287,5 MW	16,5	0,36	0,24
G3	212,5 MW	13,8	1,68	1,61

Appendix E

The parameters of the LFC system is listed in Table 13.

Table 13 - LFC parameters

Bias factor	186,5 MW/Hz	
PI	0,3	0,005
T	4 s	

The parameters of the turbine control is listed in Table 14.

Table 14 - Turbine control parameters

Time delay	4 s
Rate limiter	-0.00066 and 0.00066 (4%) -0.0016 and 0.0016 (10%)

The parameters of the speed governor system is listed in Table 13.

Table 15 – Speed governor parameters

	R	Governor gain
CHP	0.1 p.u	10 p.u
DCHP	0.04 p.u	25 p.u

Appendix F

The parameters of the CHP model is shown in Table 16.

Table 16 - CHP parameters

Parameters	Description	Variable
K	Controller gain	25 p.u
T1	Governor time constant	0.2 s
T2	Governor derivative time constant	1 s
T3	Servo time constant	0.6 s
T4	High pressure turbine time constant	0.6 s
T5	Intermediate Pressure Turbine Time Constant	0.5 s
T6	Medium Pressure Turbine Time Constant	0.8 s
T7	Low Pressure Turbine Time Constant	1 s
K1	High Pressure Turbine Factor	0.3 p.u
K2	High Pressure Turbine Factor	0 p.u
K3	Intermediate Pressure Turbine Factor	0.25 p.u
K4	Intermediate Pressure Turbine Factor	0 p.u
K5	Medium Pressure Turbine Factor	0.3 p.u
K6	Medium Pressure Turbine Factor	0 p.u
K7	Low Pressure Turbine Factor	0.15 p.u
K8	Low Pressure Turbine Factor	0 p.u

Appendix G

The parameters of the DCHP model is shown in Table 17.

Table 17 - DCHP parameters

Parameters	Description	Variable
R	Governor droop	0.1 p.u
T1	Controller time constant	0.4 s
T2	Actuator time constant	0.1 s
T3	Compressor time constant	3 s
AT	Ambient Temperature Load limit	1 p.u
Kt	Turbine Factor	2 p.u

Appendix H

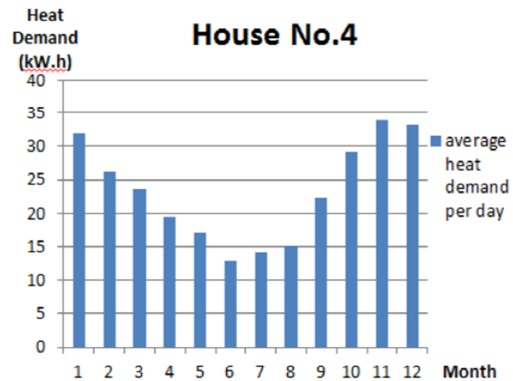
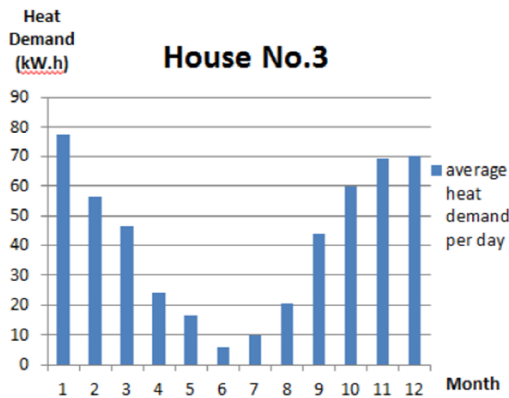
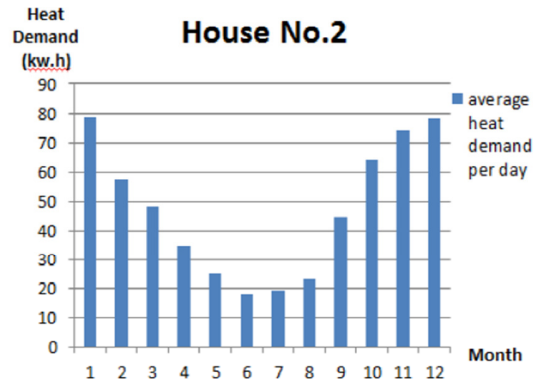
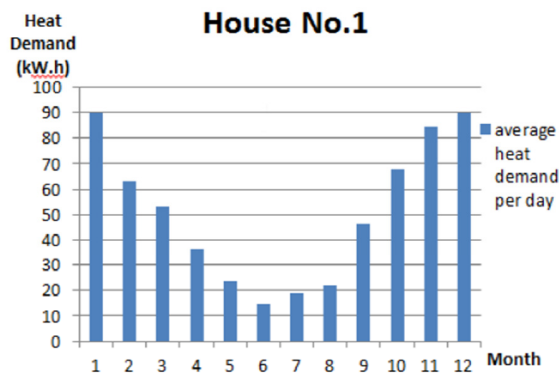
The parameters of the AE model is shown in Table 18.

Table 18 - AE parameters

	Parameters	Quantity
General	<i>Rated power (kW)</i>	355
	<i>Operation Pressure (bar)</i>	7
	<i>No. of Cells</i>	180
	<i>Max. DC Voltage (V)</i>	342
	<i>Min. DC Voltage (V)</i>	221
	<i>Max. Opert. Temp (°C)</i>	80
Cell I-U Curve	<i>r1(Ω/m²)</i>	$7.331e - 5$
	<i>r2(Ω/m²)</i>	$-1.107e - 7$
	<i>s1(V)</i>	$1.586e - 1$
	<i>s2(V/°C)</i>	$1.378e - 3$
	<i>s3(V/°C²)</i>	$-1.606e - 5$
	<i>t1(m²/A)</i>	$1.599e - 2$
	<i>t2(m²/A°C)</i>	-1.302
	<i>t3(m²/A°C²)</i>	$4.213e2$
	<i>A(m²)</i>	0.25
Faraday Efficiency	<i>a1(%)</i>	99.5
	<i>a2(m²/A)</i>	-9.5788
	<i>a3(m²/A°C)</i>	-0.0555
	<i>a4(m⁴/A)</i>	1502.7083
	<i>a5(m⁴/A°C)</i>	-70.8005
Thermal Model	<i>Rt(°C/W)</i>	0.334
	<i>Ct(J/°C)</i>	$5.38e6$
	<i>UAhx(W/°C)</i>	2100
	<i>mcool(kg/s)</i>	1.2
Compressor	<i>Rated Power (kW)</i>	70
	<i>No. of Stages</i>	2
	<i>NG (-)</i>	0.486
	<i>P2 (bar)</i>	150

Appendix I

The heat demand data is provided by Prof. Mads Pagh Nielsen in Aalborg University. The data is collected every 15 minutes over a year in four different houses, which are located in Funen. The figure below shows the average heat demand per day in a month after data arrangement.



The parameters of the HP is shown in Table 19.

Table 19 - HP parameters

Parameters			Value
Tstart	Start delay(s)		300
Thpc	Control delay(s)		30
Prated	Total Rated Power Consumption of Installed HPs (Kw)		51.3 MW (winter) 34.2 MW (Summer)
Winter	TAVG	Average value (s)	23751
	TSD	Standard deviation (s)	8550
	Erequest	Thermal energy request(kWh)	46,57
Summer	TAVG	Average value (s)	10268
	TSD	Standard deviation (s)	1781
	Erequest	Thermal energy request(kw.h)	19.35

7 Bibliography

- [1] B. K. Bose, "Global Warming: Energy, Environmental Pollution, and the Impact of Power Electronics," *Industrial Electronics Magazine, IEEE*, vol. 4, no. 1, pp. 6-17, March 2010.
- [2] GWEC, "Global wind statistics 2015," 10 Feb 2016. [Online]. Available: http://www.gwec.net/wp-content/uploads/vip/GWEC-PRstats-2015_LR.pdf.
- [3] G. G. Pillai, G. A. Putrus and N. M. Pearsall, "The potential of demand side management to facilitate PV penetration," in *Innovative Smart Grid Technologies - Asia (ISGT Asia), 2013 IEEE*, Bangalore, India, 2013.
- [4] I. B. Spliid, "Danish Energy Agency, Energistyrelsen, Stamdataregister for vindkraftanlæg," [Online]. Available: <http://www.ens.dk/info/tal-kort/statistik-noegletal/oversigt-energisektoren/stamdataregister-vindmoller>.
- [5] D. E. Agency, "Energy Strategy 2050 – from coal, oil and gas to green energy," 2011.
- [6] Danish Ministry of Climate, Energy and Building, "Smart Grid Strategy: The intelligent energy system of the future," May 2013.
- [7] A. Suwannarat, "Integration and Control of Wind Farms in the Danish Electricity," AAU, 2007.
- [8] A. M. M. O. Gillian Lalor, "Frequency Control and Wind Turbine Technologies," *IEEE Transactions On Power System*, vol. No.4, p. Vol.20, Nov 2005.
- [9] E. & D. E. Association, "Smart grid in Denmark 2.0," 2011.
- [10] C. W. Gellins, "The Concept of Demand-Side Management for Electric Utilities,IEEE," 1985.
- [11] Association of European Automotive and Industrial Battery Manufacturers(EUROBAT), "Battery Energy Storage for Smart Grid Applications," EUROBAT, 2013.
- [12] The Danish Government, "Our Future Energy," Copenhagen, Nov 2011.

- [13] T. Schaaf, J. Grünig, M. R. Schuster, T. Rothenfluh and A. Orth, "Methanation of CO₂ - storage of renewable energy in a gas distribution system," *Energy, Sustainability and Society, SpringerOpen journal*, vol. 4, no. 2, Dec 2014.
- [14] Energinet.dk, 13 Oct. 2014. [Online]. Available: <http://www.energinet.dk/da/anlaeg-og-projekter/generelt-om-elanlaeg/Sider/default.aspx>. [Accessed Sep. 2015].
- [15] Energinet.dk. [Online]. Available: <http://www.energinet.dk/DA/El/Sider/Elsystemet-lige-nu.aspx>. [Accessed 27 02 2016].
- [16] Energinet.dk. [Online]. Available: <http://www.energinet.dk/EN/KLIMA-OG-MILJOE/Miljoerapportering/VE-produktion/Sider/Vind.aspx>. [Accessed 27 02 2016].
- [17] Danish Energy Agency, "Energy Statistics 2013," Danish Energy Agency, Copenhagen, 2013.
- [18] E. Energinet.dk, "TECHNOLOGY DATA FOR ENERGY PLANTS," Energinet.dk, Energistyrelsen, May 2012.
- [19] Energinet.dk, "Gas in Danmark 2015," Energinet.dk.
- [20] E. Christian Guldager Corydon, "Udvikling i dansk vindenergi siden 2010".
- [21] Energinet.dk, "Ancillary services to be delivered in Denmark Tender conditions," Energinet.dk, 2012.
- [22] N. - N. E. Regulators, "Harmonising the balancing market - Issues to be considered," 2010.
- [23] Energinet.dk, "Regulation C2 - The balancing market and balance settlement," 2008.
- [24] Energinet.dk, "Smart grid i Danmark".
- [25] A. P. B. B.-J. Z. C. Iker Diaz de Cerio Mendaza, "Generation of Domestic Hot Water, Space Heating and Driving Pattern Profiles for Integration Analysis of Active Loads in Low Voltage Grids," 2013.
- [26] E. a. D. E. Association, "Smart grid in denmark 2.0".

- [27] L. G. a. P. S. A. Ursua, "Hydrogen production from water electrolysis: Current status and future trends," *Proceedings of the IEEE*, vol. 100, no. 2, pp. 410–426, Feb 2012.
- [28] "water electrolysis:& renewable energy ssysytems," fuel cell today, 2013. [Online]. Available: http://www.fuelcelltoday.com/media/1871508/water_electrolysis___renewable_energy_systems.pdf. [Accessed March 2016].
- [29] D. H. a. W. D'haeseleer, "The use of the natural-gas pipeline infrastructure for hydrogen transport in a changing market structure," 2007. [Online]. Available: <http://www.sciencedirect.com/science/article/pii/S0360319906004940>.
- [30] K. A. a. D. Pinchbeck, "Admissible hydrogen concentrations in natural gas systems," 2013.
- [31] "Largest power-to-gas facility now operating with hydrogenics tech," Fuel Cells Bulletin, 2013.
- [32] G. S. M. I. P. B. a. A. M. A. Schäfer, "Modeling Heat Pumps as Combined Heat andPower Plants in Energy Generation Planning," 2012.
- [33] d. foss, "DHP-A Opti air source heat pump data sheet," 26_09_2015.
- [34] Energinet.dk, "Effektiv anvendelse af vindkraftbaseret el i danmark - samspil mellemvindkraft, varmepumper og elbiler," 2009.
- [35] M. Akmal, "Impact of high penetration of heat pumps on low voltage distribution networks".
- [36] J. C. Fox, "A voltage flicker suppression device for residential air conditioners and heat pumps".
- [37] C. W. L. Y. W. a. K. S. Kwo Young, "Electric Vehicle Battery Technologies," in *Integration into Modern Power NetworksIntegration into Modern Power Networks*, springer, 2013, pp. 15-55.
- [38] N. the United Nations Environment Programme, "Hybrid Electric Vehicles: An overview of current technology and its application in developing and transitional countries," Sept 2009.

- [39] A. H. N. J. Ø. S. T. C. F. M. Y. C. C. T. Qiuwei Wu, "Driving Pattern Analysis for Electric Vehicle (EV) Grid Integration Study".
- [40] Q. W. Zhaoxi Liu, "EV Charging Analysis Based on the National Travel Surveys of the Nordic Area".
- [41] A. Y. Taisuke Masuta, "Supplementary Load Frequency Control by Use of a Number of Both Electric Vehicles and Heat Pump Water Heaters".
- [42] H. Saadat, Power System Analysis, Third edition, PSA Publishing LLC, 2010.
- [43] V. G. M. S. S. S. E. Muljadi, "Understanding Inertial and Frequency Response of Wind Power Plants".
- [44] T. N. Kazuki Watanabe, "Study on Inertial Response of Fix-speed Wind Turbine Generator".
- [45] R. T. B. J. U. A. F. I. a. P. K. M. Altin, "Methodology for assessment of inertial response from wind power plants," IEEE, 2012.
- [46] P. Kundur, Power System Stability and Control.
- [47] Energinet.dk, "Technical Regulation for Thermal Power Station Units of 1.5 MW and higher - Regulation for grid connection TF 3.2.3," 2008.
- [48] A. G. O. a. V. A. P. B. Eriksen, ""Integrating dispersed generation into the Danish power system – present situation and future prospects," Proc. of the IEEE/ PES, Montreal, 2006.
- [49] ENTSOE, "ENTSOE - Balancing and Ancillary Services Markets," 2015. [Online]. Available: <https://www.entsoe.eu/about-entso-e/market/balancing-and-ancillary-services-markets/Pages/default.aspx>.
- [50] D. S. K. T. R. Yann G. Rebours, "A Survey of Frequency and Voltage Control Ancillary Services—Part I: Technical Features," IEEE TRANSACTIONS ON POWER SYSTEMS VOL. 22, NO. 1, Feb 2007.
- [51] Energinet.dk, "Technical Regulations for thermal power station units of 1.5 MW or above," July 2006.

- [52] J. R. Pillai, "ELECTRIC VEHICLE BASED BATTERY STORAGES FOR LARGE SCALE WIND POWER INTEGRATION IN DENMARK," A Dissertation Submitted to The Faculty of Engineering, Science and Medicine, Aalborg University in Partial Fulfillment for the Degree of Doctor of Philosophy, Aalborg, December 2010.
- [53] I. P. & E. Society, "Dynamic Models for Turbine-Governors in Power System Studies," Power System Dynamic Performance Committee, Power System Stability Subcommittee, Task Force on Turbine-Governor Modeling , Jan 2013.
- [54] F. D. Bianchi, H. de Battista and R. J. Mantz, Wind Turbine Control Systems: Principles, Modelling and Gain Scheduling Design, London: Springer, 2007.
- [55] B. B.-J. Jayakrishnan Radhakrishna Pillai, "Integration of Vehicle-to-Grid in the Western Danish Power System," IEEE TRANSACTIONS ON SUSTAINABLE ENERGY, VOL. 2, NO. 1, Jan 2011.
- [56] DlgSILENT, "DlgSILENT PowerFactory 15 User Manual," DlgSILENT GmbH, Gomaringen, Germany, May 2014.
- [57] Ø. Ulleberg, "Modeling of advanced alkaline electrolyzers: a system simulation approach," *International Journal of Hydrogen Energy*, vol. 28, no. 1, p. 21–33, 2003.
- [58] I. de Cerio Mendaza, B. Bak-Jensen and Z. Chen, "Alkaline electrolyzer and V2G system DlgSILENT models for demand response analysis in future distribution networks," in *PowerTech (POWERTECH), 2013 IEEE Grenoble* , Grenoble , 2013.
- [59] Siemens, 2 July 2015. [Online]. Available: <http://www.siemens.com/innovation/en/home/pictures-of-the-future/energy-and-efficiency/smart-grids-and-energy-storage-electrolyzers-energy-storage-for-the-future.html>.
- [60] T. Masuta, A. Yokoyama and Y. Tada, "Modeling of a number of Heat Pump Water Heaters as control equipment for load frequency control in power systems," in *PowerTech, 2011 IEEE, Trondheim* , 2011.
- [61] Energinet.dk, "From wind power to heat pumps," 1 May 2013. [Online]. Available: <http://www.energinet.dk/EN/FORSKNING/Energinet-dks-forskning-og-udvikling/Sider/Fra-vindkraft-til-varmepumper.aspx>.

- [62] Danfoss A/S, "DHP-A Opti air source heat pump," 2015.
- [63] Q. W. ., L. C. A. R. Y. X. Zhaoxi Liu, "Driving pattern analysis of Nordic region based on National," 2015.
- [64] C. Copenhagen Economics, "Elbilsalget frem mod 2020," 2015.
- [65] A. N. Brooks, "Vehicle-to-Grid Demonstration Project: Grid Regulation Ancillary Service with a Battery Electric Vehicle," Dec 2002.
- [66] Teslamotors, "Model S," 2016. [Online]. Available: https://www.teslamotors.com/da_DK/models.
- [67] Chevrolet, 31 May 2016. [Online]. Available: <http://www.chevrolet.com/bolt-ev-electric-vehicle.html>.
- [68] BYD, 31 May 2016. [Online]. Available: <http://www.byd.com/la/auto/e6.html>.
- [69] D. transport, "transportvaneundersogelsen," *faktaark om biltrafik i Danmark*, 03 2014.
- [70] A. Ursua, L. Gandia and P. Sanchis, "Hydrogen Production From Water Electrolysis: Current Status and Future Trends," *Proceedings of the IEEE*, vol. 100, no. 2, pp. 410 - 426, Feb 2012.